



**Filling the gap between the Quantum and Classical Worlds
of Nanoscale Magnetism: Giant Molecular Aggregates Based
on Paramagnetic 3d Metal Ions**

Journal:	<i>Chemical Society Reviews</i>
Manuscript ID	CS-SYN-07-2015-000590.R2
Article Type:	Review Article
Date Submitted by the Author:	04-Dec-2015
Complete List of Authors:	Papatriantafyllopoulou, Constantina; University of Cyprus, Chemistry Moushi, Eleni; University of Cyprus, Department of Chemistry Christou, George; University of Florida, Department of Chemistry Tasiopoulos, Anastasios; Department of Chemistry, University of Cyprus, Chemistry

Filling the Gap between the Quantum and Classical Worlds of Nanoscale Magnetism: Giant Molecular Aggregates Based on Paramagnetic 3d Metal Ions

Constantina Papatriantafyllopoulou,^a Eleni E. Moushi,^a George Christou,^{b, *} Anastasios J. Tasiopoulos^{a, *}

^a*Department of Chemistry, University of Cyprus, 1678 Nicosia, Cyprus Fax: ++357 22895451; Tel: ++357 22892765; E-mail address: atasio@ucy.ac.cy*

^b*Department of Chemistry, University of Florida, Gainesville, FL 32611-7200, USA Fax: +1 352-392-8757; Tel: +1 352-392-8314; E-mail address: christou@chem.ufl.edu*

* Corresponding author.

Abstract

In this review, aspects of the syntheses, structures and magnetic properties of giant 3d and 3d/4f paramagnetic metal clusters in moderate oxidation states are discussed. The term “giant clusters” is used herein to denote metal clusters with nuclearity of 30 or greater. Many synthetic strategies towards such species have been developed and are discussed in this paper. Attempts are made to categorize some of the most successful methods to giant clusters, but it will be pointed out that the characteristics of the crystal structures of such compounds including nuclearity, shape, architecture, etc are unpredictable depending on the specific structural features of the included organic ligands, reaction conditions and other factors. The majority of the described compounds in this review are of special interest not only for their fascinating nanosized structures but also because they sometimes display interesting magnetic phenomena, such as ferromagnetic exchange interactions, large ground state spin values, single-molecule magnetism behaviour or impressively large magnetocaloric effects. In addition, they often possess the properties of both the quantum and the classical world, and thus their systematic study offers the potential for the discovery of new physical phenomena, as well as a better understanding of the existing ones. The research field of giant clusters is under continuous evolution and their intriguing structural characteristics and magnetism properties that attract the interest of synthetic Inorganic Chemists’ promise a brilliant future for this class of compounds.

1. Introduction

Giant molecular aggregates have become the focus of intense investigation during the last 2-3 decades. This intense interest stems from the fact that such species often possess a combination of fascinating physical properties and intriguing geometrical features (large size, high symmetry, aesthetically pleasing shapes and architectures) that provide invaluable opportunities for crossing the boundaries both within and between the fields of chemistry, physics and materials science. Several giant clusters have now been prepared and characterized, belonging to different categories on the basis of the nature of the coordinated donor atoms and the oxidation states of the involved metal ions. These categories of compounds, which in their majority are diamagnetic, include polyoxometalates (POMs), metal chalcogenides, organometallic clusters, etc and have brought to the area of molecular nanoscience all the advantages of molecular chemistry. The latter include mild synthesis conditions, monodispersity, solubility, and a shell of organic ligands that can be post-synthetically modified by standard solution chemistry methods. A particularly crucial advantage has been the crystallinity commonly exhibited by molecular species, providing a means both for attaining structural data at atomic resolution via single-crystal X-ray crystallography, and for permitting detailed studies on highly ordered assemblies in the solid state by a range of spectroscopic and physical methods. In addition, giant molecular aggregates can be employed in very important technological and industrial applications. Thus, large organometallic clusters serve as models of elemental metal catalysts of special importance for industrial and catalytic processes.¹ On the other hand, large metal chalcogenide clusters have been used for the development of new semiconductors and have been studied as models of bulk metal sulphides and quantum dots (Cd/S, Cd/Se, etc).² In addition, POMs have been employed in

molecular separation and storage applications taking advantage of their nanoscale holes and channels that can serve as filters and traps for molecular guests.³

A more recent category of giant molecular aggregates includes paramagnetic homometallic 3d and heterometallic 3d-3d' and 3d-4f compounds. It has been developed mainly during the last decade with its first member, a Mn₃₀ cluster, reported in 2001⁴ when the chemistry of the above discussed diamagnetic giant aggregates had significantly progressed. Metal clusters based on 3d ions in moderate oxidation states are strongly related to a variety of research fields, including bioinorganic chemistry, catalysis, supramolecular chemistry, magnetocalorics and molecular magnetism.⁵⁻⁷ In the field of bioinorganic chemistry, high nuclearity clusters have been studied as models in order to elucidate details of the structure and function of the active center of ferritin, which has gained significant attention due to its biological importance in the storage and recycling of iron in mammals. Ferritin contains a symmetrical spherical cell consisting of 24 polypeptide units and can encapsulate up to ca. 4500 Fe ions in an iron oxide hydroxide core.⁵ In the field of catalysis, some mixed-valence metal clusters function as homogeneous oxidation catalysts for reactions such as organic oxidations and water oxidation using activated O-atom sources as oxidants.^{6a-c} Furthermore, in supramolecular chemistry, the discovery of the C₆₀ molecule, has inspired the scientific community to develop fullerene-like metal clusters. In fact, this is a new but rapidly developing research field and includes metal clusters with multi-shell like structures.^{6d} However, the main interest in giant metal clusters comes from the areas of molecular magnetism and magnetocaloric materials.⁷

Giant 3d or 3d/4f metal clusters often exhibit interesting and sometimes exciting magnetic properties, including high ground state spin values⁸ and single-molecule magnetism (SMM) behavior.⁹ SMMs are individual molecules that behave like magnets below a blocking

temperature due to a combination of a high spin ground state, S , and a large Ising (easy-axis) magnetoanisotropy (negative zero-field splitting (zfs) parameter, D).^{7,9,10} This leads to a significant barrier (U) to magnetization reversal whose maximum value is given by $S^2|D|$ and $(S^2 - \frac{1}{4})|D|$ for integer and half-integer spin, respectively. However, in practice, quantum tunneling of the magnetization (QTM) through the barrier via higher lying M_S levels of the spin S manifold results in the actual or effective barrier (U_{eff}) being less than U . SMMs can have magnetization relaxation times that are more than 10^8 times slower than normal paramagnets. This area thus represents a molecular, “bottom-up” approach to nanoscale magnets, complementary to the standard “top-down” approach to nanoparticles of traditional magnetic materials (e.g. Fe, Fe₃O₄, CrO₂) which are atom/ion based with d- (or f-) orbital-based spin sites and with extended network in three dimensions.¹¹ SMMs have been proposed for several applications ranging from high-density information storage, molecular spintronics, and qubits for quantum computation.¹² Additionally, several other quantum mechanical phenomena have been identified in these species, such as spin-phonon coupling,^{13a-c} spin state entanglement,^{13d,e} spin parity,¹⁴ both thermally assisted and pure quantum tunneling of the magnetization (QTM),¹⁵ quantum phase interference,^{14b,16} and others.¹⁷

Mn^{III}-containing clusters have been proven one of the most fruitful sources of SMMs since the Jahn–Teller distortion of Mn³⁺ ion in octahedral coordination geometry provides molecular anisotropy. However, this class of complexes has been extended to various other metal ions including V, Fe, Co, Ni, homometallic lanthanide species and combinations of 3d with 3d, 4d, 5d and 4f paramagnetic metal ions.^{9,18}

A special class of SMMs is the one consisting of giant species, i.e. species of very large dimensions by molecular standards. There is an increasing interest in the development of

synthetic procedures towards such clusters not only for facilitating development of techniques for addressing individual SMMs in applications, but also because they represent rare examples in which the quantum world meets the size regime of the classical world. A small ‘family’ of giant SMMs has been reported including $\text{Cu}_{17}\text{Mn}_{28}$,¹⁹ $\text{Cu}_{24}\text{Dy}_8$,²⁰ $\text{Cu}_{36}\text{Ln}_{24}$,²¹ $\text{M}_{10}\text{Dy}_{42}$ ($\text{M}^{\text{II}} = \text{Co}^{\text{II}}$, Ni^{II}),²² Mn_{30} ,⁴ Mn_{32} ,^{23,24} Mn_{44} ²⁵ and Mn_{84} examples.¹¹ In fact, the last is one of the first examples of a giant metal cluster in intermediate oxidation states, displays a 4-nm-diameter torus structure, and represents the long-sought-after meeting of the bottom-up and top-down approaches to nanomagnetism.

On the other hand, high spin polynuclear clusters with small magnetic anisotropy could be used as magnetic refrigerants. Magnetic refrigeration is a cooling technique based on the magnetocaloric effect (MCE), which is defined as the response of a ferro- or ferrimagnet to an applied magnetic field resulting in the change of its temperature. MCE was first discovered in 1881 by Warburg whereas its investigation started in the mid-1920s.^{26,27} This energy efficient and environmentally friendly technique is promising for refrigeration in the ultra-low temperature region and provides a valid alternative to the use of helium-3, which is becoming rare and expensive.²⁸ There have now been isolated a few species displaying enhanced MCE, the majority of which contain the $f^7 \text{Gd}^{\text{III}}$ ion since it provides 1) zero magnetic anisotropy, and 2) weak exchange interactions mediated through its f orbitals favoring the presence of low-lying, and thus field accessible, spin states. It is noteworthy that giant clusters, such as $\text{Co}_{16}\text{Gd}_{24}$,²⁹ $\text{Cu}_{36}\text{Gd}_{24}$,²¹ $\text{M}_{10}\text{Gd}_{42}$ ($\text{M}^{\text{II}} = \text{Co}^{\text{II}}$, Ni^{II})²² and $\text{Ni}_{12}\text{Gd}_{36}$,³⁰ have been found to display enhanced cooling properties. In particular, $\text{Co}_{10}\text{Gd}_{42}$ and $\text{Ni}_{10}\text{Gd}_{42}$ exhibit impressively large MCEs²² something that reveals the potential of such clusters for use as magnetic coolants in the ultra-low temperature range.

It is the focus of this article to provide an overview of the chemistry of giant homometallic 3d and heterometallic 3d-3d' and 3d-4f clusters in moderate oxidation states. Since there is no official definition for the term “giant clusters”, we arbitrarily decided to include in this review metal clusters with nuclearity of 30 and greater; the syntheses, structures and magnetic properties of these compounds will be discussed. Apart from the category of giant clusters based on paramagnetic 3d metal ions that are the focus of this review, there are also other important families of giant molecular aggregates that will not be discussed, such as: i) *Metal chalcogenide clusters*, ii) *Polyoxometallates (POMs) and clusters based on diamagnetic early 3d metal ions in high oxidation states (e.g. Ti^{4+})*, iii) *Organometallic clusters*, iv) *Giant clusters that do not contain 3d metal ions*, and v) *Giant clusters appearing as repeating units in multidimensional coordination polymers*. The inclusion of all these categories in a review would result in an article with the size of a book; however, mainly for comparison reasons, it would still be useful to devote a few lines to these five categories of giant molecular species. Today these families number many clusters with nuclearities of 30 and greater, with the largest species in each one having sizes and molecular weights comparable to those of small proteins. Thus, the highest-nuclearity, metal chalcogenide species structurally characterized is $[Ag_{490}S_{188}(StC_5H_{11})_{144}]$, where the Ag^I/S^{2-} core can be described as a narrow-waisted cylinder of dimensions 2.8–3.1 nm.^{31a,b} Note that most of the known giant metal chalcogenide clusters come from the coordination chemistry of metal ions in oxidation state +1, and in particular from Ag^I ³¹ and Cu^I ³² cluster chemistry, although there are also compounds reported involving metal ions at higher oxidation states (e.g. Cd^{2+} , Mn^{2+} , Ni^{2+} , etc).^{2b,33} The highest nuclearity POM known is the anion $[H_xMo^{VI}_{256}Mo^V_{112}O_{1032}(SO_4)_{48}(H_2O)_{240}]^{48-}$, having approximately the size of hemoglobin.^{34a} There are also several other giant Mo, W, V, Ti and Nb POMs possessing beautiful structures

and interesting physical properties.³⁴⁻³⁹ The list of giant organometallic species includes Pd,⁴⁰ Pd/Au,^{1c,41} Pd/Ni,^{1b, 42} Pt/Ni,⁴³ Fe/Cu,⁴⁴ and Ni/Cu⁴⁵ examples with one of the most important complexes in terms of its nanosized structure being Pd₁₄₅(CO)_x(PEt₃)₃₀, which contains a capped three-shell metal core with pseudo-icosahedral symmetry.^{40a} The last two families, which have been developed very recently, include some fascinating examples. In particular, there have been reported several giant clusters that belong to the category (iv),⁴⁶ including some beautiful 4f clusters such as the Nd₁₀₄ and Gd₁₀₄ complexes that display four-shell Keplerate-type structures and are the largest known homometallic lanthanide clusters.^{46e} Another member of this category that has attracted significant attention is a recently reported Pd₈₄ ring.^{46a,b} This compound has the same nuclearity as Mn₈₄¹¹ but is assembled from a different range of building blocks and symmetry. In particular, Pd₈₄ is sevenfold symmetric and possesses Pd₁₂ building blocks whereas Mn₈₄¹¹ is sixfold symmetric with Mn₁₄ building blocks.^{46a,b} It was suggested by the authors that fairly stable building blocks that are observed in known giant complexes or in discrete lower nuclearity metal clusters can in theory appear in other compounds displaying different symmetries. In this way, some first steps can be taken towards predicting the existence of high nuclearity clusters that shall be prepared by future generations of chemists. Concerning the coordination polymers and metal organic frameworks possessing high nuclearity aggregates as repeating units, their synthesis and characterization have recently attracted the interest of the research community since such compounds could combine interesting structural architectures and topologies with novel physical properties also appearing in their building-blocks. Several such species are now known with some of them also displaying interesting magnetic properties.⁴⁷⁻⁴⁹ The most fascinating example is a Fe₁₆₈ cluster appearing as the structural repeating unit of a 3D coordination polymer; however, it should be noted that the magnetic

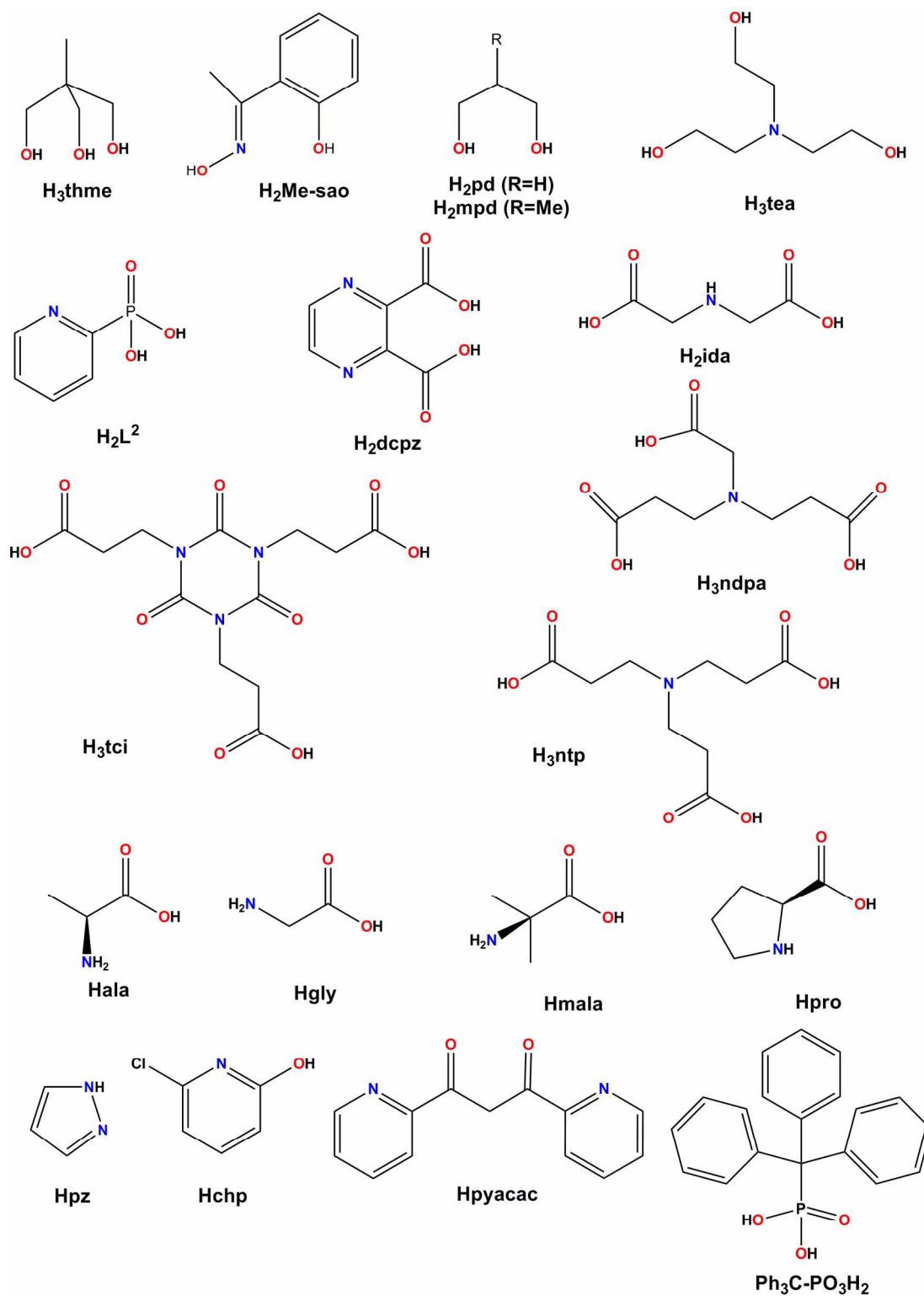
repeating unit in this case is an Fe_{28} cluster assembled through diamagnetic cubic $\{\text{Na}_4\}$ fragments to give the giant Fe_{168} cluster.⁴⁸

The review contains nine sections; the first one is introductory, the second attempts to categorize some of the main synthetic methods to giant metal clusters, the following six discuss giant Mn, Fe, Co/Ni, Cu, 3d/3d' and 3d/4f clusters, respectively, and the last one contains some concluding remarks/perspectives for this area of chemistry. This paper aims to include a discussion for every discrete giant cluster and to provide the reader with some idea of the range of chemistry that has been carried out (and remains still to be done) in this area. Emphasis will be given on synthetic, structural, and magnetic aspects of this research area. We have searched the literature up to December 2014. A review article or account on the coordination chemistry and properties of polynuclear clusters based on paramagnetic 3d metal ions with very large dimensions has never appeared in the literature.

2. Approaches for the Synthesis of Giant Clusters

Most clusters described in this paper were prepared by procedures that are based on the use of flexible ligands that impose little or no geometrical restrictions on the metal nuclearity or structure of the product. Representative examples of ligands that have been used in the synthesis of giant paramagnetic clusters are included in Scheme 1. However, it should be emphasized that although the nuclearity of paramagnetic cluster products is usually difficult to predict, the considerable forethought and choice of the ligands, metal ion sources and reaction conditions (metal ions/ligands ratio, pH, solvents, etc) has been crucial in the growth of this field of chemistry. It should also be pointed out that a continuously increasing number of giant complexes are prepared following methods that include elements of rational synthesis targeting controlled modifications in the structures of known compounds. In this paragraph we will attempt to summarize the most successful synthetic methods to giant metal clusters.

Undoubtedly, the most important organic ligands for the synthesis of metal-oxo clusters are those possessing one or more carboxylate groups. This success of carboxylate ligands can be attributed to their charged nature, resistance to oxidation, excellent bridging ability across a wide range of $M \cdots M$ separations, and their versatility due to the fact that their R groups can vary greatly from simple alkyl to phenyl or bulkier alkyl moieties; their different steric and/or electronic properties have been found to strongly affect the identity of the isolated compounds.^{9,}
⁵⁰ Such ligands also play a crucial role in the synthesis of giant clusters since they are present in most of the known giant species either together with other chelating or bridging ligands^{19,20,23,25,}
⁴⁸ or as the main organic ligand.^{4,11,21,22,24,30} Note that the carboxylates that appear most



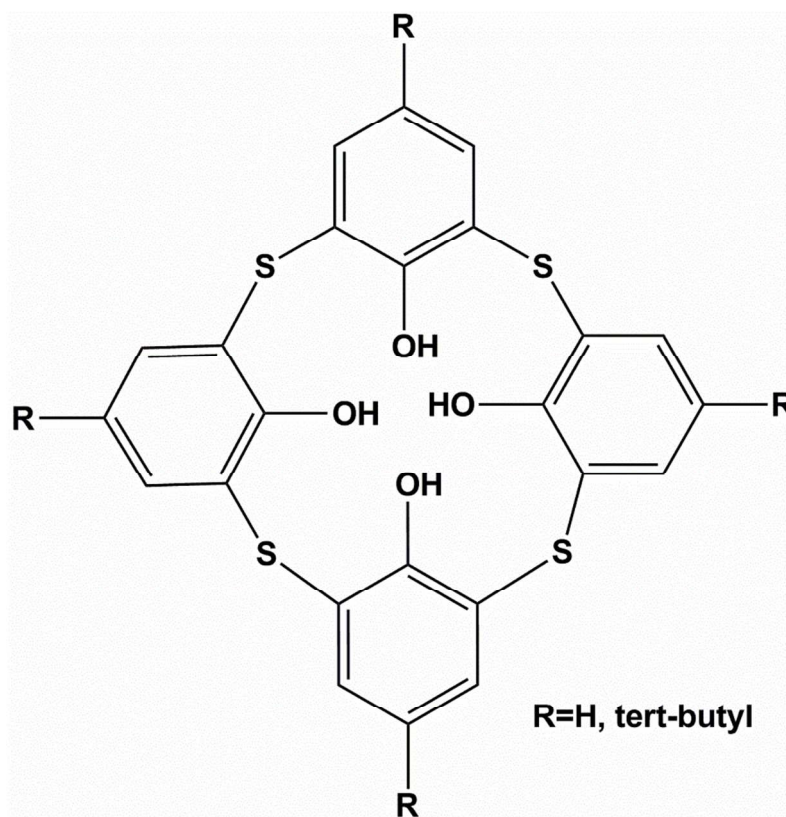
Scheme 1. Representative examples of ligands that have been employed in the synthesis of giant paramagnetic metal clusters.

often in giant species are the simplest ones (usually formates and acetates) since the presence of more bulky carboxylate ligands in such complexes would complicate significantly their structure determination. Other categories of ligands containing CO₂H groups apart from simple carboxylates have also been employed successfully in the synthesis of giant species, such as polycarboxylates, aminopolycarboxylates and amino acids.⁵¹⁻⁶⁰ These ligands have stabilized giant clusters of both M³⁺ and M²⁺ ions including Co₃₆,⁵³ Co₃₂,⁵⁴ Cu₃₆,⁵⁵ Cu₄₄,⁵⁶ Ni₇₆La₆₀,⁵⁷ Ni₃₀La₂₀^{58, 59}, Ni₅₄Gd₅₄,⁶⁰ Cu₂₄Ln₆ (Ln = Tb, Sm, La, Gd, Dy)^{51, 52} and Cu₂₆Tb₆ examples.⁵² However, it should be pointed out that depending on the relative position of their carboxylate groups, they sometimes also favor the formation of multidimensional coordination polymers.

Carboxylates are often used together with other bridging and/or chelating ligands, and in fact their combination with alkoxy-containing groups has proven a rich source of clusters with large dimensions in the coordination chemistry of metal ions that possess a variety of oxidation states, such as Fe, Co, Mn, etc. This happens because apart from the carboxylates, alkoxy-containing ligands also combine very promising features for the synthesis of giant metal clusters, mainly due to the ability of their hard RO⁻ group(s) to a) stabilize hard Mⁿ⁺ metal ions (Mⁿ⁺ = Mn³⁺, Mn⁴⁺, Fe³⁺, Co³⁺, etc), and b) act as bridges between several metal ions favoring the isolation of high nuclearity products. In addition, these ligands often promote ferromagnetic coupling between metal ions and lead to high nuclearity metal clusters with interesting magnetic properties.⁵⁰ Indeed, this approach has yielded several giant homometallic 3d and heterometallic 3d/3d' compounds including Fe₆₄,⁶¹ Mn₃₂,²⁴ Mn₄₄,²⁵ Mn₈₄,¹¹ Cu₁₇Mn₂₈¹⁹ and Mn₃₆Ni₄ species.⁶²

For the synthesis of giant clusters containing M^{II} ions (M = Co, Ni, Cu, etc), three approaches have most commonly been followed, which involve: 1) employment of ligands with suitable coordination sites, 2) use of anionic templates, and 3) combination of 3d with other 3d or

4f metal ions. The first approach is based on the use of multidentate organic ligands with suitably disposed coordination pockets, such as thiacalix[4]arene and its derivatives (Scheme 2). One such ligand is p-tert-Butylthiacalix[4]arene (H_4TCA) which has eight potential donor groups (four soft S atoms and four hard O atoms of the OH groups) and thus is able to bridge a large number of M^{II} metal ions of intermediate hardness/softness. In fact, this approach has yielded some giant clusters, including Ni_{32}^{63} and Co_{32} species.^{63b, 64} These clusters consist of a common “sandwich” - type motif involving oligonuclear units held from the quasi-planar phenolic- O_4 faces and the S atoms of calixarene ligands.



Scheme 2. Schematic representation of thiacalix[4]arenes.

The second approach of using anionic templates has been widely employed towards the synthesis of anion-specific binding agents. The design and synthesis of such molecules has been

developed into a central theme of supramolecular chemistry and several complexes displaying such properties have been already reported.⁶⁵ Apart from this, anionic species have been found to act as templates for the construction of metal clusters with large dimensions. In particular, a few Cu^{II} and $\text{Cu}^{\text{II}}/4\text{f}$ high nuclearity species, such as Cu_{36} ,⁵⁵ Cu_{44} ,⁵⁶ Cu_{31} ,⁶⁶ $\text{Cu}_{24}\text{Ln}_6$,^{51,52} possessing fascinating crystal structures and interesting magnetic properties have been found to form around an anionic template. In most cases, the anionic template comes from the metal ion salt or is formed *in-situ* during the reaction procedure.⁵⁵ However, there are also cases in which, after the realization of the role of the anion, targeted modifications were performed on the reaction mixture to study the system in detail, obtain new products and increase the size and nuclearity of the isolated clusters.⁶⁶

The third approach for the synthesis of giant clusters that contain M^{II} metal ions includes the involvement of heterometals in the reaction system; the combination of 3d with other 3d or 4f metal ions sometimes results in high, or abnormally high nuclearity heterometallic clusters with aesthetically pleasing structures. An impressive observation concerning this method comes from Ni^{2+} or $\text{Co}^{\text{n}+}$ ($n = 2,3$) cluster chemistry where although there are no homometallic complexes with nuclearity greater than 36,⁵³ the combination of $\text{Co}^{\text{n}+}$ and Ni^{2+} with 4f metal ions has led to the isolation of nanosized complexes with nuclearities up to 136.⁵⁷ Note that the first nanosized 0-D 3d/4f metal clusters were the $\text{Cu}^{2+}/4\text{f}$ complexes $\text{Cu}_{24}\text{Ln}_6$ ($\text{Ln} = \text{Tb}, \text{Gd}, \text{Sm}$ and La) and $\text{Cu}_{24}\text{Sm}_6$ containing amino acid ligands;^{51a} these compounds were reported in 2004 and after their discovery, several other nanosized $\text{Cu}^{2+}/4\text{f}$ clusters were prepared and characterized including families of $\text{Cu}_{24}\text{Ln}_6$,^{51b,52} $\text{Cu}_{26}\text{Tb}_6$,⁵² $\{[\text{Cu}_{24}\text{Ln}_6]_2\text{Cu}\}$ ($\text{Ln} = \text{Sm}, \text{Gd}$),⁵² $\text{Cu}_{24}\text{Ln}_8$ ($\text{Ln} = \text{Dy}$ and Gd)²⁰ and $\text{Cu}_{36}\text{Ln}_{24}$ ($\text{Ln} = \text{Dy}$ and Gd)²¹ complexes. The first giant heterometallic $\text{Ni}^{2+}/4\text{f}$ complex was the dual-shell cluster $[\text{Ni}_{30}\text{La}_{20}(\text{OH})_{30}(\text{ida})_{30}(\text{CO}_3)_6(\text{NO}_3)_6(\text{H}_2\text{O})_{12}](\text{CO}_3)_6$, ($\text{H}_2\text{ida} =$

iminodiacetic acid) reported in 2007.⁵⁹ The family of giant Ni²⁺/4f clusters has been expanded significantly and now includes several compounds, such as the Ni₅₄Gd₅₄,⁶⁰ Ni₇₆La₆₀,⁵⁷ Ni₁₂Gd₃₆,³⁰ and Ni₁₀Ln₄₂ (Ln = Gd³⁺, Dy³⁺)²² heterometallic species. Amongst them, Ni₇₆La₆₀ is the highest nuclearity 3d/4f metal cluster known to date and consists of 136 metal ions arranged into a four-shell, nest-like framework structure.⁵⁷ On the other hand, the family of Coⁿ⁺/4f compounds is significantly smaller including very few members, namely the Co₁₆Ln₂₄ (Ln = Gd³⁺, Dy³⁺)²⁹ and Co²⁺,Co³⁺Ln₄₂ (Ln = Gd³⁺, Dy³⁺) clusters.²² However, it should be noted that the nuclearities of the Coⁿ⁺/4f clusters are significantly larger than those of the homometallic ones. It is also very interesting to note that the picture changes if we go to Mnⁿ⁺ and Feⁿ⁺ cluster chemistry where the nuclearities of homometallic complexes are significantly higher than those of Mn/4f and Fe/4f complexes where the only complex with nuclearity greater than 30 is a Mn₁₂Ce₂₂ complex occurring as a building unit in a one-dimensional chain.⁴⁹ However, it is very difficult to comment if there is a systematic reason behind this or it is merely due to the more intense research efforts for the synthesis of high nuclearity Ni, Co/4f metal clusters. The isolation of two high nuclearity heterometallic 3d/3d clusters, Cu₁₇Mn₂₈¹⁹ and a Mn₃₆Ni₄,⁶² suggests that the use of 3d heterometals could also be a fruitful method for the isolation of giant molecular aggregates.

The growing database of such species provides valuable information that is useful for the targeted synthesis of new high nuclearity clusters. For example, the synthesis of a Mn₄₄ cluster was targeted after the isolation of its Mn₄₀Na₄ analogue in order to improve the magnetic properties of the latter.²⁵ In addition, the employment of another heterometal in the reaction mixture resulted in a new Mn₃₆Ni₄ aggregate.⁶² Note also that synthetic modifications in the reaction conditions that yielded a Ni₃₀La₂₀ cluster provided access to the family of giant Ni/4f

species possessing nuclearities up to 136 metal ions.⁵⁷⁻⁶⁰ These compounds were prepared from targeted modifications to reaction procedures that had afforded high nuclearity metal clusters and involved addition of an organic ligand to a reaction mixture containing a metal ion source and possibly other reactants. However, a new synthetic approach was recently developed and led to the rational design of new molecular species containing smaller cages as building – blocks.^{67,68} This method is based on the use of cages that display functional groups and thus can act as ligands for other metal clusters. Depending on the type of functional group, the procedure can either afford a predesigned compound or display some elements of serendipity. Thus, when the functional group is a pyridine N, compounds with completely predictable structures are formed consisting of units that are employed in the reaction procedures. However, when the functional group is a carboxylate then the central unit is assembled in the reaction solution. So far several polynuclear complexes have been prepared by employing this strategy including four compounds that will be discussed in this paper; among these compounds is an impressive Ni₁₈Cr₄₂ ring-of-rings aggregate which is one of the highest nuclearity clusters in moderate oxidation states.⁶⁷ It is clear that elements of designed synthesis have been recently added to the synthetic procedures to giant clusters and this promises the further development of this chemistry in the future, including the isolation of clusters possessing even higher nuclearities.

3. Manganese Clusters

The vast majority of the homometallic giant species in intermediate oxidation states come from Mn cluster chemistry. This is not surprising taking into account that 1) Mn can be stabilized in multiple oxidation states (such as 3+, 4+) favoring the formation and coordination of hard O^{2-} and related ions that have high bridging capability and can yield high nuclearity clusters, and 2) intense research efforts have been concentrated in Mn cluster chemistry due to its importance in the single-molecule magnetism area since most of the known SMMs, including $[Mn_{12}O_{12}(O_2CCH_3)_{16}(H_2O)_4] \cdot 4H_2O \cdot 2CH_3CO_2H$ ($Mn_{12}OAc$), ie the first one, come from this area.⁷ The result of this effort was the discovery of several high nuclearity complexes including some nanosized clusters.

The first giant Mn species $[Mn_{30}O_{24}(OH)_8((CH_3)_3CCH_2CO_2)_{32}(H_2O)_2(CH_3NO_2)_4]$ (**1**) was reported in 2001 (Fig. 1).⁴ This compound is also the first giant discrete cluster (compound with nuclearity 30 or more) based on metal ions in moderate oxidation states reported in the literature. Compound **1** was obtained by an aggregation reaction when $[Mn_{12}O_{12}((CH_3)_3CCH_2CO_2)_{16}(H_2O)_4]$ was recrystallized from $CH_2Cl_2/MeNO_2$. The structure of **1** comprises 3 Mn^{II} , 26 Mn^{III} and 1 Mn^{IV} ions and consists of a central, near-linear $\{Mn_4O_6\}$ backbone, to either side of which are attached two $\{Mn_{13}O_9(OH)_4\}$ units. (Fig. 1) The peripheral ligation around the resulting $\{Mn_{30}O_{24}(OH)_8\}$ core is completed by 32 $(CH_3)_3CCH_2CO_2^-$ ions, 2 H_2O molecules, and 4 $MeNO_2$ groups. The 24 bridging oxide ions in **1** are separated into two types: 18 are μ_3-O^{2-} and six μ_4-O^{2-} . The dominant exchange interactions between the metal ions in **1** are antiferromagnetic leading to an $S = 5$ ground state spin value. In addition, complex **1** is a

SMM with $U_{\text{eff}} = 15$ K as proven by single – crystal hysteresis studies. Although the characteristic steps of QTM were not clearly observed in the hysteresis loops, the quantum behavior of **1** was confirmed from the appearance of a “quantum hole” when the “quantum hole digging” method was employed, demonstrating for the first time that this phenomenon can be also observed in clusters with very large dimensions.

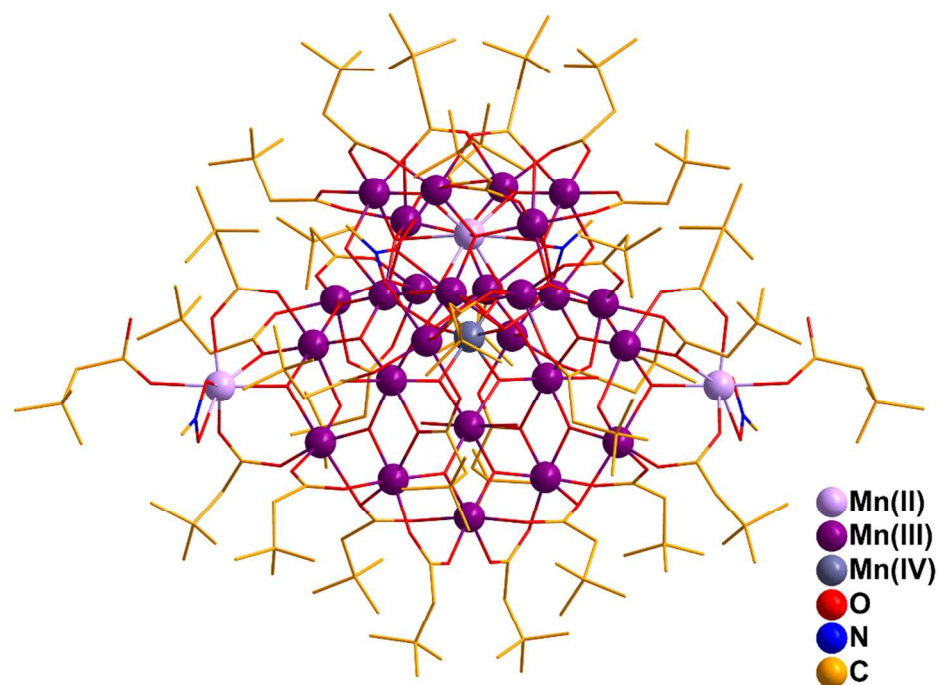


Fig. 1. The molecular structure of complex **1**.

One of the most fascinating examples of giant species is the cluster $[\text{Mn}_{84}\text{O}_{72}(\text{OH})_6(\text{CH}_3\text{CO}_2)_{78}(\text{OMe})_{24}(\text{MeOH})_{12}(\text{H}_2\text{O})_{42}]$ (**2**)¹¹ (Fig. 2) that was formed from the reaction of Mn_{12}OAc and $(\text{N}^t\text{Bu}_4)(\text{MnO}_4)$ in the presence of $\text{CH}_3\text{CO}_2\text{H}$ in MeOH. The structure of **2** consists of alternating near-linear $\{\text{Mn}_3\text{O}_4\}$ and cubic $\{\text{Mn}_4\text{O}_2(\text{OMe})_2\}$ structural units held together to form a $\{\text{Mn}^{\text{III}}_{84}\}$ giant wheel. It has a diameter of about 4.2 nm and a thickness of

about 1.2 nm, with a central hole of diameter 1.9 nm, thus being of comparable size to the smallest nanoparticles. Magnetic studies on **2** revealed the existence of dominant antiferromagnetic exchange interactions leading to a relatively small spin ground state of $S = 6$.

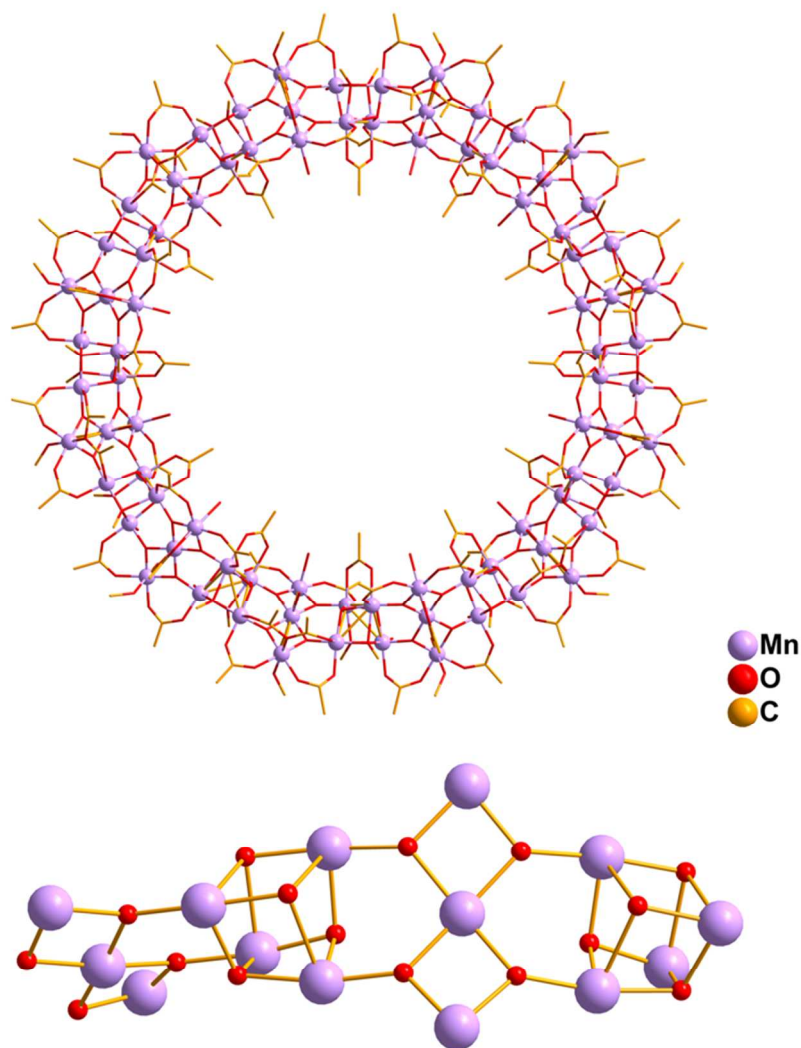


Fig. 2. The molecular structure of complex **2** (top) and the Mn/O core of its $\{\text{Mn}_{14}\}$ repeating unit (bottom).

Single-crystal hysteresis studies proved that **2** is a new SMM and the “quantum hole digging” method revealed that this compound displays QTM. Thus, although **2** is comparable in

size with the smaller magnetic nanoparticles, it still possesses the quantum properties of molecular species. The occurrence of QTM was also confirmed by obtaining magnetization relaxation rate ($1/\tau$) data from out-of-phase AC susceptibility (χ_M'') data at different AC frequencies, and DC magnetization versus time decay studies. These data were plotted as τ versus $1/T$ (Fig. 3) and fitted to the Arrhenius equation, which gave $U_{\text{eff}}=18$ K and $\tau_0=5.7 \times 10^{-9}$ s, where τ is the relaxation time and τ_0 is the preexponential factor. The relaxation rate is temperature-independent at the lowest temperatures, as expected for relaxation only by QTM. This Mn_{84} torus represents the first meeting point of the top-down and bottom-up approaches to nanoscale magnetic materials and although over 10 years have passed from its preparation, it is still the largest known SMM and Mn cluster.

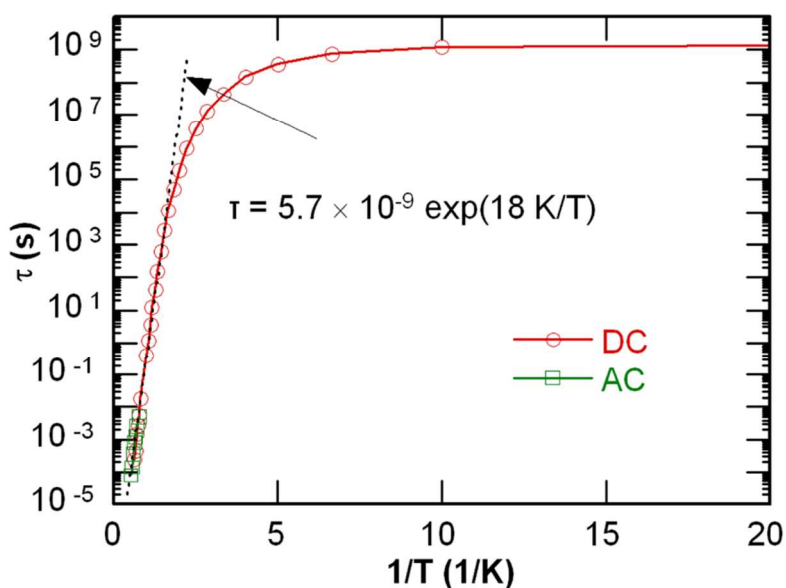


Fig. 3. Arrhenius plot constructed by using a combination of out-of-phase AC susceptibility (χ_M'') and DC magnetization decay data for compound **2**. The dashed line is a fit of the thermally activated region to the Arrhenius relationship. Adapted from reference 11 with permission.

The reaction of $[\text{Mn}_2(\text{Hthme})_2(\text{bpy})_4](\text{ClO}_4)_2$, $\text{CH}_3\text{CO}_2\text{Na}$ and NaN_3 in MeCN yielded the mixed-valent cluster $\{\text{Mn}(\text{bpy})_3\}_{1.5}[\text{Mn}_{32}(\text{thme})_{16}(\text{bpy})_{24}(\text{N}_3)_{12}(\text{CH}_3\text{CO}_2)_{12}](\text{ClO}_4)_{11}$ (**3**), where $\text{H}_3\text{thme} = 1,1,1$ -tris(hydroxymethyl)ethane and $\text{bpy} = 2,2'$ -bipyridine.⁶⁹ The cation $[\text{Mn}_{32}(\text{thme})_{16}(\text{bpy})_{24}(\text{N}_3)_{12}(\text{CH}_3\text{CO}_2)_{12}]^{8+}$ (Fig. 4) consists of eight $\{\text{M}_4\}$ star-shaped units linked together to form a truncated cube. Each $\{\text{Mn}_4(\text{thme})_2\}^{4+}$ unit comprises a central Mn^{IV} ion and three peripheral Mn^{II} ions; the Mn^{II} ions are linked to the Mn^{IV} ion through the alkoxy arms of two thme^{3-} ligands, whereas the neighbouring units are held together through CH_3CO_2^- and N_3^- ions. The cation of **3** possibly displays a ground state spin value of $S = 9$ or 10 , although it is very difficult to confirm this beyond any doubt since this complex contains several Mn^{2+} ions. The latter exhibit weak exchange interactions that lead to low-lying excited states that complicate the magnetic analysis.

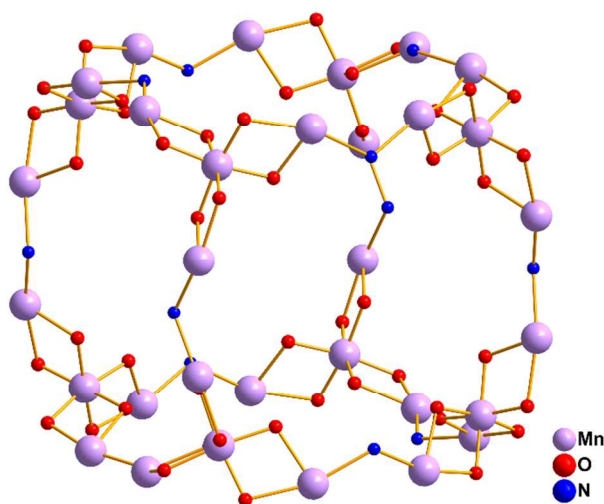


Fig. 4. Representation of the core of the $[\text{Mn}_{32}(\text{thme})_{16}(\text{bpy})_{24}(\text{N}_3)_{12}(\text{CH}_3\text{CO}_2)_{12}]^{8+}$ cation of compound **3**.

Recently, two new Mn_{32} clusters possessing SMM behavior were reported. The first one is a double-decker wheel with the formula $[\text{Mn}_{32}\text{O}_8(\text{OH})_6(\text{Me}-$

sao)₁₄(CH₃CO₂)₁₈Br₈(H₂O)₁₀](OH)₂ (**4**).²³ It was formed by the reaction of MnBr₂·4H₂O, NaO₂CMe, 2-phenyl-1,2-propanediol (Ph-pdH₂), and 2'-hydroxyacetophenone oxime (H₂Me-sao) in a 1:1:1:1 molar ratio in MeCN. The diol does not appear in the final product, but its presence in the reaction mixture was proven to be crucial for isolation of **4**. The cation of **4** is a centrosymmetric, mixed-valent {Mn^{II}₁₈Mn^{III}₁₄} double-decker wheel (Fig. 5), comprising two parallel {Mn^{II}₇Mn^{III}₇} crown-shaped wheels that enclose a {Mn^{II}₄} rectangle in their inner cavity.

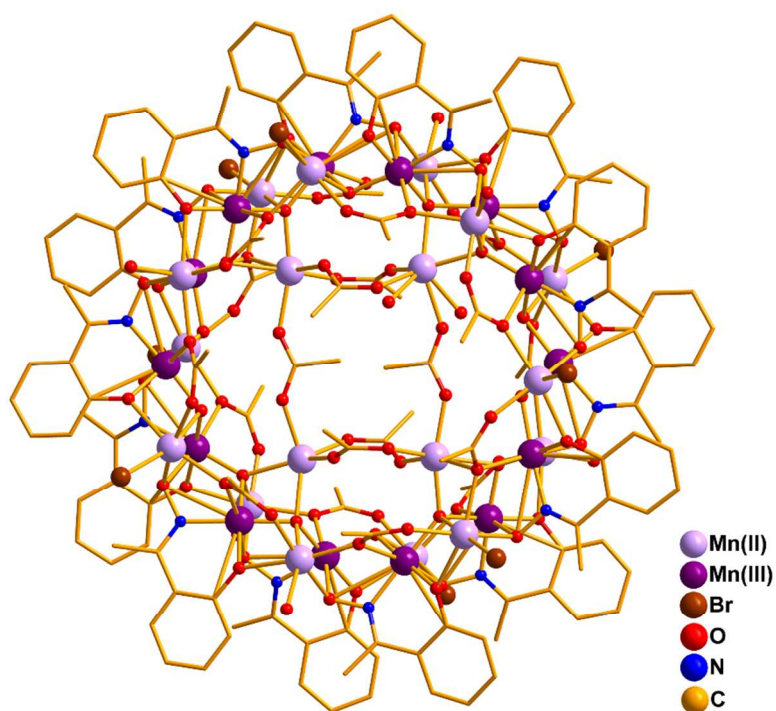


Fig. 5. Representation of the molecular structure of the cation of **4**.

Each {Mn₁₄} unit consists of seven Mn^{III} and seven Mn^{II} ions located alternately to form a single-stranded wheel. The two {Mn₁₄} units are held together through the oximate μ-O atoms of the 14 Me-sao²⁻ ligands, the 6 μ₃-OH⁻ units, and the 8 μ₄-O²⁻ atoms. The latter also connect the resulting {Mn₂₈} double-decker to the central {Mn^{II}₄} rectangle, in which the four Mn^{II} ions are linked through four η¹:η¹:μ CH₃CO₂⁻ ions. The metal–oxygen core of the cluster comprises four

pairs of edge-sharing $\{M_4O\}$ tetrahedra situated at the “corners” of the wheel linked to each other alternately by one and two vertex-sharing $\{Mn_3O\}$ triangles revealing a fictitious “Maltese Cross”-like cavity.

DC and AC magnetic susceptibility measurements revealed the existence of competing ferro- and antiferromagnetic exchange interactions in **4**. The existence of frequency dependent out-of-phase ac signals suggested that **4** is a SMM; this conclusion was confirmed by single – crystal hysteresis measurements (Fig. 6). The U_{eff} value of **4** was found to be 44.5 K, one of the highest observed to date for a $Mn^{II/III}$ mixed-valent complex⁷⁰ and the highest observed for any molecular wheel.

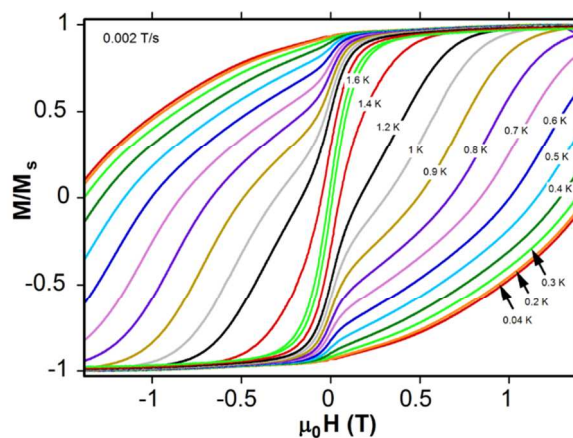
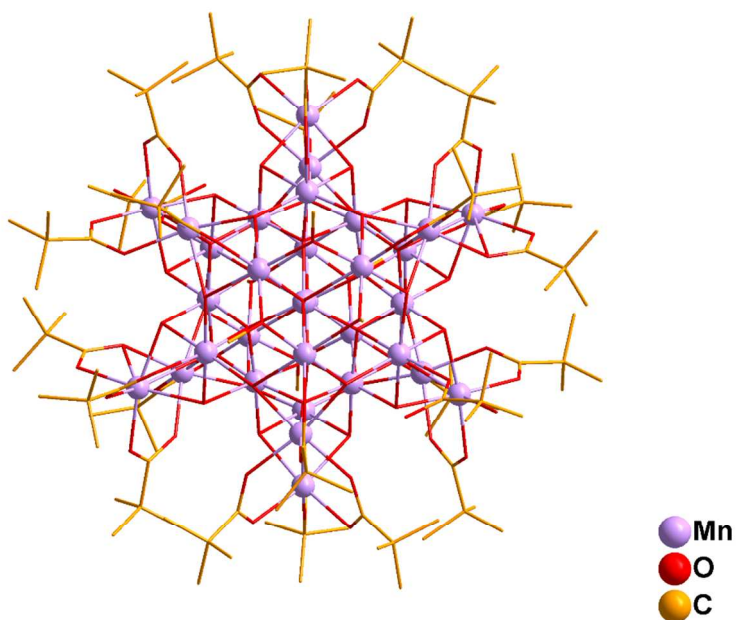


Fig. 6. Magnetization (M) versus applied magnetic field (μ_0H) hysteresis loops for a single crystal of **4**·3MeCN at the indicated temperatures and a fixed field sweep rate of 0.002 T s⁻¹. M is normalized to its saturation value (M_s). Adapted from reference 23 with permission.

The other Mn_{32} cage with the formula $[Mn^{II}_{18}Mn^{III}_{10}Mn^{IV}_4O_{14}(OH)_{24}(OMe)_6((CH_3)_3CCO_2)_{24}(H_2O)_{2.6}]$ (**5**) (Fig. 7, top) was prepared from the reaction of $Mn(O_3SC_6H_4CH_3)_2 \cdot 6H_2O$, pivalic acid and triethylamine in MeOH and recrystallization of the obtained product from

CH_2Cl_2 .²⁴ The crystal structure of complex **5** contains 18 Mn^{II} , 10 Mn^{III} and 4 Mn^{IV} ions held together through 10 $\mu_4\text{-O}^{2-}$, 4 $\mu_3\text{-O}^{2-}$ and 12 $\mu_3\text{-OH}^-$ bridges. The structural core of **5** contains a central $\{\text{Mn}^{\text{II}}_{10}\text{Mn}^{\text{III}}_4\text{Mn}^{\text{IV}}_4\text{O}_{12}(\text{OH})_{12}\}^{12+}$ fragment which displays six distorted cubanes sharing two vertices to form a ring. (Fig. 7, bottom, left) The six remaining Mn^{III} sites form two incomplete $\{\text{Mn}_3\text{O}(\text{OMe})_3\}^{4+}$ cubanes, each missing one metal vertex, which are capped by eight Mn^{II} sites (Fig. 7, bottom, right). The capped incomplete cubanes lie above and below the main cubane fragment and are linked to it through O^{2-} , OH^- and pivalate ligands. Complex **5** possesses an $S = 5$ ground state spin value and possible SMM behavior as indicated by the existence of out-of-phase ac magnetic susceptibility ‘tails’ at very low temperatures.



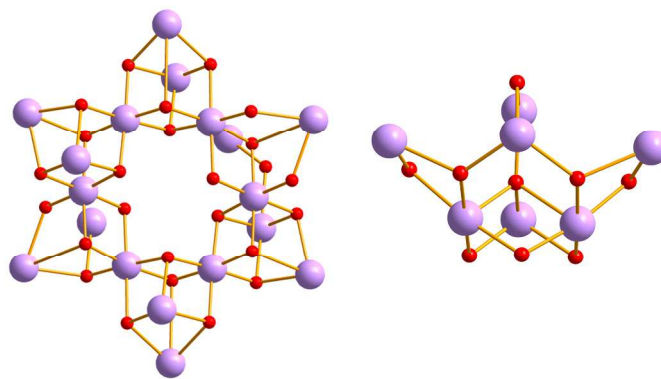


Fig. 7. Representation of a) the molecular structure of **5** (top), b) the vertex sharing cubanes in a ring configuration (bottom, left) and c) the capped incomplete cubane fragment (bottom, right) present in the structural core of **5**.

Recently, a family of $\text{Mn}_{40}\text{Na}_4$ and Mn_{44} loops was reported consisting of four smaller Mn_{10}M ($\text{M} = \text{Na}^+$ or Mn^{2+}) wheels, i.e. these compounds displayed a ‘loop-of-loops’ topology.²⁵ Complexes $[\text{Mn}_{10}\text{NaO}_2(\text{CH}_3\text{CO}_2)_{13}(\text{pd})_6(\text{py})_2]_4$ (**6**) (Fig. 8, left) and $[\text{Mn}_{10}\text{NaO}_2(\text{CH}_3\text{CO}_2)_{13}(\text{mpd})_6(\text{py})(\text{H}_2\text{O})]_4$ (**7**) were prepared from reactions of $[\text{Mn}_3\text{O}(\text{CH}_3\text{CO}_2)_6(\text{py})_3] \cdot \text{py}$ with 1,3-propanediol (H_2pd) or 2-methyl-1,3-propanediol (H_2mpd) in the presence of NaN_3 respectively. The two compounds are essentially isostructural, consisting of four Mn_{10} loops linked through Na^+ ions. Each loop contains two Mn^{II} and eight Mn^{III} ions and consists of two $\{\text{Mn}^{\text{III}}_3\text{O}\}^{7+}$ triangles and two dinuclear $\text{Mn}^{\text{II}}\text{Mn}^{\text{III}}$ subunits linked by L^{2-} ($\text{L}^{2-} = \text{pd}^{2-}$ in **6**; mpd^{2-} in **7**) $\mu\text{-O}$ atoms, and both $\mu\text{-MeCO}_2^-$ and $\eta^2:\eta^2:\mu_4\text{-CH}_3\text{CO}_2^-$ groups (Fig. 8, right). The triangles are connected by the alkoxo arms of two L^{2-} ligands, whereas the $\text{Mn}^{\text{II}}\text{Mn}^{\text{III}}$ units are connected by two $\mu\text{-alkoxo O}$ atoms and one $\mu\text{-CH}_3\text{CO}_2^-$ group. The Mn ions of the triangular units are held together through a $\mu_3\text{-O}^{2-}$ ion, two L^{2-} and one acetate $\mu\text{-O}$ atoms, and two $\mu_3\text{-CH}_3\text{CO}_2^-$ ligands. The latter and an additional acetate group link each Mn_3 unit to a Na^+ ion; the two Na^+ ions attached to the Mn_{10} loop connect it in an equivalent way to a neighbouring

one resulting in the formation of a large tetrameric loop-of-loops supramolecular aggregate with a saddle-like configuration.

DC magnetic susceptibility measurements on compound **6** revealed the existence of dominant antiferromagnetic exchange interactions between the metal centers that lead to a ground state spin value of $S = 4$ for the Mn_{10} loop. The latter was also confirmed by AC

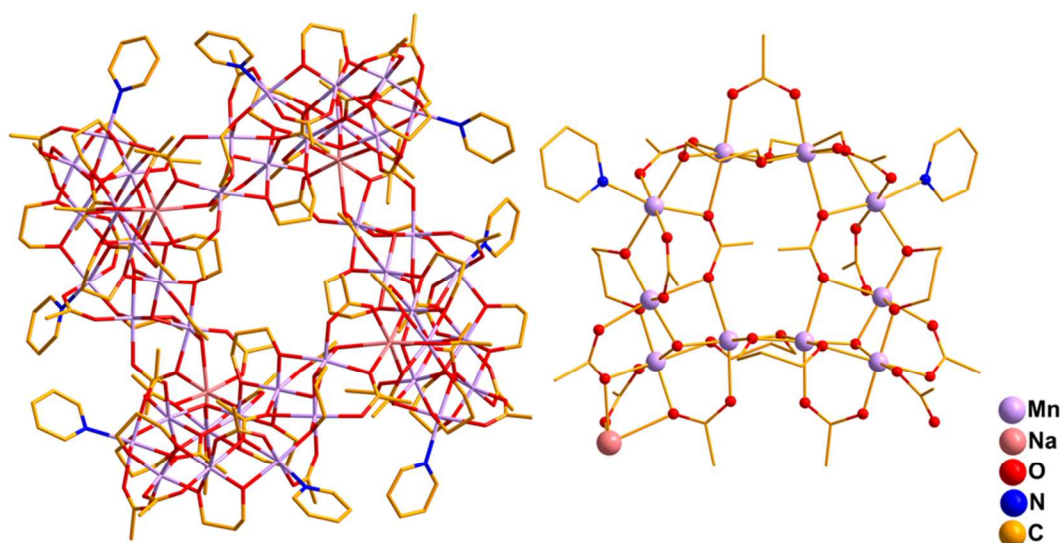


Fig. 8. The molecular structure of the compound **6** (left) and its Mn_{10}Na subunit (right).

measurements which also displayed frequency-dependent out-of-phase signals below 3.5 K. The existence of out-of-phase signals suggested that **6** might possess SMM behavior, thus magnetization measurements vs applied dc field were performed. The obtained magnetization responses at different temperatures and a fixed field sweep rate of 0.070 T/s are shown in Fig. 9, left. Hysteresis loops become evident at 4 K, displaying a small coercivity which increases, but only slightly, with decreasing temperature down to 0.04 K. This behavior was attributed to the combination of an intrinsic barrier to magnetization relaxation for each Mn_{10} unit and weak exchange interactions between the neighboring decanuclear units.

Since the weak exchange interactions between the neighboring Mn_{10} units prevented **6** from displaying SMM behavior, the isolation of the magnetically discrete, homometallic analogue (Mn_{44}) was then targeted as a means of strengthening the inter-loop interactions and potentially thus yielding structurally and magnetically discrete Mn_{44} clusters that might be new SMMs. This objective was realized by the preparation of the Mn_{44} complex **8** with the formula $[\text{Mn}_{44}\text{O}_8(\text{CH}_3\text{CO}_2)_{52}(\text{pd})_{24}(\text{py})_8](\text{ClO}_4)(\text{OH})_3$ (**8**). The latter was obtained from the reaction that yielded **6** but with the use of $\text{Mn}(\text{ClO}_4)_2 \cdot 6\text{H}_2\text{O}$ instead of a Na^+ salt. The structure of the cation of **8** is essentially identical to those of **6** and **7**, with the most significant difference being that the four Na^+ ions of **6** and **7** have been replaced by Mn^{2+} ions. However, the magnetic study of **8** revealed that it possesses a spin ground state value $S = 6$ and is a new SMM as confirmed by the observation of hysteresis loops below 0.7 K whose coercivities increase with decreasing temperature and with increasing field sweep rate (Fig. 9, right). Thus, complex **8** is the second largest Mn cluster and SMM reported to date after Mn_{84} (complex **2**).

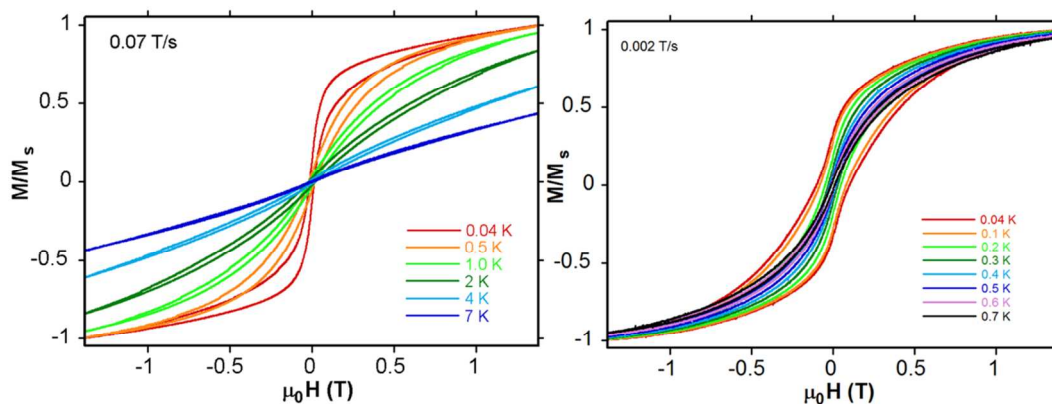


Fig. 9. Magnetization (M) vs applied magnetic field ($\mu_0 H$) hysteresis loops for a single crystal of **6**·9.6H₂O (left) and **8**·(6+x)H₂O (right) at the indicated temperatures and a fixed field sweep rate of 0.07 T/s (for **6**·9.6H₂O) and 0.002 T/s (for **8**·(6+x)H₂O). The magnetization is normalized to its saturation value (M_s). Adapted with permission from reference 25a.

4. Iron Clusters

High nuclearity iron clusters remain a synthetic target of many research groups around the world not only because of their interesting magnetic and catalytic properties but also their relevance to the Fe-storage ferritin proteins.⁵ The first such species was reported in 1999 as a part of a fascinating work on the size control of clusters with icosahedral symmetry of the type $\{(\text{pentagon})_{12}(\text{linker})_{30}\}$, known as Keplerate solids.⁷¹ The latter is a mixed 4d/3d $\text{Mo}^{\text{VI}}_{72}\text{Fe}^{\text{III}}_{30}$ metal cluster and typically should not be discussed in detail in this review since the giant $\text{Fe}^{\text{III}}_{30}$ subunit is part of a large POM compound. However, this $\text{Fe}^{\text{III}}_{30}$ fragment is the first giant species based on 3d paramagnetic metal ions reported, thus we chose to make an exception and include it, as well as a few other members of this family, in this review. The reported compound displays the formula $[(\text{Mo}^{\text{VI}}_6\text{O}_{21}\text{L}^1_6)_{12}\{\text{Fe}^{\text{III}}(\text{H}_2\text{O})\text{L}^1\}_{30}]$ (**9**), where $\text{L}^1 = \text{H}_2\text{O} / \text{CH}_3\text{CO}_2^- / \text{Mo}_2\text{O}_{8/9}^{n-}$;⁷¹ the H_2O , CH_3CO_2^- and $\text{Mo}_2\text{O}_{8/9}^{n-}$ ligands have been denoted as L^1 because they are coordinated to the metal ions in the same manner. Compound **9** was formed in high yield from the reaction of $\text{FeCl}_3 \cdot 6\text{H}_2\text{O}$ with the previously reported anion $[\{\text{Mo}^{\text{VI}}_6\text{O}_{21}(\text{H}_2\text{O})_6\}_{12}\{\text{Mo}^{\text{V}}_2\text{O}_4(\text{CH}_3\text{CO}_2)\}_{30}]^{42-}$ (Mo_{132}).⁷² Mo_{132} cluster is also a keplerate solid which contains $\{(\text{Mo})\text{Mo}_5\}$ pentagons and Mo^{V}_2 linkers; during its reaction with Fe^{III} salts, the Mo^{V}_2 linkers are substituted by aqua-ligand- Fe^{III} polyhedra. The crystal structure of **9** (Fig. 10) has an approximately icosahedral symmetry and consists of twelve $\{(\text{Mo})\text{Mo}_5\text{O}_{21}\}$ pentagonal fragments containing a central bipyramidal MoO_7 unit surrounded by five MoO_6 octahedra. These fragments are connected through the Fe^{III} linkers each of which bridges two MoO_6 octahedra of two neighbouring pentagonal units. The thirty Fe

centres form an icosidodecahedron, one of the Archimedean solids, consisting of twenty triangles and twelve pentagons.

It is noteworthy that the family of the molybdenum oxide-based keplerate solids of the type $\{(\text{Mo})_{72}\{\text{linker}\}_{30}\}$ has now been expanded and includes the compounds $\{\text{Na}(\text{H}_2\text{O})_{12}\}[\text{Mo}^{\text{VI}}_{72}\text{Cr}^{\text{III}}_{30}\text{O}_{252}(\text{CH}_3\text{CO}_2)_{19}(\text{H}_2\text{O})_{94}]$ **(10)**^{35c} and $[\text{K}_{10}\subset\{(\text{Mo}^{\text{VI}})\text{Mo}^{\text{VI}}_5\text{O}_{21}(\text{H}_2\text{O})_3(\text{SO}_4)\}_{12}\{(\text{V}^{\text{IV}}\text{O})_{30}(\text{H}_2\text{O})_{20}\}]^{26-}$ **(11)**.^{35h} Compounds **10** and **11** possess similar structures to **9**, with the $\text{Mo}^{\text{VI}}_{72}\text{Cr}^{\text{III}}_{30}$ analogue also encapsulating a $\{\text{Na}(\text{H}_2\text{O})_{12}\}$ species in its cavity. The analogous polyoxotungstate clusters $\text{Na}_6(\text{NH}_4)_{20}(\text{Fe}^{\text{III}}(\text{H}_2\text{O})_6)_2[\{(\text{W}^{\text{VI}})\text{W}^{\text{VI}}_5\text{O}_{21}(\text{SO}_4)\}_{12}\{(\text{Fe}(\text{H}_2\text{O}))_{30}\}(\text{SO}_4)_{13}(\text{H}_2\text{O})_{34}]$ **(12)**^{37a} and $\text{K}_{14}(\text{VO})_2[\text{K}_{20}\subset\{(\text{W})\text{W}_5\text{O}_{21}(\text{SO}_4)\}_{12}(\text{VO})_{30}(\text{SO}_4)(\text{H}_2\text{O})_{63}]$ **(13)**^{37b} have been also synthesized and characterized. Furthermore, this chemistry has been expanded to 3d/4f metal clusters and in this context the $\{\text{Capsule content} \subset [\text{Mo}_{72}\text{Fe}_{24}\text{Ln}_6\text{O}_{252}(\text{H}_2\text{O})_{105}]\}$ **(14/Ln; Capsule content: ca. $\text{Mo}_{18}\text{O}_{66}\text{Ln}_2(\text{H}_2\text{O})_n$; Ln = Ce, Pr)**,³⁵ⁱ keplerate solids have been reported. This research area has attracted significant interest and several other compounds are now known including keplerate solids containing 2 or 3 different metal ions in the M_{30} units, such as $\{\text{Mo}_{72}\text{Mo}_8\text{V}_{22}\}$, $\{\text{Mo}_{72}\text{V}_{15}\text{Fe}_7\text{Mo}_8\}$, and $\{\text{Mo}_{72}\text{V}_{11}\text{Fe}_{11}\text{Mo}_8\}$, or keplerate solids with partially reduced $\{(\text{Mo})\text{Mo}_5\}$ building blocks, such as $\text{K}_{13}\text{Na}_3\{\text{VO}(\text{H}_2\text{O})_5\}_{3-}[\{(\text{Mo}_6\text{O}_{21}(\text{H}_2\text{O})_3(\text{SO}_4)\}_{12}(\text{Fe}(\text{H}_2\text{O})_2)_{30}]$.^{37c-e} However, it would be beyond the scope of this review to discuss in detail, and list in table 1, all of these compounds and thus we chose to discuss only the representative clusters **9-14**. The fact that several such molecular spheres have been isolated reveals that their targeted synthesis based on a careful selection of appropriate pentagonal ligands and metal ions with specific coordination behaviour is very likely to be feasible. The isolation of a large number of complexes possessing essentially the same crystal

structure with some differences in the constituent metal ions, ligands, etc confirms that several elements of rational design have been included in this type of chemistry.

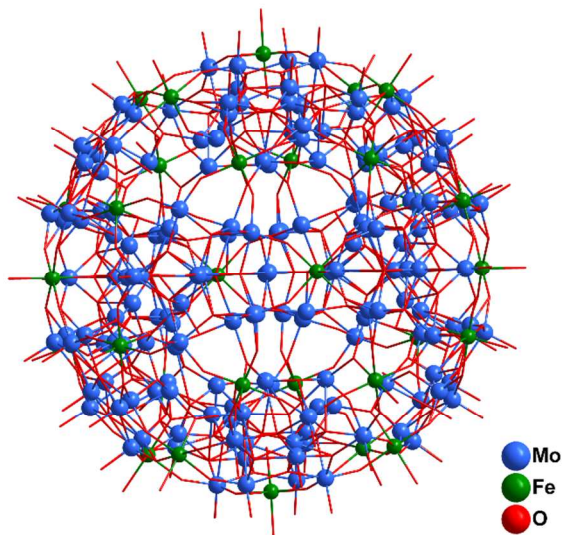


Fig. 10. Representation of the spherical Mo/Fe/O core of **9**.

The first (chronologically) discrete giant Fe cluster was prepared nine years after compound **9** was reported. It was a $\text{Fe}^{\text{III}}_{64}$ cluster with the formula $[\text{Fe}^{\text{III}}_{64}\text{O}_{24}(\text{tea})_8(\text{Htea})_{24}(\text{HCO}_2)_{60}](\text{ClO}_4)_{12}$ (**15**), where H_3tea is triethanolamine.⁶¹ Compound **15** was isolated by a very slow mixing of two different methanol solutions separated by H_2O ; the first solution included the ligands HCO_2H and H_3tea , and the second one the salt $\text{Fe}(\text{ClO}_4)_2 \cdot 6\text{H}_2\text{O}$. The cation of **15** (Fig.11, left) can be described as a cubic cage consisting of eight octanuclear $[\text{Fe}^{\text{III}}_8\text{O}_3(\text{tea})(\text{Htea})_3(\text{HCO}_2)_6(\text{HCO}_2)_{3/2}]$ subunits (Fig. 11, right) located at its corners. Each Fe^{III}_8 unit comprises three flattened $\{\text{Fe}_4(\mu_4\text{-O})\}$ tetrahedra sharing the central Fe – Fe axis of the core and displaying a propeller-like configuration. Each Fe_8 corner is connected through three formate ligands to three other Fe_8 units forming the Fe_{64} cube. Magnetism studies revealed the existence of antiferromagnetic exchange interactions between the metal ions in **15**

leading to a diamagnetic ground state ($S = 0$). The isolation of **15** demonstrated the potential of HCO_2^- ions, when they are used together with other flexible ligands (e.g. various polyols), to result in high nuclearity clusters likely due to their small steric hindrance. Compound **15** is the largest discrete Fe^{III} cluster and the second largest homometallic 3d metal cluster after Mn_{84} although an Fe_{168} complex being the repeating unit of a 3-D coordination polymer was reported recently.⁴⁸

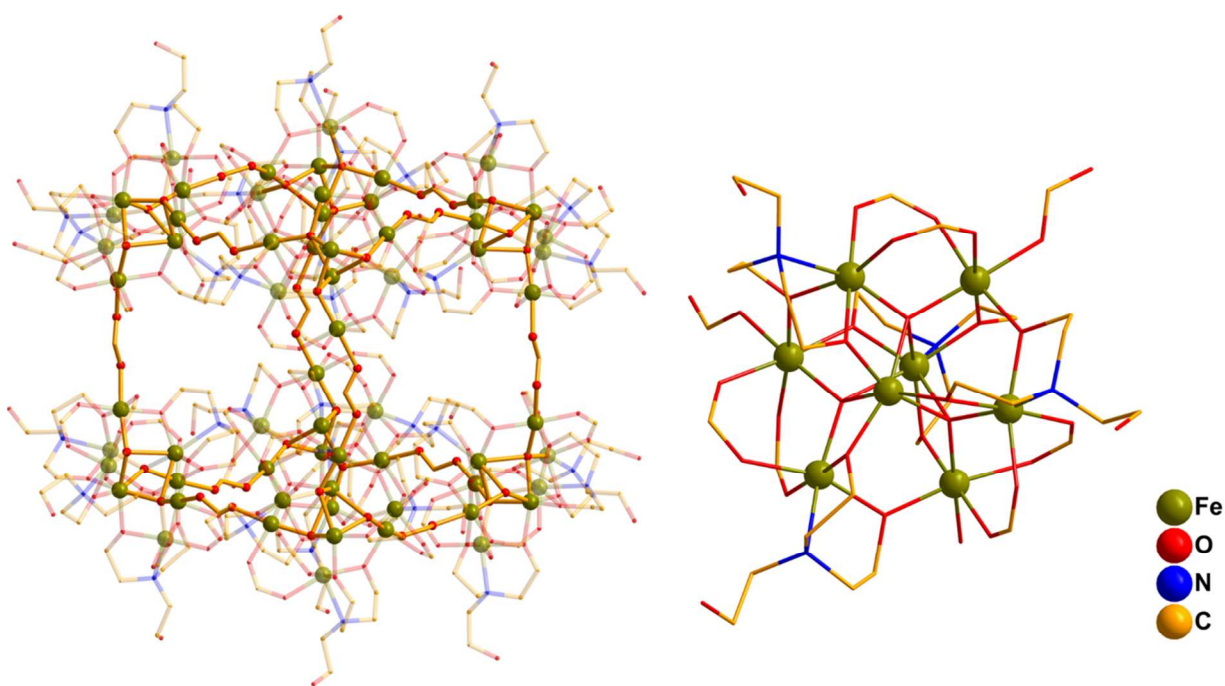


Fig. 11. Representations of the molecular structure of the cation of **15** (left) and its Fe_8^{III} building unit (right).

The most recent Fe complex with nuclearity greater than thirty to be prepared and characterized is an Fe_{36} phosphonate cage. The crystallography in this case was a very challenging task due to the poor quality of the crystals, large void space in the structure and existence of severely disordered lattice solvent molecules. To unequivocally determine the atom

connectivity and structure of the Fe_{36} cage, two analogous compounds possessing the same $[\text{Fe}^{\text{III}}_{36}(\text{L}^2)_{44}(\text{H}_2\text{O})_{48}]^{20+}$ ($\text{H}_2\text{L}^2 = 2$ -pyridylphosphonic acid) cation and differing only in their counterions (ClO_4^- , NO_3^- and OH^- in **16**; CF_3SO_3^- and OH^- in **17**) were prepared.⁷³ The cationic cage (Fig.12) has nearly O_h symmetry and displays a dual-shell configuration in which the 36 metal centers are held together through the $\eta^1:\eta^1:\eta^1:\eta^1:\mu_3$ 2-pyridylphosphonate groups. The

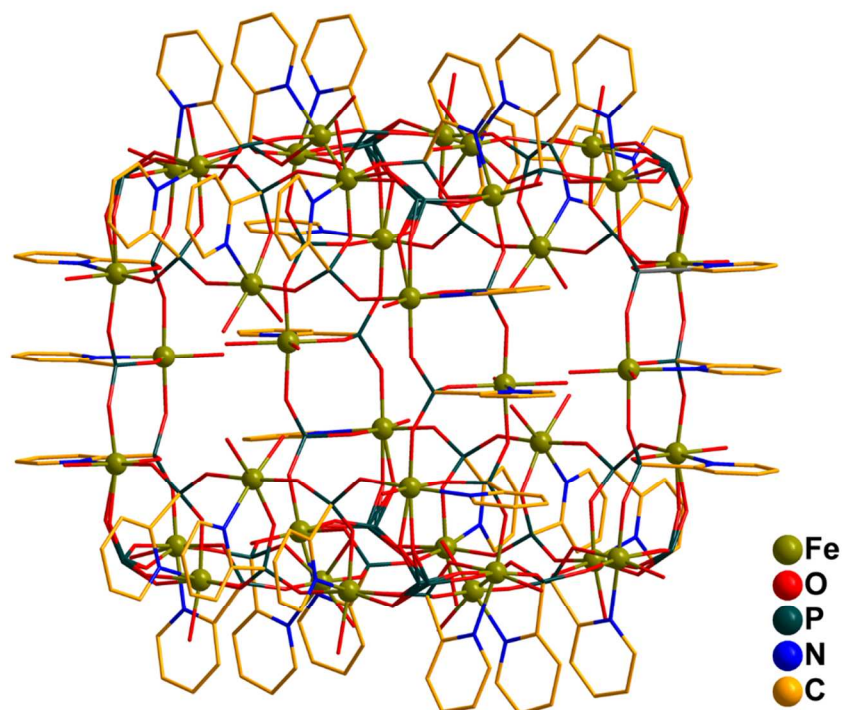


Fig. 12. Representation of the molecular structure of the $[\text{Fe}^{\text{III}}_{36}(\text{L}^3)_{44}(\text{H}_2\text{O})_{48}]^{20+}$ cation present in compounds **16** and **17**.

coordination sphere of the Fe^{III} ions of the outer shell is completed by four phosphonate oxygen atoms, one pyridyl nitrogen atom and a H_2O molecule whereas the inner iron atoms have three sites occupied by phosphonate oxygen atoms, a pyridyl nitrogen atom, and two H_2O molecules. The magnetic properties of complex **16** were studied and revealed that the exchange interactions between the metal centers are antiferromagnetic leading to a very small ground state spin value.

5. Cobalt and Nickel Clusters

The employment of polytopic organic ligands has been proven a successful route for the synthesis of high nuclearity Ni and Co clusters. In particular, the highest nuclearity Co species known to date, $[\text{Co}_{36}\text{O}_8(\text{OH})_{16}((\text{CH}_3)_3\text{CCO}_2)_{36}((\text{CH}_3)_3\text{CCO}_2\text{H})_4(\text{dcpz})_2(\text{Hdcpz})_4(\text{H}_2\text{O})_{16}(\text{MeCN})_6]$ (**18**),⁵³ was formed from the reaction of $[\text{Co}_2((\text{CH}_3)_3\text{CCO}_2)_4((\text{CH}_3)_3\text{CCO}_2\text{H})_4(\text{H}_2\text{O})]$ and 2,3-dicarboxypyrazine (H_2dcpz) in MeCN. The crystal structure of complex **18** (Fig.13) consists of a central Co_{12} unit, comprising four fused edge-sharing cubanes, which is attached to two Co_{11} wings. Each Co_{11} wing is further linked to a pendant arm containing a mononuclear Co unit; thus, the overall arrangement of **18** can be described as a central Co_{12} multiple heterocubane subunit linked to two identical Co_{12} wings forming the Co_{36} cluster. Each “wing” consists of a central Co^{II}_5 moiety linked to two Co^{II}_3 fragments through the dcpz ligand resulting the $\text{Co}^{\text{II}}_{11}$ unit; the latter is additionally linked to a Co^{II} moiety through the organic ligand.

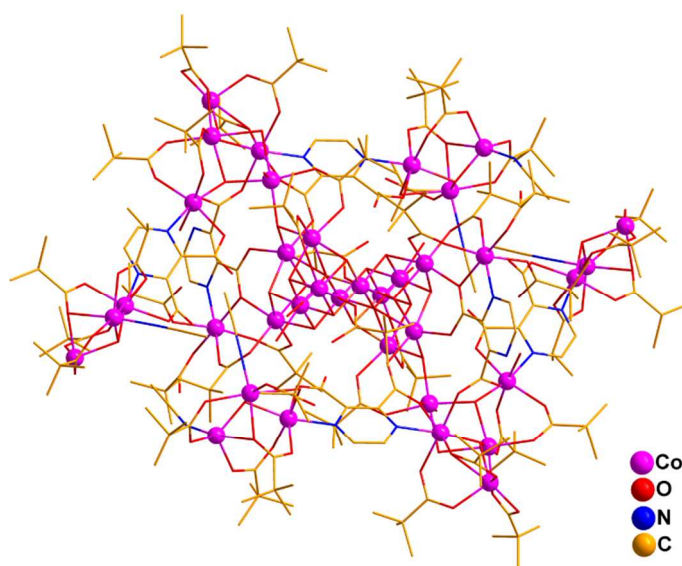


Fig. 13. Representation of the molecular structure of **18**.

Magnetism studies revealed the existence of dominant antiferromagnetic interactions between the metal centers in **18** leading to an $S = 6$ ground state spin value.

A second compound that was isolated from the use of polytopic carboxylate ligands in Co chemistry is a new Co_{32} compound with the formula $[\text{Co}_{32}\text{O}_{16}(\text{tci})_{16}(\text{H}_2\text{O})_{12}]$ (**19**), where $\text{H}_3\text{tci} = \text{tris}(2\text{-carboxyethyl})\text{isocyanurate}$.⁵⁴ It was formed from the reaction between $\text{CoCl}_2 \cdot 6\text{H}_2\text{O}$, H_3tci and NEt_3 in $\text{H}_2\text{O}/\text{acetone}$ under solvothermal conditions, and its structure consists of four mixed-valent octanuclear units $\{\text{Co}^{\text{II}}_4\text{Co}^{\text{III}}_4(\mu_4\text{-O})_4\}^{12+}$ linked through the carbonyl oxygen atoms of the tci^{3-} ions (Fig. 14), which adopt a $\eta^2:\eta^2:\eta^2:\mu_4$ coordination mode. Each octanuclear unit consists of a central cubane $\{\text{Co}^{\text{III}}_4\text{O}_4\}^{4+}$ which is connected to four Co^{II} ions through four $\mu_4\text{-O}^{2-}$ ions. The metal ions of each unit are held together through four tci^{3-} ligands, each carboxyl group of which links the outer Co^{II} ions with the cubane Co^{III} ions. The magnetic interactions between the paramagnetic Co^{II} ions in **19** are antiferromagnetic and the compound has a small ground state spin value.

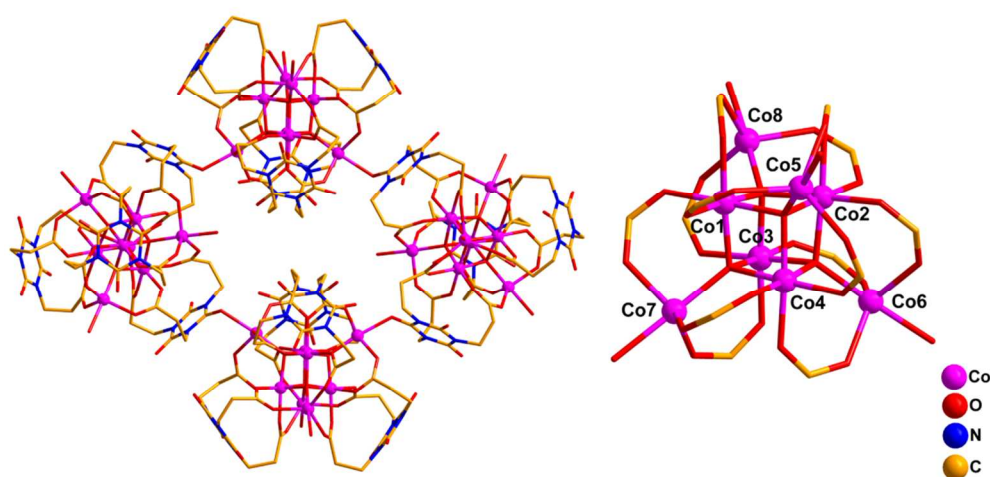


Fig. 14. Representations of the molecular structure (left) and octanuclear building unit (right) of **19**.

The ligand *p*-tert-butylthiacalix[4]arene (H₄TCA) has been employed by several groups for the synthesis of high nuclearity clusters and SMMs.⁷⁴ This ligand has also afforded some giant M₃₂ (M = Co^{II/III}, Co^{II}, Ni^{II}) clusters. The first nanosized Co species with H₄TCA was prepared in 2009,⁶⁴ and since then a few more giant species were reported by other groups.⁶³ In particular, the solvothermal reaction of Co(CH₃CO₂)₂·4H₂O and H₄TCA in MeOH/CHCl₃/H₂O at 130 °C provided access to three isomers of the [Co^{II}₂₄Co^{III}₈O₂₄(TCA)₆(H₂O)₂₄] (**20**) nanospherical cluster, differing in their packing arrangements. The spherical units are composed of six Co^{II}₄(TCA) subunits located around a Co^{III}₈ cubane (Fig. 15).⁶⁴ The Co^{III} ions are held together through 24 μ₃-O²⁻ bridges. The coordination sphere of each Co^{III} site is completed by three μ₃-O atoms and three terminal H₂O molecules. Each Co^{II} ion is coordinated by two phenoxy O groups and one S atom from the TCA⁴⁻ ligand, two μ₃-O bridges and two monodentate H₂O molecules. An interesting feature of **20** is that the Co^{II} ions form a sodalite cage that hosts the Co^{III}₈ cube; although the sodalite topology is common in zeolite-related

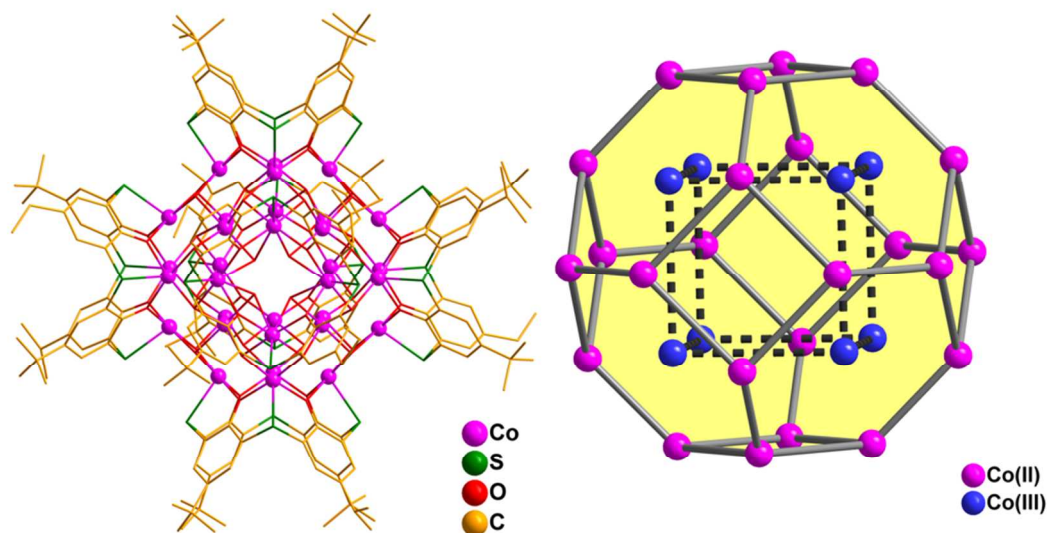


Fig. 15. Representations of the molecular structure of **20** (left) and its metallic skeleton from a view that emphasizes the sodalite-type Co^{II}₂₄ fragment and the encapsulated Co^{III}₈ cube (right).

compounds, it is rarely observed in metal cluster chemistry. Magnetism studies showed the presence of dominant antiferromagnetic exchange interactions between the paramagnetic Co^{II} ions in **20** that lead to a small ground state spin value.

The diffusion of a DMF solution of $[\text{Co}(\text{DMSO})_6](\text{BF}_4)_2$ into a DMF solution of H_4TCA and Et_3N yielded $[\text{Co}^{\text{II}}_{32}\text{O}_{16}(\text{OH})_8(\text{TCA})_6(\text{MeOH})_6]$ (**21/Co**),^{63b} which is very similar to **20** with the main differences being: 1) the oxidation states of the metal ions: all Co ions in **21/Co** are in the +2 oxidation state whereas compound **20** is mixed-valent; 2) eight of the O^{2-} - bridges in **20** have been replaced by OH^- groups in **21/Co**; and 3) the terminally coordinated solvent molecules are different in the two compounds (H_2O , **20**; MeOH , **21/Co**).

The employment of H_4TCA for the synthesis of giant clusters has proven to favor the formation of M_{32} nanospheres, thus a similar synthetic procedure to the one that yielded compound **21/Co**, but using $[\text{Ni}(\text{DMSO})_6](\text{BF}_4)_2$ or $[\text{Ni}(\text{DMSO})_6](\text{ClO}_4)_2$ instead of $[\text{Co}(\text{DMSO})_6](\text{BF}_4)_2$ yielded clusters $[\text{Ni}^{\text{II}}_{32}\text{O}_{16}(\text{OH})_8(\text{TCA})_6(\text{MeOH})_6]$ (**21/Ni**) or $[\text{Ni}_{32}(\text{OH})_{40}(\text{TCA})_6]$ (**22**), respectively.⁶³ The structures of complexes **21/Ni** and **22** are related to each other and also to those of the $\text{Co}^{\text{n+}}$ analogues **20** and **21/Co** and especially the homovalent complex (**21/Co**). The main difference between **21/Ni** and **22** is the presence of 40 OH^- bridging ligands in the second one instead of 16 O^{2-} and 8 OH^- in the first.

6. Copper Clusters

There are five giant Cu(II) clusters known to date; four of these were grown around anionic templates and published in the same year (2004) whereas the fifth one was published a year earlier, i.e. in 2003. In particular, the compounds $\{K_4(\mu\text{-MeOH})_4\}[\text{Cu}^{\text{II}}_{36}(\text{OH})_{36}(\text{OMe})_4\text{Cl}_6(\text{ndpa})_8(\text{H}_2\text{O})_5\{\text{KCl}_6\}]\text{Cl}$ (**23**) and $\{\text{Cu}^{\text{I}}_2\text{K}_4\text{Cl}_3(\text{H}_2\text{O})_3\}[\text{Cu}^{\text{II}}_{36}(\text{OH})_{37}(\text{OMe})_3\text{Cl}_6(\text{ndpa})_8(\text{H}_2\text{O})_4\{\text{KCl}_6\}]$ (**24**) were formed in good yield from the reaction of (nitrilodipropionic)acetic acid (H_3ndpa), KOH and $\text{CuCl}_2 \cdot 2\text{H}_2\text{O}$ in MeOH;⁵⁵ **23** was formed over a period of two weeks in solutions of reagent grade MeOH, whereas **24** was isolated after two months from absolute MeOH solution. The crystal structures of **23** and **24** are essentially identical with the $\text{Cu}^{\text{II}}_{36}$ aggregate being built around a central $\{\text{KCl}_6\}^{5-}$ moiety (Fig. 16, left). The latter likely acts as a template around which an inorganic hydroxo/methoxo bridged Cu_{28} framework is constructed. The Cu_{28} unit is encapsulated by $(\text{Cu}(\text{ndpa})\text{Cl})^{2-}$ and $\{\text{Cu}_2\text{Cl}(\text{ndpa})_2\}^{3-}$ moieties resulting in the formation of the Cu_{36} aggregate. The main difference between the two compounds is the existence of two Cu^{I} centres attached to the $\text{Cu}^{\text{II}}_{36}$ aggregate in **24**. The further development of the use of anionic templates for the synthesis of high nuclearity metal clusters, led to the isolation of the largest Cu^{II} aggregate known to date, namely $[\text{Cu}_{44}(\text{OH})_{40}\text{Br}_{10}(\text{ntp})_{12}(\text{H}_2\text{O})_{28}]\text{Br}_2$ (**25**), where H_3ntp is 3,3',3''-nitrilotripropionic acid.⁵⁶ Complex **25** was formed from the reaction of CuBr_2 , H_3ntp and $\text{CsOH} \cdot \text{H}_2\text{O}$ in H_2O and displays a zeotypic superstructure. The Cu^{II} ions are held together through OH^- and Br^- bridges forming a cuboidal construction around the two central Br^- ions, which are the templates for the structure (Fig. 16, right). Neighboring molecules of **25** are packed in parallel layers forming an open

structure displaying a nanosized cavity that contains a large amount of H₂O molecules and the two Br⁻ ions. Clusters **23**, **24** and **25** display dominant antiferromagnetic exchange interactions between their Cu²⁺ ions exhibiting small, ground state spin values.

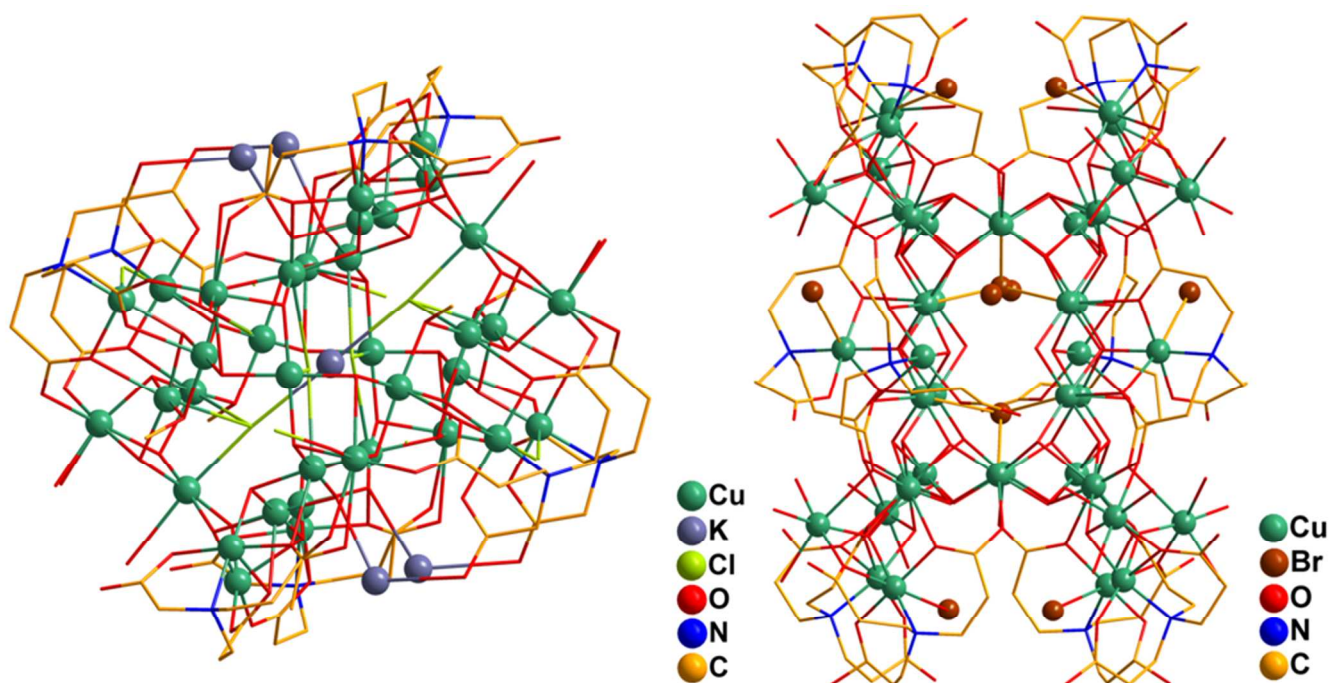


Fig. 16. Representations of the molecular structure of the Cu^{II}₃₆ aggregate present in the crystal structure of **23** (left) and the Cu^{II}₄₄ aggregate present in the crystal structure of **25** (right).

The same year, a series of Cu^{II} rings templated around various anions were reported. The highest nuclearity among these is the giant (PPN)₂[(SO₄)₂⊂{Cu(OH)(pz)}₈₊₁₄₊₉] (**26**) (PPN = bis(triphenylphosphoranylidene)ammonium cation and Hpz = pyrazole) consisting of 31 Cu^{II} ions.⁶⁶ Compound **26** was co-crystallized with (PPN)[Cl⁻⊂{[Cu(OH)(pz)]₆₊₁₂}₂] and formed serendipitously in an attempt to remove the Cl⁻ ions from compound (PPN)₂[Cu₃O(pz)₃Cl₃]. The crystal structure of **26** contains [{cis-Cu^{II}(μ-OH)(μ-pz)}_n] rings whose structures resemble those of crown ethers and natural ionophores consisting of distorted square planar Cu^{II} ions held

together through μ -OH and μ -pz ligands. The latter are located on the outer surface of the rings whereas OH⁻ groups are located on the inner surface thus defining hydrophobic and hydrophilic domains, respectively. The larger ring acts as host for smaller rings, stabilizing them with multiple weak Cu \cdots O interactions. In particular, the 14-membered ring acts as a host, binding to the Cu ions of the eight- and nine-membered rings, which, in turn, bind the encapsulated sulfate ion (Fig. 17). Several hydrogen-bonding interactions are observed which contribute to the stabilization of such a high nuclearity aggregate.

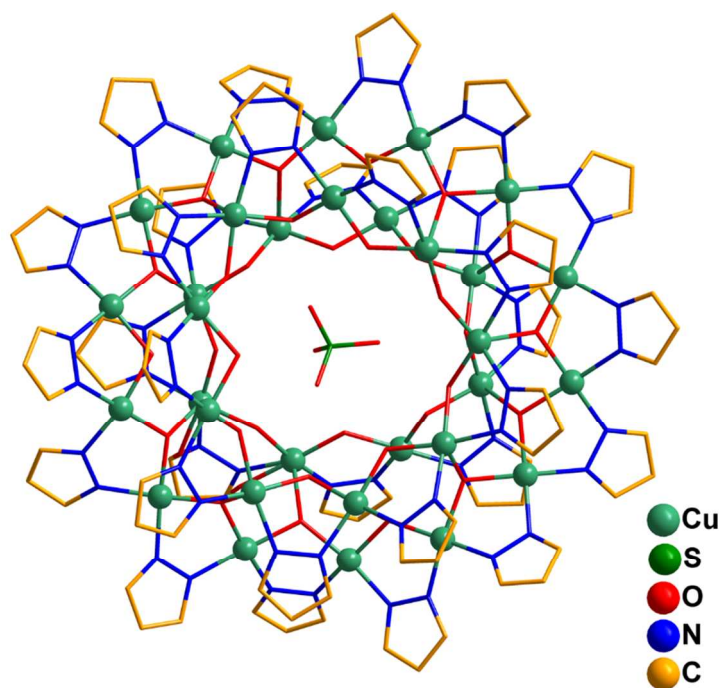


Fig. 17. Representation of the molecular structure of **26**.

The last compound discussed in this section is the one that was prepared slightly earlier than the other four. Compound $[\text{Cu}_{36}(\mu_3\text{-OH})_8(\text{dpocco})_{12}(\text{CH}_3\text{CO}_2)_{16}(\text{H}_2\text{O})_x]$ (**27**) (Figure 18, bottom) was isolated from the reaction of $\text{Cu}(\text{CH}_3\text{CO}_2)_2$ with the extended tritopic picolinic dihydrazide ligand H_4dpocco (Figure 18, top).⁷⁵ The Cu^{II} ions of **27** are held together through 12 dpocco

ligands and 8 μ_3 -OH⁻ ions adopting a spheroidal conformation. The diazine nitrogen atoms of each dpocco ligand bridge a central Cu^{II} ion to two terminal copper ions; the two latter are part of a OH-centered Cu₃ triangular unit bridged by oxime linkages from three interconnecting ligands. In the center of the spheroidal cluster there is a hole surrounded by a sheath of coordinated water molecules and acetate groups, several of which could not be included in the final structure which is of poor quality ($R_1=0.152$). However, there is no doubt about the main core of the Cu₃₆ compound. DC magnetic susceptibility studies on **27** revealed antiferromagnetic exchange interactions between the metal centres leading to a diamagnetic ground state.

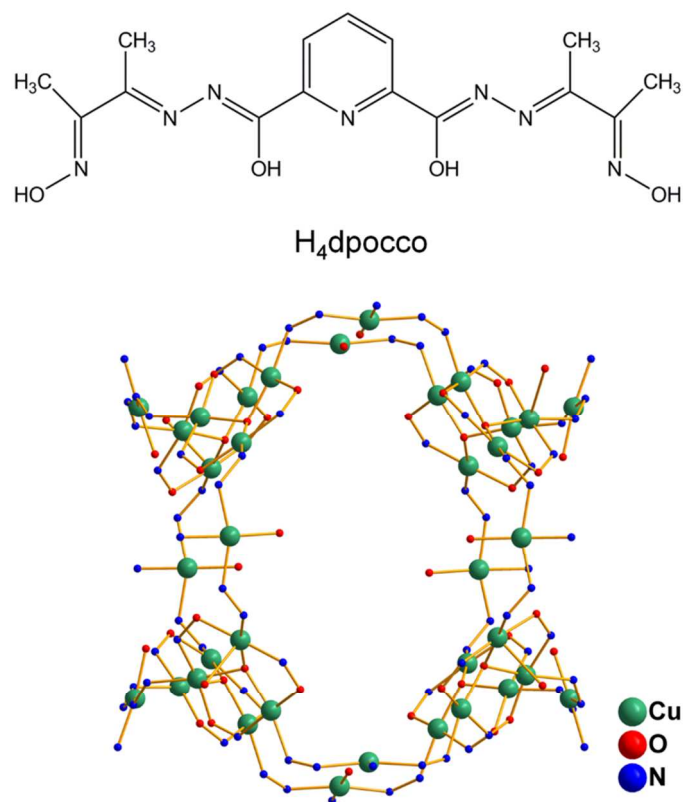


Fig. 18. Representations of the H₄dpocco ligand (top) and the core of compound **27** (bottom).

7. 3d-3d' Clusters

Although quite a few giant homometallic 3d and heterometallic 3d-4f (*vide infra*) clusters in intermediate oxidation states have been reported, the corresponding 3d-3d' species are fairly scarce. In fact, there have been published only six such compounds, with two of them displaying interesting magnetic properties. In 2007, the first giant heterometallic 3d-3d' cluster was reported, namely $[\text{Cu}_{17}\text{Mn}_{28}\text{O}_{40}(\text{tea})_{12}(\text{HCO}_2)_6(\text{H}_2\text{O})_4]$ (**28**) (Fig. 19), where H_3tea is triethanolamine.¹⁹ Compound **28** was formed from the reaction of Cu powder, $\text{Mn}(\text{CH}_3\text{CO}_2)_2 \cdot 4\text{H}_2\text{O}$ and H_3tea in 1:2:1 ratio in DMF at 85 °C. It consists of 4 Cu^{I} , 13 Cu^{II} , 4 Mn^{II} , 12 Mn^{III} and 12 Mn^{IV} ions held together through 28 μ_4 - and 12 μ_3 - O^{2-} ions forming a giant $\{\text{Cu}_{17}\text{Mn}_{28}\text{O}_{40}\}^{42+}$ core which displays T_d symmetry. All the tea^{3-} ligands adopt the $\eta^1:\eta^2:\eta^2:\eta^2:\mu_4$ coordination mode bridging one Cu^{II} , one Mn^{II} and two Mn^{III} ions. The 28 Mn atoms form 6 $\text{Mn}^{\text{III}}_2\text{Mn}^{\text{IV}}_2\text{O}_4$ and 4 $\text{Mn}^{\text{II}}\text{Mn}^{\text{IV}}_3\text{O}_4$ cubanes which are further linked, through all the Mn^{IV} ions, to construct a large adamantane – like Mn_{28} cage based on Mn_4O_4 cubanes. DC magnetic susceptibility measurements on **28** revealed that the $\chi_M T$ value increases with decreasing temperature suggesting a high ground state spin value of $S = 51/2$. The latter was further confirmed from the fit of magnetization data (plotted as reduced magnetization, $M/N\beta$, versus H/T) assuming that there is an $S = 63/2$ excited state lying 5 K above the $S = 51/2$ ground state. AC magnetic susceptibility studies were also performed at $H_{ac} = 5$ G and $H_{dc} = 0$ and revealed the existence of frequency-dependent AC out-of-phase tails of peaks at very low temperatures.

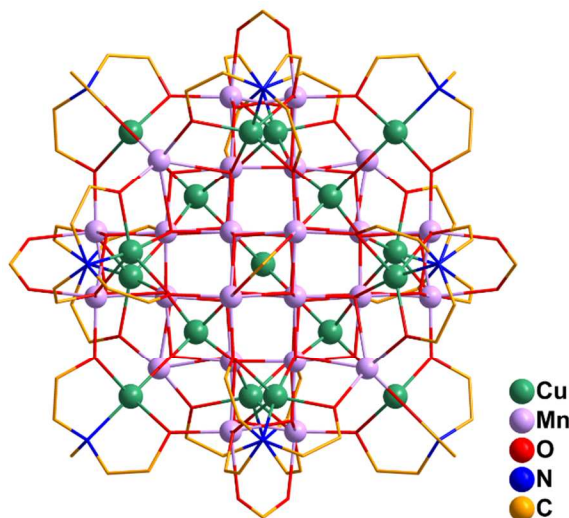


Fig. 19. Representation of the molecular structure of **28**.

Recently, we reported on the synthesis and characterization of the molecular aggregate $[\text{Mn}_{36}\text{Ni}_4\text{O}_{12}\text{Cl}_{10}(\text{CH}_3\text{CO}_2)_{26}(\text{pd})_{24}(\text{py})_4(\text{H}_2\text{O})_2]$ (**29**) (H_2pd = 1,3-propanediol) that possesses an unprecedented ‘loop-of-loops-and-supertetrahedra’ structural topology (Fig. 20).⁶² Compound **29** was isolated from the reaction of $[\text{Mn}_3\text{O}(\text{CH}_3\text{CO}_2)_6(\text{py})_3]\cdot\text{py}$ (py = pyridine) with H_2pd and $\text{NiCl}_2\cdot 6\text{H}_2\text{O}$ in CH_3CN . This $\text{Mn}_{36}\text{Ni}_4$ aggregate consists of two mixed-metal $\{\text{Mn}^{\text{III}}_8\text{Ni}_2(\mu_3\text{-O})_2(\text{CH}_3\text{CO}_2)_{12}(\text{pd})_6(\text{py})_2\}$ loops (Fig. 20, bottom, right) and two $\{\text{Mn}^{\text{III}}_6\text{Mn}^{\text{II}}_4(\mu_4\text{-O})_4(\mu_3\text{-Cl})_4(\text{CH}_3\text{CO}_2)\text{Cl}(\text{pd})_6(\text{H}_2\text{O})\}$ supertetrahedral subunits (Fig. 20, bottom, left). Each $\text{Mn}^{\text{III}}_8\text{Ni}_2$ unit comprises two $\{\text{Mn}^{\text{III}}_3\text{O}\}^{7+}$ triangles and two dinuclear $\text{Mn}^{\text{III}}\text{Ni}^{\text{II}}$ fragments connected through $\eta^2:\eta^2:\mu_3$ pd^{2-} ligands and CH_3CO_2^- groups. The $\text{Mn}^{\text{III}}_8\text{Ni}_2$ loops are related to the $\text{Mn}^{\text{III}}_8\text{Mn}^{\text{II}}_2$ loops that are present in the Mn_{40}M_4 clusters **6-8** with the main difference being the existence of the two Ni^{II} ions in the former in the place of two Mn^{II} ions.⁶²

The Mn_{10} supertetrahedron is based on the $\{\text{Mn}^{\text{III}}_6\text{Mn}^{\text{II}}_4(\mu_4\text{-O})_4\}^{18+}$ core and contains nine Mn ions in two stacked Mn_6 and Mn_3 isosceles triangles, and a tenth Mn ion at the apex position held together through the four $\mu_4\text{-O}^{2-}$ ions. The peripheral ligation is completed by one *syn,syn-*

$\eta^1:\eta^1:\mu_2$ CH_3CO_2^- group, six $\eta^2:\eta^2:\mu_3$ pd^{2-} ligands, four μ_3 and one terminal Cl^- ions and one monodentate H_2O molecule. An unusual feature in the structure of **29** is that it represents a rare example of a large cluster consisting of covalently linked polynuclear M_x ($x > 6$) complexes and the only one that contains a magnetically interesting polynuclear M_x repeating unit.⁶²

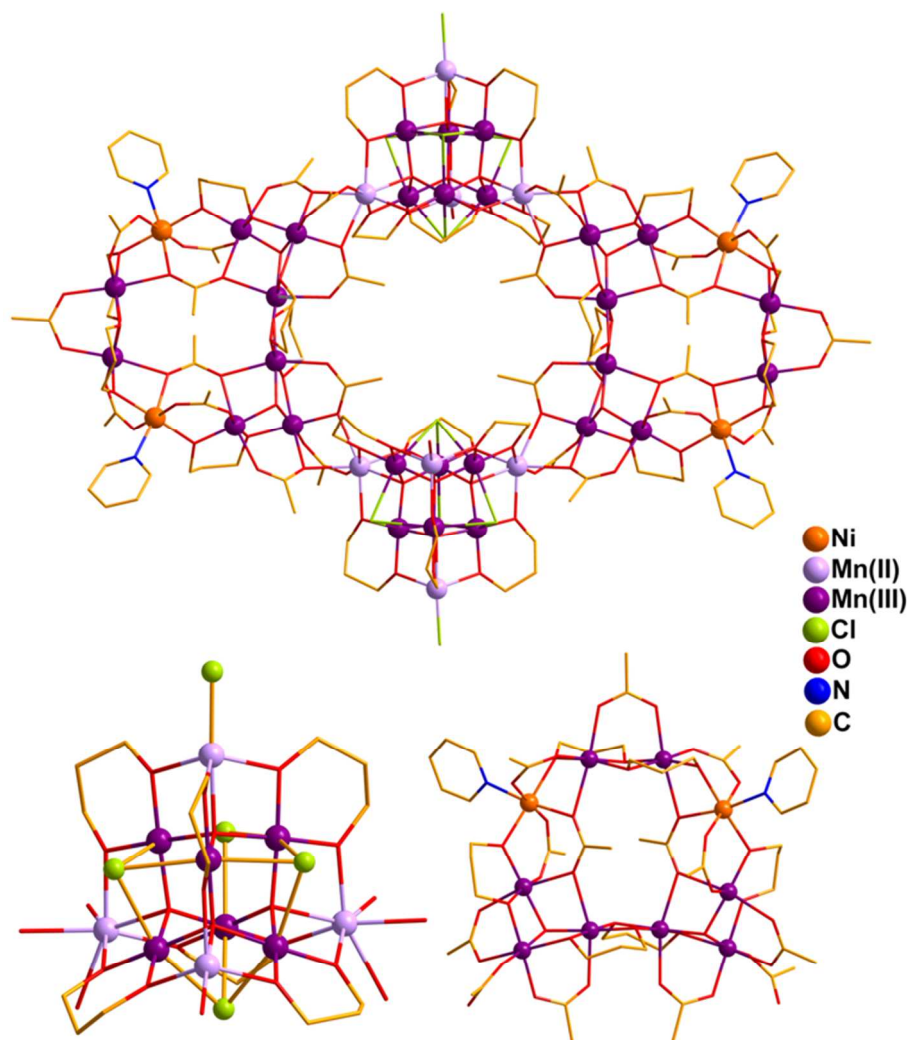


Fig. 20. Representations of the molecular structure of **29** (top) and its $\text{Mn}^{\text{III}}_6\text{Mn}^{\text{II}}_4$ supertetrahedral (bottom, left) and $\text{Mn}^{\text{III}}_8\text{Ni}_2$ loop (bottom, right) subunits.

Compound **29** displays dominant ferromagnetic exchange interactions and a high $S = 26 \pm 1$ spin ground state, the highest yet observed in a heterometallic cluster. Despite this large spin ground state value it does not display SMM behavior as proven by magnetization versus DC field scans performed on a single crystal of **29**·2CH₃CN·12.30H₂O. It is interesting to note the similar magnetic properties of compound **29** and its Mn^{III}₆Mn^{II}₄ supertetrahedral building block since both compounds display ferromagnetic exchange interactions, large spin ground state values, nearly zero D and do not exhibit SMM behaviour.

A series of high nuclearity clusters were isolated following a method which is based on the connection of a polynuclear cage that can act as a Lewis base with other cages that can act as Lewis acids. In all cases the Lewis base was the heterometallic {Cr₇Ni} ring containing a pyridine N functional group. Thus, the reaction between [NH₂Pr₂][Cr₇NiF₈((CH₃)₃CCO₂)₁₅(C₅H₄NCO₂)] and the dodecametallic SMM [Ni₁₂(chp)₁₂(CH₃CO₂)₁₂(H₂O)₆(THF)₆] yielded the 60-metal ring of rings, [Ni₁₂(chp)₁₂(CH₃CO₂)₁₂(H₂O)₆{[NH₂Pr₂][Cr₇NiF₈((CH₃)₃CCO₂)₁₅(C₅H₄NCO₂)]₆} (**30**), where Hchp=6-chloro-2-hydroxypyridine.⁶⁷ The structure of **30** (Fig. 21) consists of a central {Ni₁₂} ring in which six {Cr₇Ni} units are attached. Interestingly, the structural features of the discrete clusters {Ni₁₂} and {Cr₇Ni} remain unchanged in complex **30**. It is noteworthy that compound **30** is not an SMM although one of its main components, the central {Ni₁₂} ring, displays SMM behavior. This is likely due to the existence of weak exchange interactions between the central {Ni₁₂} ring and the {Cr₇Ni} rings which provide additional relaxation pathways. Following the same synthetic procedure, a second high nuclearity cage-of-cages was isolated using as a Lewis acid the compound [Mn^{II}₄Mn^{III}₂(μ₄-O)₂((CH₃)₃CCO₂)₁₀(THF)₄] and as a Lewis base the {Cr₇Ni} ring. The four terminal THF ligands of the {Mn₆} cluster were substituted by the pyridine of the

{Cr₇Ni} ring discussed above giving rise to the giant cage-of-cages [$\{\text{Mn}^{\text{II}}_4\text{Mn}^{\text{III}}_2(\mu_4\text{-O})_2((\text{CH}_3)_3\text{CCO}_2)_{10}\}[\text{NH}_2\text{Pr}_2][\text{Cr}_7\text{NiF}_8((\text{CH}_3)_3\text{CCO}_2)_{15}(\text{C}_5\text{H}_4\text{NCO}_2)]\}_4$] (**31**) consisting of thirty eight metal centers.

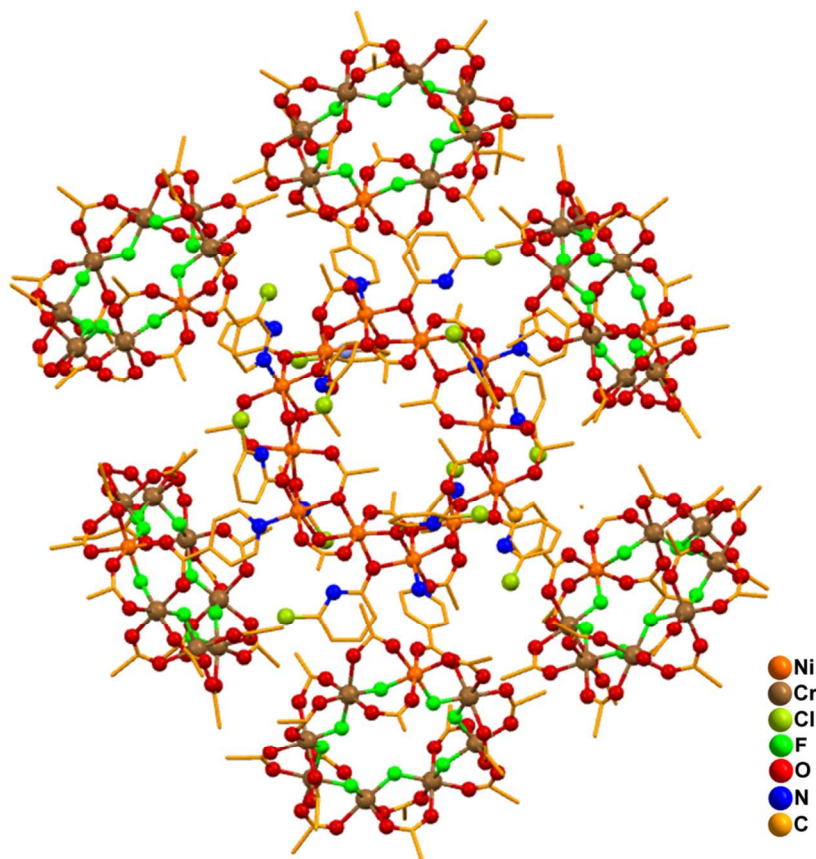
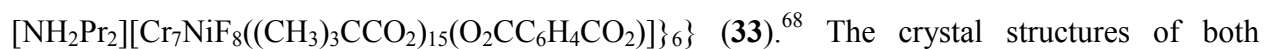
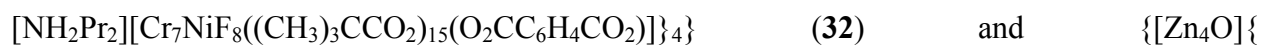


Fig. 21. Representation of the molecular structure of compound **30**.

Extending and expanding this strategy, a carboxylate functional group was introduced on the {Cr₇Ni} ring. In this case the central cage is assembled *in situ* in the presence of simple metal salts, thus this synthetic method also includes elements of serendipity. The reaction of a monosubstituted analogue of the {Cr₇Ni} ring with isophthalic acid, [NH₂Pr₂][Cr₇NiF₈((CH₃)₃CCO₂)₁₅(O₂CC₆H₄CO₂H)] and Cu(ClO₄)₂ or Zn(ClO₄)₂ provided access to two new giant clusters namely, $\{[\text{Cu}_4(\text{OH})_4(\text{Me}_2\text{CO})]\}$



compounds consist of a central tetranuclear unit $\{\text{Cu}_4(\text{OH})_4(\text{Me}_2\text{CO})\}$ in **32** or $\{\text{Zn}_4\text{O}\}$ in **33**

which is surrounded by $\{\text{Cr}_7\text{Ni}\}$ rings (4 rings in **32** and 6 rings in **33**). In **32**, the central

tetranuclear unit displays a square topology with the four five-coordinate copper(II) sites being

bridged on each edge by a hydroxide and a carboxylate group of a dicarboxylic ligand that

connects the central $\{\text{Cu}_4\}$ unit with a $\{\text{Cr}_7\text{Ni}\}$ ring. In **33**, the $\{\text{Zn}_4\text{O}\}$ unit has a tetrahedral

arrangement and is linked to the $\{\text{Cr}_7\text{Ni}\}$ rings through six isophthalate groups. The six

heterometallic rings adopt a slightly distorted octahedral conformation around the $\{\text{Zn}_4\text{O}\}$ unit.

A representation of the molecular structure of **32** is shown on Figure 22. The magnetic properties

of both compounds have been studied and revealed the presence of antiferromagnetic exchange

interactions between the metal centers.

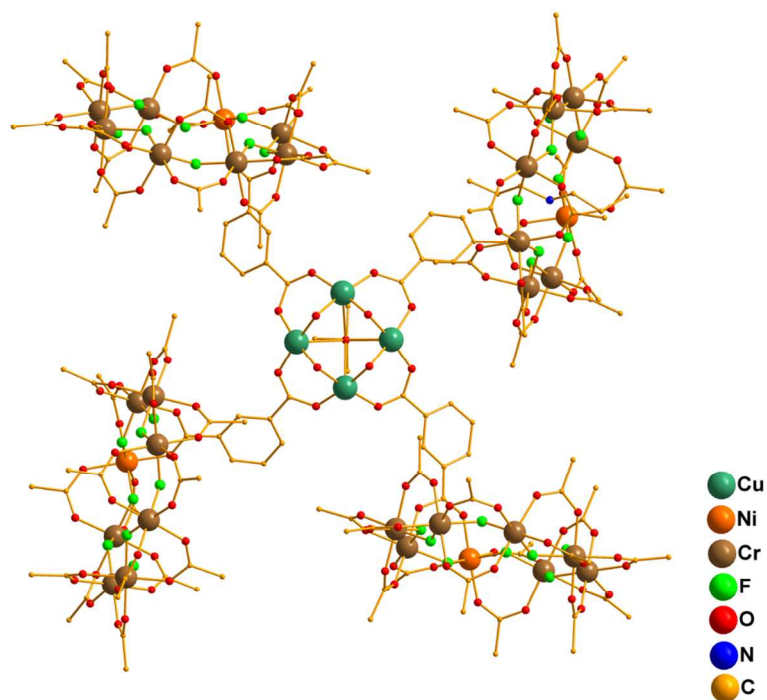


Fig. 22. Representation of the molecular structure of **32**.

8. 3d-4f Clusters

The synthesis and characterization of polynuclear 3d-4f metal clusters has recently attracted significant attention, mainly due to two reasons: 1) most trivalent lanthanides possess high single-ion anisotropy, thus such species have been investigated as an alternative approach for the synthesis of molecule-based magnets; and 2) the combination of 3d and 4f metal ions often yields high nuclearity metal clusters and has been successfully employed for the synthesis of giant species. As a result, an appreciable number of 3d/4f metal clusters are now known with the vast majority of them being Ni/4f and Cu/4f species.^{20,21,30,51,52,57-60} In the next two paragraphs, the syntheses, structures and physical properties of these compounds will be described.

8.1. Ni/Ln and Co/Ln clusters

Although the first giant 3d/4f species were Cu/4f,^{51a} the highest nuclearity complexes come from a fascinating work, which involved the use of iminodiacate (ida^{2-} , Scheme 1) ligand in Ni/4f cluster chemistry. Ida^{2-} is an excellent ligand for the construction of high nuclearity 3d/4f metal clusters since it has the capability to bridge several metal ions due to the two carboxylate groups that it contains and can also control the hydrolysis of the lanthanide ions resulting in the formation of discrete hydroxo-bridged polynuclear clusters. Thus, the reactions of H_2ida with simple metal salts resulted in several Ni/4f clusters, including $\text{Ni}_{30}\text{La}_{20}$,^{58,59} $\text{Ni}_{21}\text{Ln}_{20}$ ($\text{Ln} = \text{Pr}, \text{Nd}$),⁵⁸ $\text{Ni}_{54}\text{Gd}_{54}$,⁶⁰ and $\text{Ni}_{76}\text{La}_{60}$ ⁵⁷ examples. In particular, the solvothermal reaction of $\text{Ni}(\text{NO}_3)_2 \cdot 6\text{H}_2\text{O}$, $\text{Ln}(\text{NO}_3)_3 \cdot 6\text{H}_2\text{O}$ ($\text{Ln} = \text{La}, \text{Pr}$ and Nd) and H_2ida in 1.5 : 1 : 2 molar ration in H_2O yielded the cationic clusters $[\text{Ni}_{30}\text{La}_{20}(\text{OH})_{30}(\text{ida})_{30}(\text{CO}_3)_6(\text{NO}_3)_6(\text{H}_2\text{O})_{12}](\text{CO}_3)_6$ (**34**)^{58,59} and $[\text{Ni}_{21}\text{Ln}_{20}(\text{OH})_{24}(\text{ida})_{21}(\text{C}_2\text{H}_2\text{O}_3)_6(\text{C}_2\text{O}_4)_3(\text{NO}_3)_9(\text{H}_2\text{O})_{12}](\text{NO}_3)_9$ (**35**/Ln; $\text{Ln} = \text{Pr}$,

Nd),⁵⁸ revealing that the nature of the 4f ion affects the identity of the reaction product. The $\text{C}_2\text{H}_2\text{O}_3^{2-}$ (glycolate) and $\text{C}_2\text{O}_4^{2-}$ (oxalate) ions appearing in compounds **35**/Ln come from the hydrothermal decomposition of H_2ida . The metal centers in **34** display a keplerate - type double shell conformation with an outer $\text{Ni}^{\text{II}}_{30}$ shell encapsulating an inner $\text{La}^{\text{III}}_{20}$ sphere (Fig. 23). The 30 Ni(II) ions are connected exclusively by the carboxylate groups of the ida^{2-} ligands in an anti-syn fashion forming 12 pentagonal and 20 triangular faces, thus they span the Archimedean solid icosidodecahedron. The 20 La(III) ions are linked through $\mu_3\text{-OH}^-$ ions, $\mu_2\text{-H}_2\text{O}$ molecules, CO_3^{2-} and NO_3^- ions and are located on the vertices of a perfect dodecahedron, one of the Platonic solids. Thus, the two distinct sets of metal ions that form the $\text{Ni}_{30}\text{La}_{20}$ cage display icosahedral symmetry (I_h), the highest possible for molecules. The two metal spheres are linked by bridging ida^{2-} ligands and triply bridging $\mu_3\text{-OH}$ groups. The coordination sphere of the metal ions in **34** is

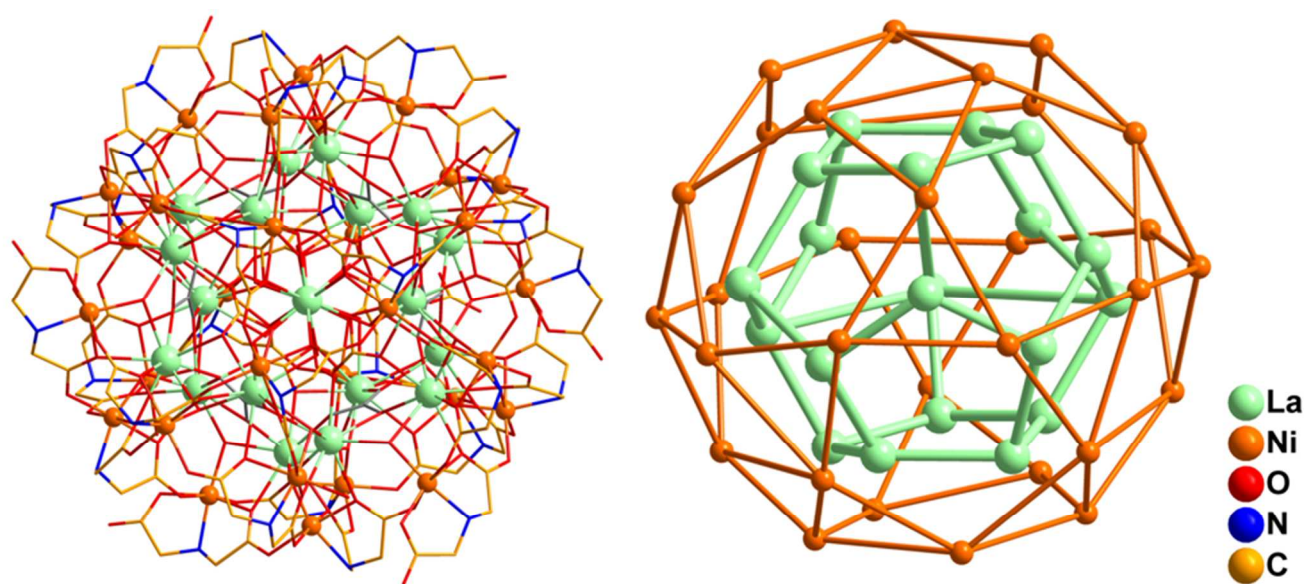


Fig. 23. Representation of the molecular structure of the cation of **34** (left) and its metallic skeleton (right). The solid lines connecting the metal ions are used to emphasize on the shapes of the outer Ni_{30} icosidodecahedron and the inner La_{20} dodecahedron cages.

completed by additional ida^{2-} ligands, bridging H_2O molecules, $\mu_3\text{-OH}$ groups, NO_3^- , and CO_3^{2-} ions. Magnetic susceptibility studies of **34** revealed the $\chi_{\text{M}}T$ value to increase with decreasing temperature suggesting the existence of dominant ferromagnetic exchange interactions between the paramagnetic Ni(II) ions (Fig. 24). $\chi_{\text{M}}T$ reaches a maximum of $264.81 \text{ cm}^3 \text{ mol}^{-1} \text{ K}$ at 16 K and then decreases, possibly due to antiferromagnetic inter-cluster interactions and zero-field splitting of the ground state. The maximum at 16 K suggests an $S \sim 20$ ground state spin for **34**.

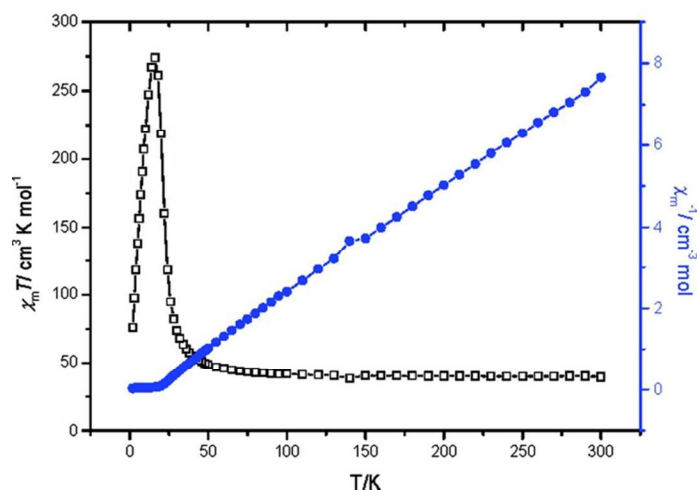


Fig. 24. Plots of the temperature dependence of $\chi_{\text{M}}T$ and χ^{-1} for **34** at 1000 Oe. Adapted from reference 58 with permission.

The crystal structures of the two **35/Ln** analogues (Fig. 25, left) are essentially identical differing mainly in the Ln ion (Ln = Pr, Nd) and also in metric parameters (bond lengths and angles), as expected since they consist of different lanthanide ions and the number of crystallization water molecules.⁵⁸ Their metal core can be described as consisting of two bowl-shaped fragments, each comprising a bowl of Ln_{10} encapsulated in the outer bowl of Ni_9 (Fig. 25, right). The two Ni_9 fragments are linked through three additional Ni(II) ions and bridging NO_3^- and oxalate groups resulting in the formation of a closed-shell structure consisting of an outer

shell of 21 Ni(II) ions encapsulating a Ln₂₀ unit. The Ni^{II} ions of the outer shell in the crystal structures of **35**/Ln are connected through the carboxylate groups of ida²⁻ ions in the anti-syn fashion, similarly to **34**. The Ln^{III} ions are held together through μ_3 -OH⁻ ions, bridging H₂O molecules, and oxalate and NO₃⁻ groups. The μ_3 -OH group bridges one Ni^{II} and two Ln^{III} ions forming one vertex of a distorted cube. The Ni^{II}₂₁ and Ln^{III}₂₀ spheres are linked by bridging ida²⁻ ligands and triply bridging μ_3 -OH⁻ groups forming the dual shell structure of **35**/Ln. Variable temperature DC magnetic susceptibility studies for compounds **35**/Ln revealed the presence of dominant antiferromagnetic exchange interactions between the metal ions that result in non-zero ground state spin values for both complexes.

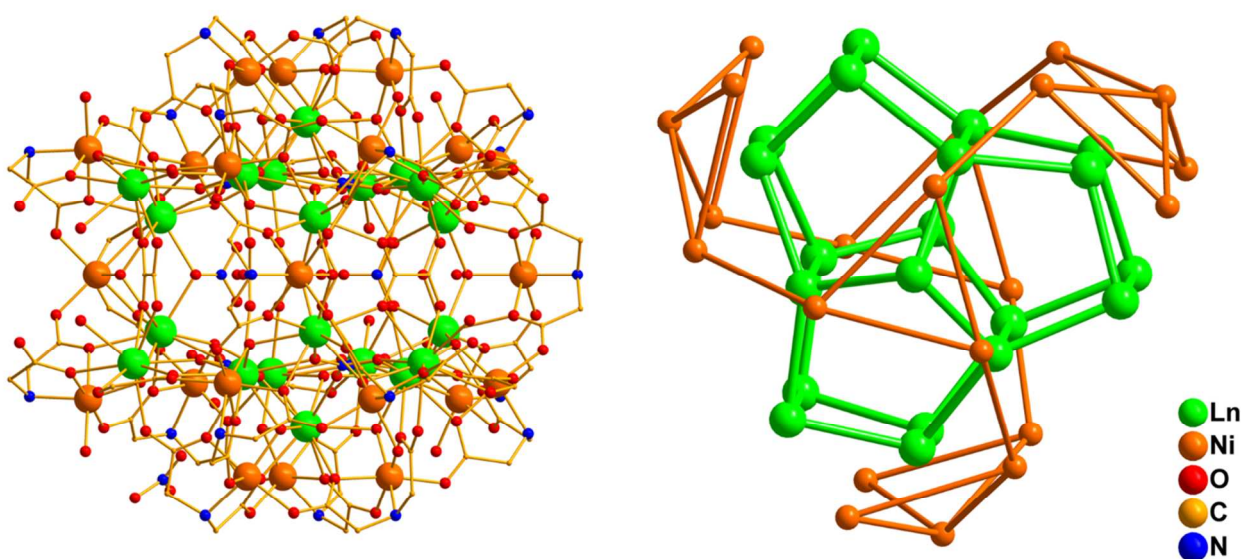


Fig. 25. Representation of the molecular structure (left) and the metallic skeleton (right) of the cation of **35**/Ln.

Since the reaction system that included mixing of Ni(NO₃)₂·6H₂O, Ln(NO₃)₃·6H₂O, H₂ida and NaOH in water afforded high nuclearity complexes with novel structural topologies and geometries, it was further studied in detail. Thus, various alterations in the synthetic

parameters of the reaction system that yielded clusters **34**, **35**/Ln were performed that included use of different Ln ions, different molar ratios, different reaction conditions (e.g. use of ambient reaction conditions instead of hydrothermal ones), etc. The result of these investigations was the isolation of two more giant clusters $[\text{Ni}_{54}\text{Gd}_{54}(\text{OH})_{144}(\text{ida})_{48}(\text{CO}_3)_6(\text{H}_2\text{O})_{25}](\text{NO}_3)_{18}$ (**36**)⁶⁰ and $[\text{Ni}_{76}\text{La}_{60}(\text{OH})_{158}(\text{ida})_{68}(\text{NO}_3)_4(\text{H}_2\text{O})_{44}](\text{NO}_3)_{34}$ (**37**)⁵⁷ which are the two highest nuclearity 3d/4f clusters reported in the literature. Compound **36** was prepared from the reaction of $\text{Ni}(\text{NO}_3)_2 \cdot 6\text{H}_2\text{O}$, $\text{Gd}(\text{NO}_3)_3 \cdot 6\text{H}_2\text{O}$ and H_2ida in water under hydrothermal conditions and consists of 4 shells, thus it can be described as containing a nesting or Russian doll-like configuration (Fig. 26, left). The innermost shell (shell 1) contains 6 Ni^{II} and 2 Gd^{III} ions which are located in the vertices of a cube. The Gd^{III} ions are disposed diagonally and linked through a bridging H_2O molecule. The second shell (shell 2) consists of 20 Gd^{III} ions and is linked to the first shell through $\mu_3\text{-OH}^-$ ions; each OH^- ion bridges two neighboring metal ions (Gd or Ni) from shell 1 within the cube and a Gd^{III} ion located at the edge center of shell 2. The framework of the Gd^{III} ions in shell 2 displays a cubic configuration with 8 of the metal ions being located at the vertices and the remaining lying in the middle of the cube edges. Shell 2 is linked to the two neighbouring shells (1 and 3) through $\mu_3\text{-OH}^-$ ions with those linking shells 2 and 3 coordinated to both the edge and vertex Gd ions of shell 2. Shell 3 consists of 32 Gd^{III} ions that form a cube with two Gd^{III} ions being located on each edge. There are three $\mu_3\text{-OH}$ groups between each pair of edge Gd^{III} ions, one of which bridges an edge Gd^{III} ion in shell 2 with the other two being coordinated to two separate Ni^{II} ions from the outermost shell (shell 4). The latter contains 48 Ni^{II} ions and can be described as a truncated cube with each of its vertex occupied by a triangular Ni^{II}_3 unit and two Ni^{II} ions being located in its edges. The inter-shell connections through the $\mu_3\text{-OH}^-$ ions in **36** result in the formation of a highly compact, brucite-like structure. Its magnetic

properties were investigated and revealed the existence of dominant antiferromagnetic exchange interactions between the metal centres. The $\chi_{\text{M}}T$ value at low temperature is $402.7 \text{ cm}^3 \text{ mol}^{-1} \text{ K}$ suggesting a large ground state spin value for **36**.

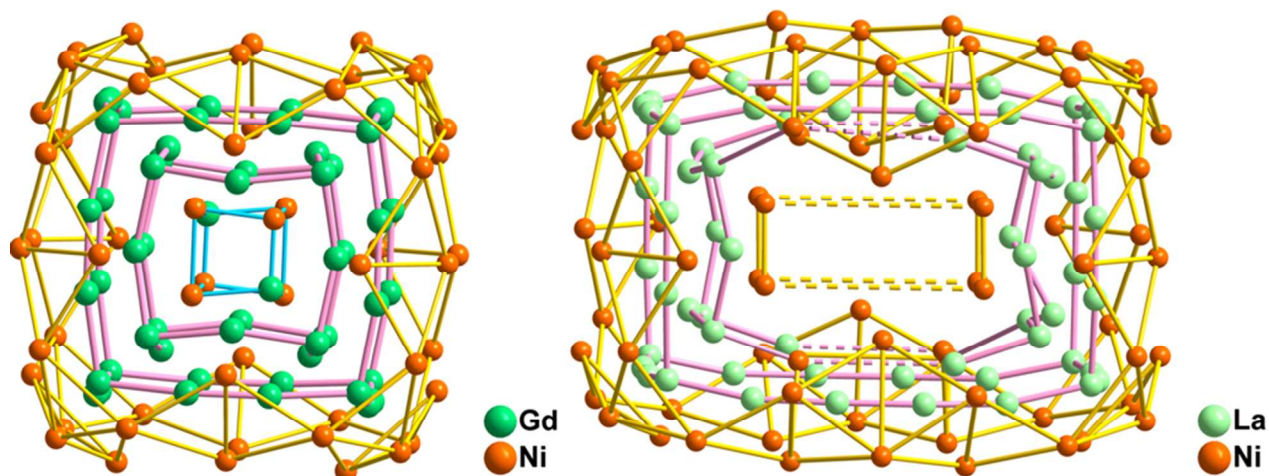


Fig. 26. The metallic skeletons of the cations of **36** (left) and **37** (right) from views that emphasize their four-shell nesting doll-like structure. The solid and dashed lines connecting the metal ions are to emphasize the structure topology of each shell and the overall structure.

Compound **37** was prepared from the reaction of $\text{Ni}(\text{NO}_3)_2 \cdot 6\text{H}_2\text{O}$, $\text{La}(\text{NO}_3)_3 \cdot 6\text{H}_2\text{O}$ and H_2id in the presence of NaOH in water under ambient pressure conditions (the reaction mixture was refluxed) and contains 136 metal ions organized in 4 distinct shells (Fig. 26, right). Thus, its crystal structure can be viewed as an elongation along one of the axes of the cube-shaped cluster **36**. The innermost shell (shell 1) contains 8 pentacoordinate Ni^{II} ions bridged only through $\mu_3\text{-OH}^-$ ions which also link them to neighbouring La^{III} and Ni^{II} ions of shell 2. The latter contains a La_2Ni_4 unit in a rectangular parallelepiped configuration with dimensions $7.8 \times 7.8 \times 15.3 \text{ \AA}^3$. The two opposite faces of the rectangular parallelepiped consist of 8 $\text{La}(\text{III})$ ions, whereas its four longer edges consist of one $\text{Ni}(\text{II})$ and one $\text{La}(\text{III})$ ion that connect the opposite faces,

completing the core structure. The coordination sphere of the La^{III} ions located in the vertices is completed through $\mu_3\text{-OH}^-$ ions which also connect metal ions of shell 2 with metal ions of the two neighbouring shells. The Ni^{II} ions are tetracoordinate and their coordination sphere is completed through 3 $\mu_3\text{-OH}^-$ ions and one carboxylate O atom from a ida^{2-} ligand. The third shell consists of 40 La^{III} ions which form a rectangular parallelepiped of dimensions 12.0 x 12.0 x 19.8 Å³. Six triply-bridging OH^- ions and 3 carboxylate O atoms from different ida^{2-} ligands connect the La^{III} ions of the vertices with one La^{III} ion of shell 2, 3 La^{III} ions of shell 3, and 3 Ni^{II} ions of shell 4. The latter contains 64 Ni^{II} ions in a truncated rectangular parallelepiped configuration; the vertices of the parallelepiped are occupied by triangular Ni_3^{II} units, whereas each of its shorter and longer edges is occupied by 2 and 6 Ni^{II} ions, accordingly. Compound **37** is the highest nuclearity 3d-4f cluster reported to date. Magnetism studies revealed the existence of weak ferromagnetic exchange interactions between the paramagnetic Ni^{II} ions.

The cationic clusters $[\text{Ni}_{12}\text{Gd}_{36}\text{O}_6(\text{OH})_{84}(\text{CH}_3\text{CO}_2)_{18}(\text{H}_2\text{O})_{54}(\text{NO}_3)\text{Cl}_2](\text{NO}_3)_6\text{Cl}_9$ (**38**)³⁰ $[\text{M}_{10}\text{Ln}_{42}(\text{OH})_{68}(\text{CO}_3)_{12}(\text{CH}_3\text{CO}_2)_{30}(\text{H}_2\text{O})_{70}] \cdot (\text{ClO}_4)_x$ [**39**/Ln: M = Ni, Ln = Gd, Dy, x = 24; **40**/Ln: M = Co, Ln = Gd, Dy, x = 25)²² were isolated from reactions that involved use of acetate as the only organic ligand. The crystal structure of **38** (Fig. 27) consists of 36 Gd^{III} and 12 Ni^{II} ions that are held together through 84 triply bridging OH^- and 6 $\mu_4\text{-O}^{2-}$ ions. The peripheral ligation is completed by 54 H_2O molecules, 18 acetate ligands, one NO_3^- and two Cl^- ions. The metal ions adopt a tubular arrangement that is very rare in metal cluster chemistry. The $\{\text{Ni}_{12}\text{Gd}_{36}(\mu_3\text{-OH})_{84}(\mu_4\text{-O})_6\}^{36+}$ structural core can be described as a “sandwich” of two different kinds of cluster wheels. The two external layers are 18-metal hexagonal wheels based on six vertex-sharing cubic $\{\text{NiGd}_3(\mu_3\text{-OH})_4\}^{7+}$ units. The inner layer is a 24-metal hexagonal wheel $\{\text{Gd}_{24}(\mu_4\text{-O})_6(\mu_3\text{-OH})_{36}\}^{24+}$ constructed from six $\{\text{Gd}_5(\mu_4\text{-O})(\mu_3\text{-OH})_4\}^{9+}$ units joined together

with two identical neighbours by sharing two basal Gd atoms of the roughly square-pyramidal fragment. The three layers are connected by sharing 6 Gd^{III} ions of adjacent wheels forming the

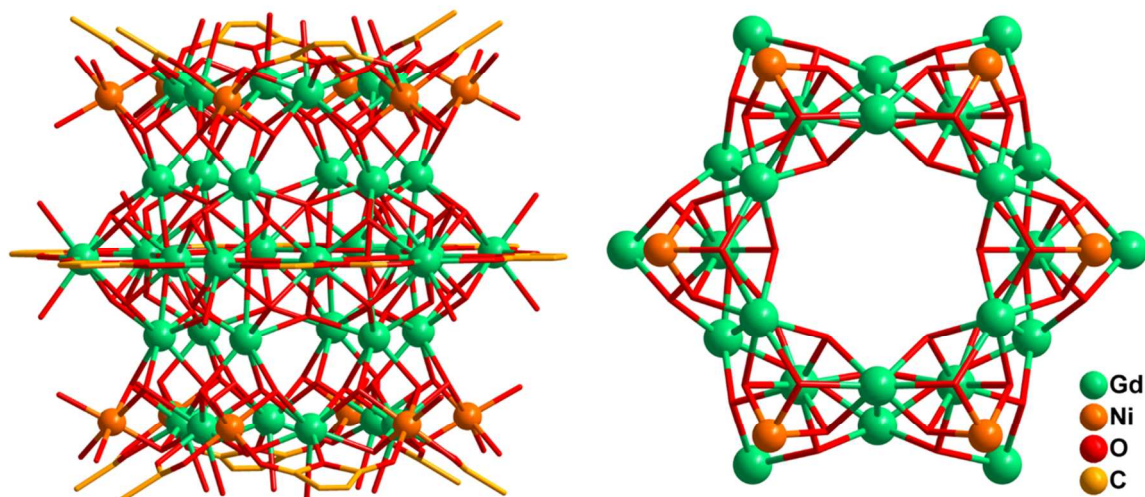


Fig. 27. Representation of the molecular structure of the cation of **38** (left) and its structural core (right).

tube-like core of **38**. This compound displays remarkably large MCE ($-\Delta S_m = 36.3 \text{ J kg}^{-1} \text{ K}^{-1}$ at 3 K for $\Delta H = 7 \text{ T}$) (Fig. 28), which may be attributed to the large metal/ligand mass ratio and the

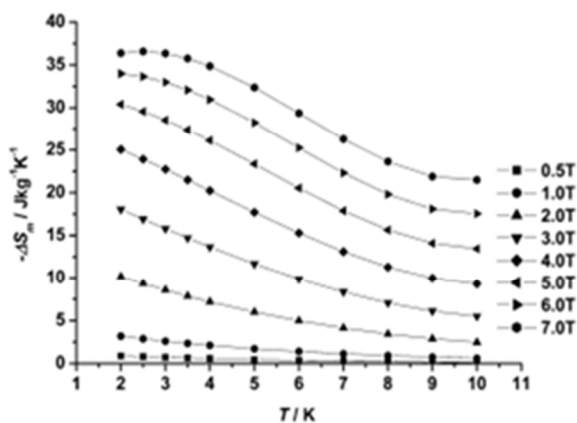


Fig. 28. Magnetic entropy changes ($-\Delta S_m$) vs T for **38** as obtained from magnetization data at various fields and temperatures. Adapted from reference 30 with permission.

use of low molecular weight ligands. Thus, complex **38** could have great potential for use in magnetic cooling applications.

Clusters **39/Ln** and **40/Ln** are nearly identical differing only in the 3d metal ions they contain (Ni in case of **39/Ln** and Co in **40/Ln**) and the number of ClO_4^- counterions that balance the metal ion charges in the crystal structures.²² In particular, in complexes **39/Ln** there are 24 ClO_4^- ions, whereas in **40/Ln** 25 ClO_4^- ions. This happens because **39/Ln** consists of only divalent Ni^{2+} ions whereas in **40/Ln** apart from Co^{2+} there is also one Co^{3+} ion. Thus, only the crystal structure of the representative cluster **39/Gd** will be described here. It consists of 10 Ni^{II} and 42 Gd^{III} ions that are held together through $\mu_3\text{-OH}^-$, CH_3CO_2^- and CO_3^{2-} bridges with the latter coming from the atmospheric CO_2 . The structure contains a bowl-like cationic core $\{\text{Ni}_{10}\text{Gd}_{42}(\mu_3\text{-OH})_{68}(\text{CO}_3)_{12}\}^{54+}$ (Fig. 29, top) which is constructed from three different types of building units (A, B, and C, Fig. 29, bottom). Type A contains one $\{\text{Gd}_5(\mu_3\text{-OH})_5\}^{10+}$ square pyramid and one cubane-like $\{\text{Gd}_4(\mu_3\text{-OH})_4\}^{8+}$ unit that share one common Gd^{3+} vertex forming a $\{\text{Gd}_8(\mu_3\text{-OH})_9\}^{15+}$ unit. Type B consists of two distorted cubane-like $\{\text{NiGd}_3(\mu_3\text{-OH})_4\}^{7+}$ units and one cuboidal $\{\text{Gd}_3(\mu_3\text{-OH})_4\}^{5+}$ unit sharing three Gd^{3+} vertices and constructing a $\{\text{Ni}_2\text{Gd}_6(\mu_3\text{-OH})_{12}\}^{10+}$ subunit. Type C can be described as a distorted tetrahedron $\{\text{Ni}_4(\mu_3\text{-OH})(\text{CO}_3)_3\}^+$ displaying a $\mu_3\text{-OH}$ capped trimetallic basal plane with each of its three metal ions connected to the fourth one through a bridging CO_3^{2-} ion. Three type-A and three type-B units are joined together alternately through nine CO_3^{2-} and one $\mu_3\text{-OH}^-$ ions, constructing the bowl-like $\{\text{Ni}_6\text{Gd}_{42}(\mu_3\text{-OH})_{64}(\text{CO}_3)_9\}^{56+}$ core in the center of which is located one type-C unit which is held to the main body of the cage through CO_3^{2-} ligands. The magnetic properties of **39/Ln** and **40/Ln** were studied and revealed that the Dy^{III} containing clusters display slow relaxation of

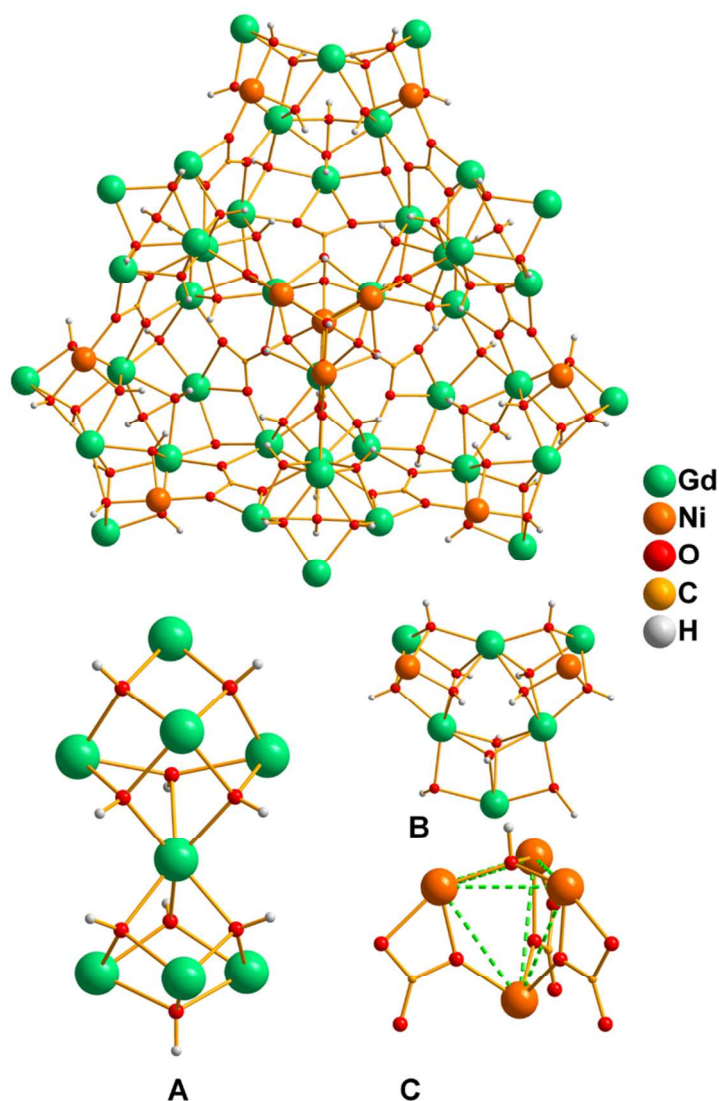


Fig. 29. Representations of the structural core of the cation of **39/Gd** (top) and its three structural subunits (type A: $\{\text{Gd}_8(\mu_3\text{-OH})_9\}^{15+}$, type B: $\{\text{Ni}_2\text{Gd}_6(\mu_3\text{-OH})_{12}\}^{10+}$ and type C: $\{\text{Ni}_4(\mu_3\text{-OH})(\text{CO}_3)_3\}^+$) (bottom).

magnetization albeit with a small energy barrier (Fig. 30). On the other hand the Gd^{III} containing clusters possess large MCE ($-\Delta S_{\text{m}}=38.2 \text{ J kg}^{-1} \text{ K}^{-1}$ at 2 K for $\Delta H=7 \text{ T}$, **39/Gd**; $-\Delta S_{\text{m}}=41.26 \text{ J kg}^{-1} \text{ K}^{-1}$ at 2 K for $\Delta H=7 \text{ T}$, **40/Gd**) (Fig. 31) which may be attributed to the large metal/ligand ratio,

as in the case of **38**. Thus, these species could also be valuable for the development of magnetic cooling technology.

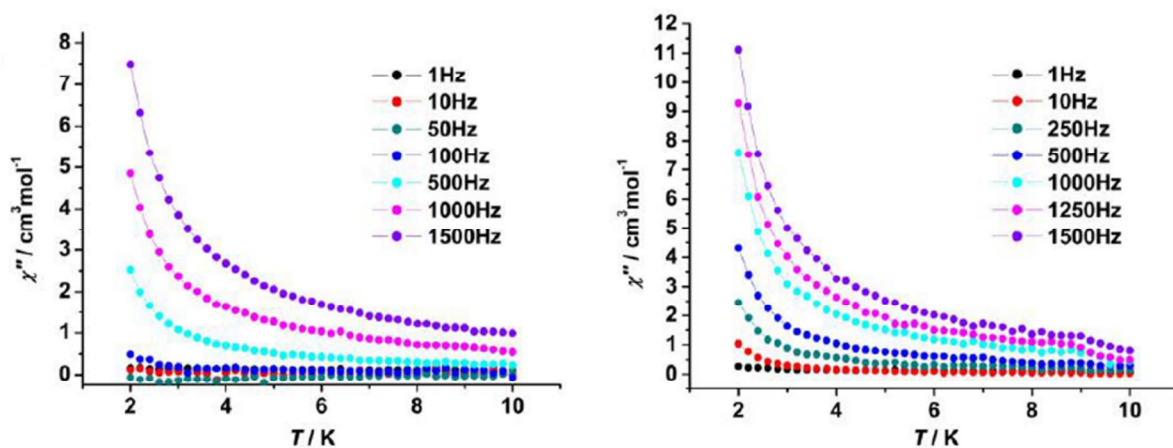


Fig. 30. Plots of the out-of-phase ac susceptibility (χ''_M) signals as χ''_M vs T for **39/Dy** (left) and **40/Dy** (right) oscillating at the indicated frequencies. Adapted from reference 22 with permission.

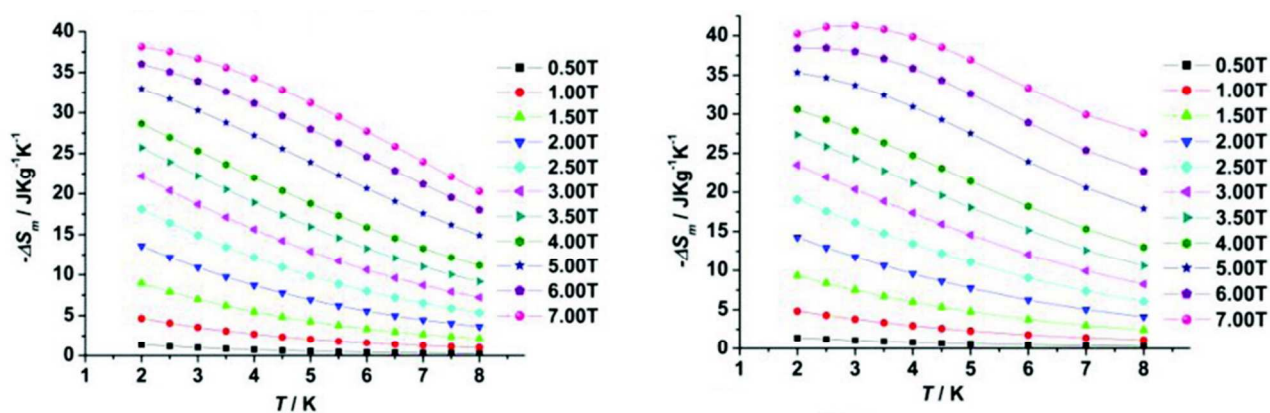


Fig. 31. Magnetic entropy changes ($-\Delta S_m$) vs T for **39/Gd** (left) and **40/Gd** (right) as obtained from magnetization data at various fields (0.5–7 T) and temperatures (2–8 K). Adapted from reference 22 with permission.

Recently, the synthesis and characterization of two new wheel - shaped clusters $[\text{Co}_{16}\text{Ln}_{24}(\text{OH})_{50}(\text{pyacac})_{16}(\text{NO}_3)_{18}(\text{H}_2\text{O})_{12}][\text{Ln}(\text{H}_2\text{O})_8]_2(\text{NO}_3)_{16}(\text{OH})_{10}$ (**41**/Ln, Ln = Dy, Gd), where Hpyacac is 1,3-di(2-pyridyl)-1,3-propanedione, were reported. Compounds **41**/Ln were prepared from reactions of $\text{Co}(\text{NO}_3)_2 \cdot 6\text{H}_2\text{O}$ and $\text{Ln}(\text{NO}_3)_3 \cdot 6\text{H}_2\text{O}$ (Ln = Dy or Gd) with Hpyacac in the presence of NEt_3 in MeOH.²⁹ Compounds **41**/Ln are nearly isostructural containing a $\{\text{Co}_{16}\text{Ln}_{24}\}$ core constructed from a $\{\text{Ln}_{24}\}$ super-square unit and a $\{\text{Co}_{16}\}$ octagonal prism (Fig. 32, top). The super-square fragment contains two kinds of subunits (A and B) with the type A units acting as edges and the type B ones as vertices (Fig. 32, bottom-a,b). Subunit A formulated as $\{\text{Ln}_4(\mu_3\text{-OH})_2(\mu\text{-O})_5\}$ displays a “butterfly” conformation with the two $\mu_3\text{-OH}^-$ ions located at the same side of the Ln_4 plane forming a “cis-butterfly” structural motif. Subunit B is the tetranuclear fragment $\{\text{Ln}_4(\mu_3\text{-OH})_2(\mu\text{-O})_5\}$ which forms a distorted tetrahedron. Four subunits A are connected with four subunits B to form the super-square $\{\text{Ln}_{24}\}$ fragment through sharing Ln^{III} vertices. Four Co^{II} ions are located at the four corresponding sides of each subunit of type B and are linked to the neighbouring Ln^{III} ions through a $\mu_3\text{-OH}^-$ ion and two O atoms of pyacac⁻ ligands (Fig. 32, bottom-c). All the pyacac⁻ ligands in **41**/Ln adopt the $\eta^1:\eta^2:\eta^2:\eta^1:\mu_3$ coordination mode. The super-square unit is encapsulated in the flat octagonal prismatic fragment constructed from the 16 Co^{II} ions forming the $\{\text{Co}_{16}\text{Ln}_{24}\}$ metal cluster. Magnetism studies revealed the existence of competing ferromagnetic and antiferromagnetic exchange interactions for both complexes. DC and AC magnetic susceptibility studies were performed for **41**/Gd and **41**/Dy and revealed the existence of competing ferromagnetic and antiferromagnetic interactions, as well as possible SMM behaviour for **41**/Dy. In addition, **41**/Gd displays large MCE ($-\Delta S_m = 26.0 \text{ J kg}^{-1} \text{ K}^{-1}$ at 3.8 K and $\Delta H=7 \text{ T}$), thus it is a potential candidate for use in low temperature magnetic cooling processes.

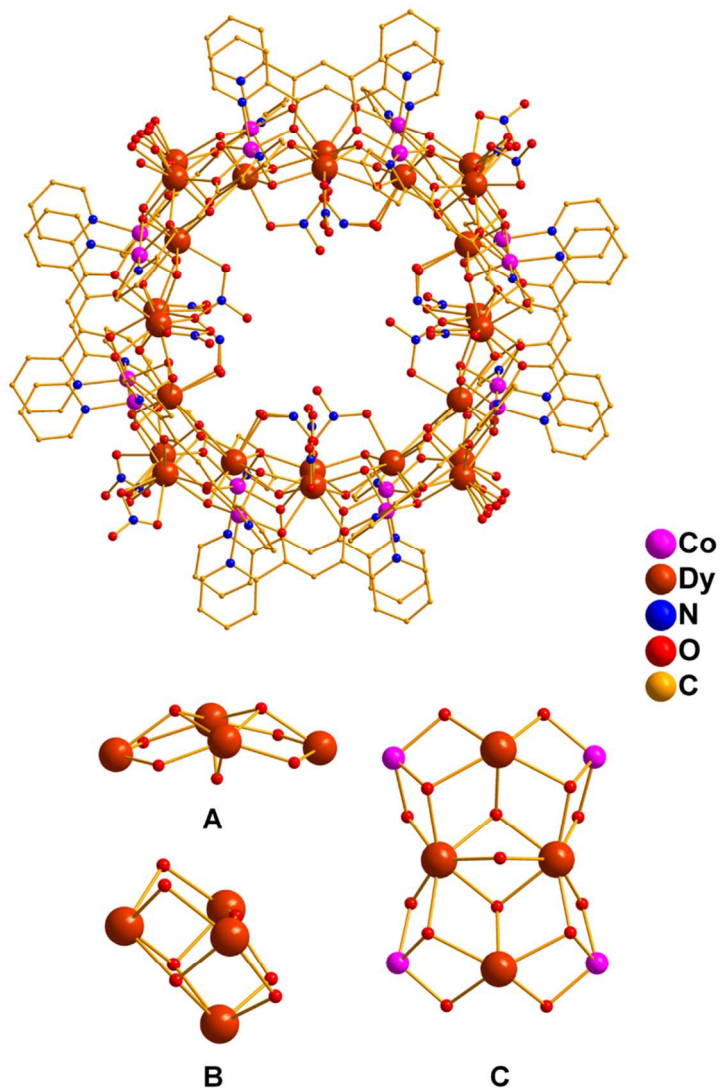


Fig. 32. The molecular structure of the $\text{Co}^{\text{II}}_{16}\text{Dy}_{24}$ cation of **41/Dy** (top) and its structural subunits (bottom).

8.2. *Cu/Ln clusters*

Indisputably one of the most important sub-categories of giant 3d/4f compounds, together with the family of Ni/4f complexes discussed above, is that of the Cu/4f clusters. One method that has afforded several giant complexes involves the use of various amino acids such as glycine

(Hgly), L-alanine (Hala), 2-methylalanine (Hmala), L-proline (Hpro) in Cu/4f chemistry. This synthetic method has led to the isolation of a large family of related $\text{Cu}_{24}\text{Ln}_6$ ($\text{Ln} = \text{Tb, Gd, Sm, La, Dy}$) species.^{51,52} A series of compounds formulated as $[\text{Cu}_{24}\text{Ln}_6(\text{OH})_{30}(\text{ala})_{12}(\text{CH}_3\text{CO}_2)_6(\text{ClO}_4)(\text{H}_2\text{O})_{12}](\text{ClO}_4)_{10}(\text{OH})_7$ (**42**/Ln) ($\text{Ln} = \text{Tb, Gd, Sm}$ and La) were prepared from the use of Hala and, in particular, from the reaction of $\text{Cu}(\text{ClO}_4)_2 \cdot 6\text{H}_2\text{O}$, $\text{Ln}(\text{ClO}_4)_3 \cdot 6\text{H}_2\text{O}$, Hala and $\text{CH}_3\text{CO}_2\text{Na} \cdot 3\text{H}_2\text{O}$ in a 6 : 1 : 1 : 4 molar ratio in H_2O .^{51a} The molecular structure of the Tb analogue (**42**/Tb) (Fig. 33, left), the only member of this family that was crystallographically characterized, will be described below and will be compared with the structures of related compounds that contain other amino acids. The six Tb^{III} ions of **42**/Tb construct an octahedron with twelve Cu^{II} ions located in the middle of its edges. There are twelve additional Cu^{II} ions located in the outer sphere of the octahedron; each Tb^{III} ion is linked to two such Cu^{II} ions through one $\mu_3\text{-OH}^-$ group and two ala ligands (Fig. 33, right). The surfaces of the octahedron are composed of three Tb^{III} and three Cu^{II} ions linked by three $\mu_3\text{-OH}^-$ ions. The dimensions of the resulting cage are $2.38 \times 2.38 \times 2.38 \text{ nm}^3$. The coordination sphere of each Tb^{III} ion is completed by 5 $\mu_3\text{-OH}^-$ ions, 2 carboxylate O atoms and 2 H_2O molecules resulting in a monocapped square antiprismatic geometry. The inner Cu^{II} ions display a slightly distorted six-coordinated octahedral configuration with four $\mu_3\text{-OH}^-$ ions located in the equatorial positions, and two O atoms (one from one ClO_4^- and one from the CH_3CO_2^- ions) in the apical ones. The twelve outer Cu^{II} ions are four-coordinated displaying square planar coordination geometry with each one linked to three O and one N donor atoms, although two additional O atoms from H_2O molecules weakly interact with these Cu^{II} ions ($\text{Cu} \cdots \text{O}$ distances $\sim 2.5 \text{ \AA}$) and thus their geometry can be considered as pseudo-octahedral. One ClO_4^- ion is encapsulated in the octahedral cage, possibly acting as template for the formation of the compound. The ala⁻ ligands

in **42**/Ln adopt the $\eta^1:\eta^2:\eta^1:\mu_3$ coordination mode. DC magnetic susceptibility measurements revealed that the $\chi_M T$ value at 300 K is $\sim 73 \text{ cm}^3 \text{ mol}^{-1} \text{ K}$

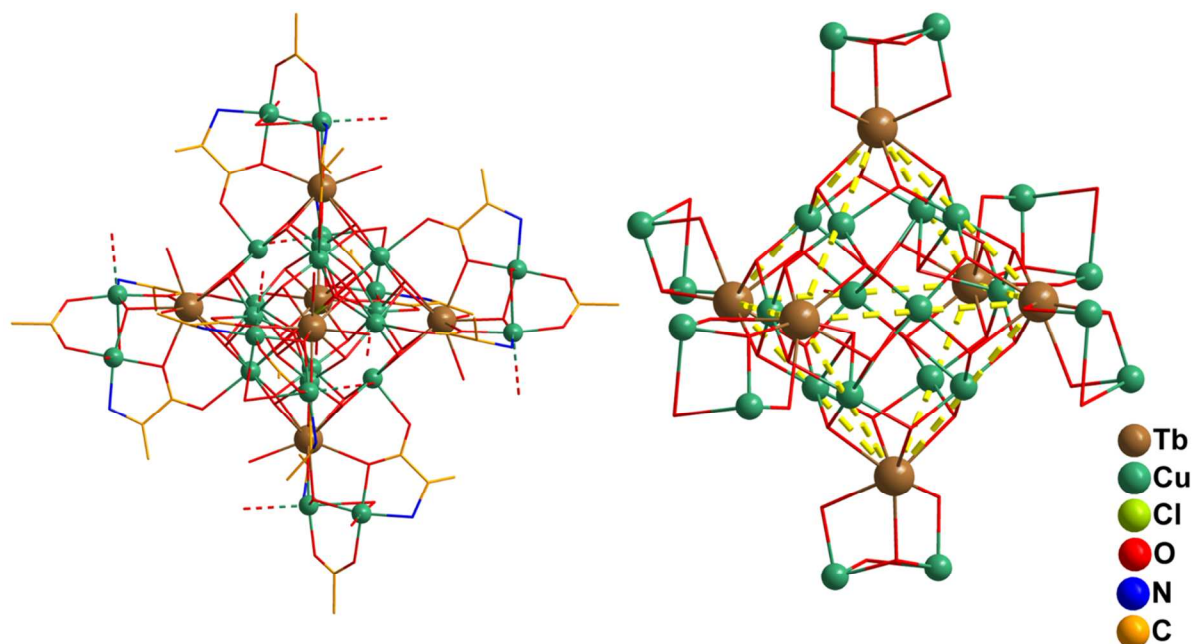


Fig. 33. Representation of the molecular structure of the cation of **42**/Tb (left) and its structural core (right). The yellow dashed lines emphasize the octahedron formed by the Tb^{III} ions.

and remains essentially constant down to 20 K and then sharply decreases to $\sim 60 \text{ cm}^3 \text{ mol}^{-1} \text{ K}$ at 5 K indicating the presence of dominant ferromagnetic interactions between the metal ions of **42**/Tb. A similar magnetic behaviour was also observed for the Gd-analogue (**42**/Gd) where the $\chi_M T$ value remains almost constant at $\sim 56 \text{ cm}^3 \text{ mol}^{-1} \text{ K}$ down to 75 K, where it begins to increase smoothly until it reaches a maximum of $\sim 68 \text{ cm}^3 \text{ mol}^{-1} \text{ K}$ at around 5 K. This behavior was attributed to the presence of dominant ferromagnetic exchange interactions between the Cu^{II} and Gd^{III} ions leading to an appreciable spin ground state for **42**/Gd (the low T $\chi_M T$ value corresponds to $S = 11$). Interestingly, in the case of the **42**/La and **42**/Sm the magnetic behavior was entirely different since the $\chi_M T$ values continuously decrease with decreasing T from 300 to 5 K, suggesting the presence of dominant antiferromagnetic exchange interactions between the

metal ions. Another $\text{Cu}_{24}\text{Ln}_6$ analogue of **42**/Ln that was reported recently (in 2014) is $\text{Na}[\text{Cu}_{24}\text{Ln}_6(\text{OH})_{30}(\text{ala})_{12}(\text{CH}_3\text{CO}_2)_6(\text{NO}_3)_4(\text{H}_2\text{O})_{20}] (\text{NO}_3)_8(\text{OH})_7$ (**43**/Ln; Ln = Gd, Dy).^{51b} The main differences between **43**/Ln and **42**/Ln include: (i) the presence of a Na^+ ion in the former; (ii) different type and number of ligated and lattice counter-anions (NO_3^- in **43**/Ln, ClO_4^- in **43**/Ln); and (iii) different coordination numbers and geometries of the constituent metal ions of the two compounds. In addition, in the case of **42**/Ln the $\text{Cu}_{24}\text{Dy}_6$ analogue had not been reported. DC magnetic susceptibility studies revealed that **43**/Gd displays a very similar behavior to **42**/Gd, i.e. weak ferromagnetic exchange interactions and a large spin ground state value. In addition, it displays a significant MCE with the maximum entropy change value $-\Delta S_m = 21.2 \text{ J kg}^{-1} \text{ K}^{-1}$ obtained at 2.5 K for $\Delta H = 7 \text{ T}$. AC studies revealed that **43**/Dy displays out-of-phase ac signals, the maxima of which could not be seen in the absence of a DC field. When a 5000 Oe DC field was applied, the peak maxima of the out-of-phase signals were observed and the data were fitted to the Arrhenius equation providing the energy barrier U_{eff} (34 K) and the pre-exponential factor τ_0 ($8.16 \times 10^{-7} \text{ s}$) (Fig. 34).

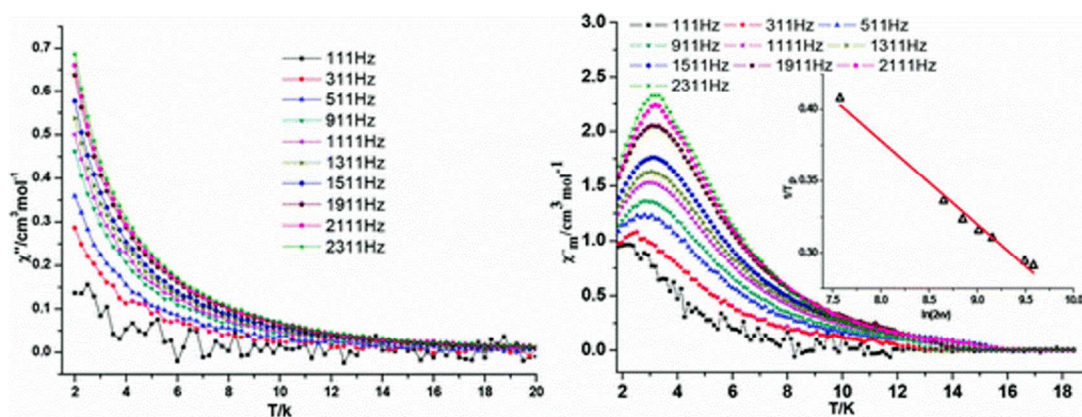


Fig. 34. The temperature dependence of the out-of-phase (χ''_M) ac susceptibility at the indicated frequencies for **43**/Dy under a zero dc field (left) and 5000 Oe (right). The inset of the

right figure is the Arrhenius plot for **43**/Dy; the solid line is the best fit of the data to the Arrhenius equation (see text for details). Adapted from reference 51b with permission.

When the reaction that led to **42**/Sm was repeated with the use of Hgly instead of Hala a compound similar to **42** was isolated, formulated as $[\text{Cu}_{24}\text{Sm}_6(\text{OH})_{30}(\text{gly})_{12}(\text{CH}_3\text{CO}_2)_{12}(\text{ClO}_4)(\text{H}_2\text{O})_{16}](\text{ClO}_4)_9(\text{OH})_2$ (**44**).^{51a} Compound **44** has the same metal core topology and overall is very similar to **42**/Tb with the main differences being the different amino acid and the number of CH_3CO_2^- ligands (**44** contains 12 CH_3CO_2^- whereas **42**/Tb only 6).

Since the use of amino acids in Cu/4f cluster chemistry afforded giant metal clusters with beautiful crystal structures, various modifications in the reaction mixtures were performed. These modifications involved use of different reagent ratios, reaction conditions, etc. Several other compounds were obtained from this reaction system, with crystal structures related to those of **42**/Tb and **44** discussed above. One such example is compound $\text{Na}_4[\text{Cu}_{26}\text{Tb}_6(\text{OH})_{30}(\text{gly})_{18}(\text{ClO}_4)(\text{H}_2\text{O})_{22}](\text{ClO}_4)_{25}$ (**45**)⁵² which is related to the two compounds discussed above since it consists of a $\text{Tb}_6\text{Cu}_{24}$ subunit, very similar to the one appearing in **42** and **44**, linked to two $\{\text{Cu}(\text{gly})(\text{H}_2\text{O})_2\}^+$ fragments. The use of the amino acid Hmala in similar reactions to those that afforded **42**, **44** and **45** resulted in compound $[\text{Cu}_{24}\text{Gd}_6(\text{OH})_{30}(\text{mala})_{16}(\text{ClO}_4)(\text{H}_2\text{O})_{22}](\text{ClO}_4)_{17}(\text{OH})_2$ (**46**), which possesses an analogous structural core to those of the other $\text{Cu}_{24}\text{Ln}_6$ clusters. Employment of the amino acid Hpro in Cu/4f cluster chemistry led to compound $\{[\text{Cu}_{24}\text{Ln}_6(\text{OH})_{30}(\text{pro})_{12}(\text{CH}_3\text{CO}_2)_6(\text{ClO}_4)(\text{H}_2\text{O})_{13}]_2\text{Cu}(\text{pro})_2\}(\text{ClO}_4)_{18}(\text{OH})_{16}$ (**47**/Ln, Ln = Sm, Gd), one of the larger 3d/4f metal clusters. Compounds **47**/Ln consist of two $\text{Cu}_{24}\text{Ln}_6$ units linked

through a Cu(pro)₂ mononuclear subunit. Clearly, the Cu/4f/amino acid reaction system has been proven one of the most fruitful sources of giant species.

The combination of carboxylate and phosphonate ligands in Cu/4f coordination chemistry has provided access to two new giant species, namely [H₃O][Cu₂₄Dy₈(OH)₄₂(Ph₃C-PO₃)₆(Ph₃C-PO₃H)₆(CH₃CO₂)₁₂(CH₃CO₂H)₆(NO₃)(H₂O)₆] (**48**) and [(Me₄N)₂K₂][Cu₂₄Gd₈(OH)₄₂(Ph₃C-PO₃)₆(Ph₃C-PO₃H)₆(CH₃CO₂)₁₂(CH₃CO₂H)₁₂(NO₃)](OH)₃ (**49**). Both compounds were obtained from the reaction of Ln(NO₃)₃·xH₂O (Ln = Dy or Gd), Cu(CH₃CO₂)₂·H₂O and tritylphosphonic acid in the presence of base.²⁰ They display related crystal structures differing mainly in the nature of the counterions and terminal ligands, thus only one of them will be described below. The crystal structure of compound **48** consists of a Dy^{III}₈ cube which encapsulates a cuboctahedron constructed from 12 Cu^{II} ions (Fig. 35). There are also 12 outer Cu^{II} ions that are divided into 6 dimers with each dimer capping one square face of the Dy^{III} cube. In addition, each Dy^{III} caps a triangular face of the cuboctahedral fragment forming a Cu₃Dy tetrahedron. The metal sites in the Cu₂ dimers are held together through one hydroxy and one phosphonate bridges and are connected to the Cu₁₂Dy₈ core through one acetate and two phosphonate bridges. The twelve inner Cu^{II} ions are connected by one NO₃⁻ and twenty four OH⁻ bridging ligands. The coordination sphere of the metal centers is completed by 12 phosphonate ions (6 of them being monoanionic and 6 dianionic), and 12 acetate ions and 6 acetic molecules. Phosphonate ligands adopt the η¹:η¹:η¹:μ₃ and η¹:η¹:μ coordination modes in **48**. Magnetism studies revealed that compound **48** is a SMM, albeit with a very small energy barrier ($U_{\text{eff}} = 4.6$ K). This was confirmed by magnetization versus dc field scans on a single crystal of **48**, which revealed the existence of hysteresis loops the coercivity of which increases with decreasing temperature (Fig. 36) and increasing scan rates.

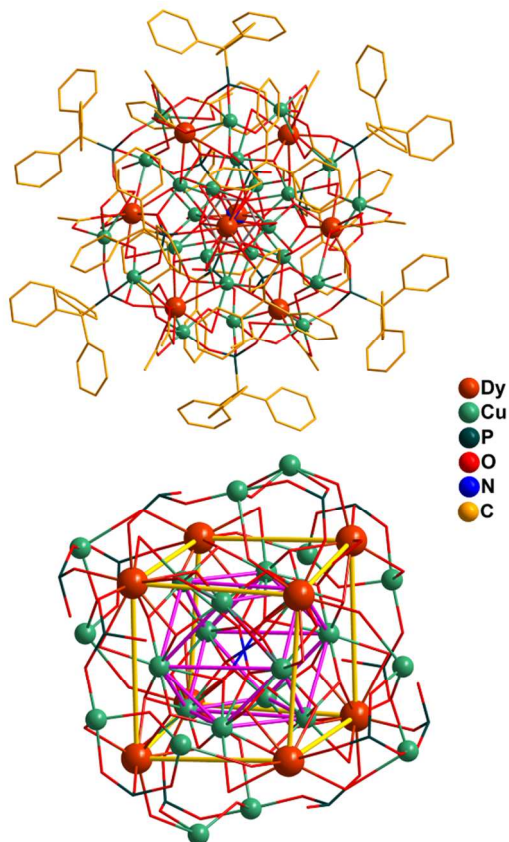


Fig. 35. Representation of the molecular structure (top) and the structural core (bottom) of the anion of **48**. The yellow and purple solid lines in the bottom figure are to emphasize the Dy₈ cubic and Cu₁₂ cuboctahedral subunits; see text for details.

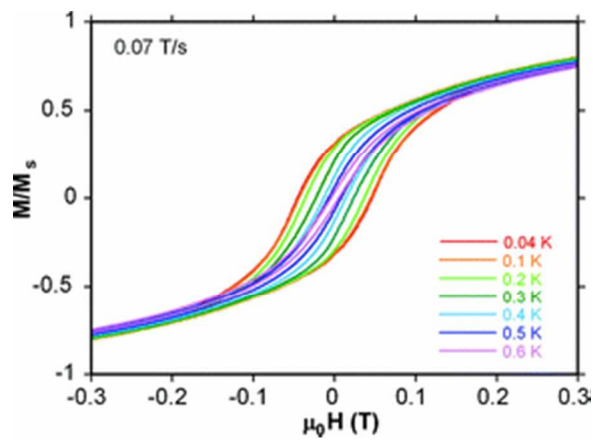


Fig. 36. Hysteresis loops for **48** measured at 0.04 to 0.6 K. Adaped from reference 20 with permission.

The employment of carboxylate ions in the absence of other organic (chelating or bridging) ligands in Cu/4f coordination chemistry has provided access to a family of giant heterometallic species possessing a fascinating crystal structure. Thus, compounds $[\text{Cu}_{36}\text{Ln}_{24}(\text{OH})_{72}(\text{NO}_3)_6(\text{PhCO}_2)_{60}(\text{MeOH})_m(\text{H}_2\text{O})_n](\text{NO}_3)_6$ (Ln = Dy, $m = 14$, $n = 0$ **50**/Dy; Ln = Gd, $m = 6$, $n = 12$, **50**/Gd).²¹ The two compounds were prepared from the reaction of $\text{Cu}(\text{NO}_3)_2 \cdot 3\text{H}_2\text{O}$ and $\text{Ln}(\text{NO}_3)_3 \cdot 6\text{H}_2\text{O}$ (Ln = Dy or Gd) with PhCO_2H and NEt_3 in MeCN/MeOH. The two members of this family are essentially isostructural and thus only the structure of **50**/Dy will be discussed in detail. The molecular structure of **50**/Dy (Fig. 37, top) consists of a $\text{Cu}^{\text{II}}_{36}\text{Dy}^{\text{III}}_{24}$ ring with hexagonal configuration based on two different kinds of alternating building units; the first one is a cubane-like $\{\text{Dy}_4(\text{OH})_4\}$ unit (Fig. 37, bottom) whereas the second consists of six Cu^{II} sites held together through eight OH^- and one NO_3^- ions displaying a “boat”-like conformation (Fig. 37, bottom). The neighbouring units are linked by 3 $\mu_3\text{-OH}^-$ ions forming the $\text{Cu}^{\text{II}}_{36}\text{Ln}^{\text{III}}_{24}$ ring. The coordination spheres of the metal ions are completed by 60 PhCO_2^- groups in the common *syn, syn*, μ -bridging mode and 14 terminal MeOH molecules. The hexagonal ring possesses a diagonal dimension of ~ 4.6 nm, a height (referring to the height of the hexagon) of ~ 4.2 nm, a thickness of ~ 1.8 nm and a central hole with a diameter of ~ 0.8 nm. Magnetism studies revealed the existence of dominant antiferromagnetic exchange interactions between the metal ions in both **50**/Gd and **50**/Dy and frequency dependent out-of-phase ac signals below 4 K indicative of slow relaxation of the magnetization in **50**/Dy. In addition, **50**/Gd displays large MCE ($-\Delta S_m = 21 \text{ J kg}^{-1} \text{ K}^{-1}$ at 2.1 K for $\Delta H = 7 \text{ T}$), although smaller than that of other reported compounds.²¹

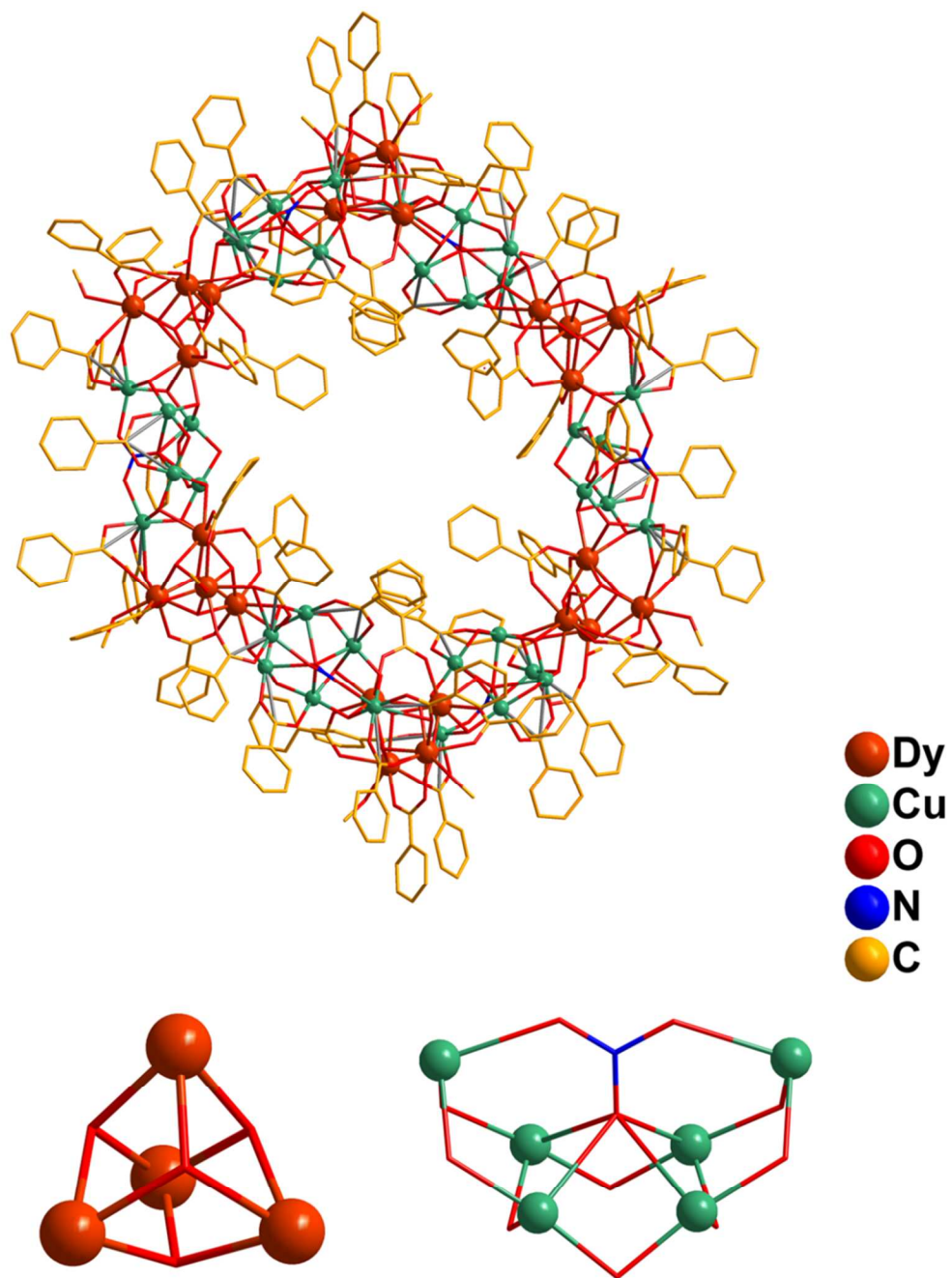


Fig. 37. Representation of the molecular structure of the cation of **50/Dy** (top), and the structural core of its cubic (bottom, left) and boat-like (bottom, right) subunits.

Table 1

Chemical formulae and magnetic properties of paramagnetic 3d and 3d/4f metal clusters in moderate oxidation states with nuclearities of 30 and greater.^a

No	Complex	Magnetic Properties	Ref.
1	[Mn ₃₀ O ₂₄ (OH) ₈ ((CH ₃) ₃ CCH ₂ CO ₂) ₃₂ (H ₂ O) ₂ (CH ₃ NO ₂) ₄]	dominant AF; <i>S</i> = 5; SMM; <i>U</i> _{eff} = 15 K	4
2	[Mn ₈₄ O ₇₂ (OH) ₆ (CH ₃ CO ₂) ₇₈ (OMe) ₂₄ (MeOH) ₁₂ (H ₂ O) ₄₂]	dominant AF; <i>S</i> = 6; SMM; <i>U</i> _{eff} = 18 K	11
3	{Mn(bpy) ₃ } _{1.5} [Mn ₃₂ (thme) ₁₆ (bpy) ₂₄ (N ₃) ₁₂ (CH ₃ CO ₂) ₁₂](ClO ₄) ₁₁ ^{1,2}	dominant AF; <i>S</i> = 9 or 10	69
4	[Mn ₃₂ O ₈ (OH) ₆ (Me-sao) ₁₄ (CH ₃ CO ₂) ₁₈ Br ₈ (H ₂ O) ₁₀](OH) ₂ ³	competing F and AF; SMM; <i>U</i> _{eff} = 44.5 K	23
5	[Mn ₃₂ O ₁₄ (OH) ₂₄ (OMe) ₆ ((CH ₃) ₃ CCO ₂) ₂₄ (H ₂ O) _{2.6}]	dominant AF; <i>S</i> = 5; possible SMM	24
6	[Mn ₁₀ NaO ₂ (CH ₃ CO ₂) ₁₃ (pd) ₆ (py) ₂] ₄ ⁴	dominant AF; <i>S</i> = 4	25
7	[Mn ₁₀ NaO ₂ (CH ₃ CO ₂) ₁₃ (mpd) ₆ (py)(H ₂ O)] ₄ ⁵	not applicable	25a
8	[Mn ₄₄ O ₈ (CH ₃ CO ₂) ₅₂ (pd) ₂₄ (py) ₈](ClO ₄)(OH) ₃ ⁴	<i>S</i> = 6; SMM; <i>U</i> _{eff} = 10 K	25a
9	[(Mo ^{VI} ₆ O ₂₁ L ^I ₆) ₁₂ {Fe ^{III} (H ₂ O)L ^I } ₃₀] ⁶	dominant AF; small <i>S</i>	71
10	{Na(H ₂ O) ₁₂ } [Mo ^{VI} ₇₂ Cr ^{III} ₃₀ O ₂₅₂ (CH ₃ CO ₂) ₁₉ (H ₂ O) ₉₄]	dominant AF; small <i>S</i>	35c
11	[K ₁₀ ⊂{(Mo ^{VI})Mo ^{VI} ₅ O ₂₁ (H ₂ O) ₃ (SO ₄) ₁₂ {(V ^{IV} O) ₃₀ (H ₂ O) ₂₀ }] ²⁶⁻	dominant AF; small <i>S</i>	35h
12	Na ₆ (NH ₄) ₂₀ (Fe ^{III} (H ₂ O) ₆) ₂ [(W ^{VI})W ^{VI} ₅ O ₂₁ (SO ₄) ₁₂ {(Fe(H ₂ O)) ₃₀ }(SO ₄) ₁₃ (H ₂ O) ₃₄]	dominant AF; small <i>S</i>	37a
13	K ₁₄ (VO) ₂ [K ₂₀ ⊂{(W)W ₅ O ₂₁ (SO ₄) ₁₂ (VO) ₃₀ (SO ₄)(H ₂ O) ₆₃]	dominant AF; <i>S</i> = 0	37b
14/Ln; Ln = Ce, Pr	{Capsule content ⊂ [Mo ₇₂ Fe ₂₄ Ln ₆ O ₂₅₂ (H ₂ O) ₁₀₅]} (Capsule content: ca. Mo ₁₈ O ₆₆ Ln ₂ (H ₂ O) _n)	dominant AF; small <i>S</i>	35i
15	[Fe ₆₄ O ₂₄ (tea) ₈ (Htea) ₂₄ (HCO ₂) ₆₀](ClO ₄) ₁₂ ⁷	dominant AF; <i>S</i> = 0	61
16, 17	[Fe ₃₆ (L ²) ₄₄ (H ₂ O) ₄₈]X ₂₀ ⁸	dominant AF; small <i>S</i>	73

18	$[\text{Co}_{36}\text{O}_8(\text{OH})_{16}((\text{CH}_3)_3\text{CCO}_2)_{36}((\text{CH}_3)_3\text{CCO}_2\text{H})_4(\text{dcpz})_2(\text{Hdcpz})_4(\text{H}_2\text{O})_{16}(\text{MeCN})_6]^{9}$	dominant AF; $S = 6$	53
19	$[\text{Co}_{32}\text{O}_{16}(\text{tci})_{16}(\text{H}_2\text{O})_{12}]^{10}$	dominant AF; small S	54
20	$[\text{Co}_{32}\text{O}_{24}(\text{TCA})_6(\text{H}_2\text{O})_{24}]^{11}$	dominant AF; small S	64
21/M; M = Co, Ni	$[\text{M}_{32}\text{O}_{16}(\text{OH})_8(\text{TCA})_6(\text{MeOH})_6]^{11}$	not applicable	63b
22	$[\text{Ni}_{32}(\text{OH})_{40}(\text{TCA})_6]^{11}$	not applicable	63a
23	$\{\text{K}_4(\text{MeOH})_4\}[\text{Cu}_{36}(\text{OH})_{36}(\text{OMe})_4\text{Cl}_6(\text{ndpa})_8(\text{H}_2\text{O})_5\{\text{KCl}_6\}]\text{Cl}^{12}$	dominant AF	55
24	$\{\text{Cu}^{\text{I}}_2\text{K}_4\text{Cl}_3(\text{H}_2\text{O})_3\}[\text{Cu}^{\text{II}}_{36}(\text{OH})_{37}(\text{OMe})_3\text{Cl}_6(\text{ndpa})_8(\text{H}_2\text{O})_4\{\text{KCl}_6\}]^{12}$	dominant AF	55
25	$[\text{Cu}_{44}(\text{OH})_{40}\text{Br}_{10}(\text{ntp})_{12}(\text{H}_2\text{O})_{28}]\text{Br}_2^{13}$	dominant AF; small S	56
26	$(\text{PPN})_2[(\text{SO}_4)\text{C}\{\text{Cu}(\text{OH})(\text{pz})\}_{8+14+9}]^{14}$	not applicable	66
27	$[\text{Cu}_{36}(\mu_3\text{-OH})_8(\text{dpocco})_{12}(\text{CH}_3\text{CO}_2)_{16}(\text{H}_2\text{O})_x]^{15}$	dominant AF; small S	75
28	$[\text{Cu}_{17}\text{Mn}_{28}\text{O}_{40}(\text{tea})_{12}(\text{HCO}_2)_6(\text{H}_2\text{O})_4]^7$	dominant F; $S = 51/2$; possible SMM	19
29	$[\text{Mn}_{36}\text{Ni}_4\text{O}_{12}\text{Cl}_{10}(\text{CH}_3\text{CO}_2)_{26}(\text{pd})_{24}(\text{py})_4(\text{H}_2\text{O})_2]^4$	dominant F; $S = 26 \pm 1$	62
30	$[\text{Ni}_{12}(\text{chp})_{12}(\text{CH}_3\text{CO}_2)_{12}(\text{H}_2\text{O})_6\{[\text{NH}_2\text{Pr}_2][\text{Cr}_7\text{NiF}_8((\text{CH}_3)_3\text{CCO}_2)_{15}(\text{C}_5\text{H}_4\text{NCO}_2)]\}_6]^{16}$	It does not display SMM behaviour. ²⁴	67
31	$[\text{Mn}^{\text{II}}_4\text{Mn}^{\text{III}}_2(\mu_4\text{-O})_2((\text{CH}_3)_3\text{CCO}_2)_{10}\{[\text{NH}_2\text{Pr}_2][\text{Cr}_7\text{NiF}_8((\text{CH}_3)_3\text{CCO}_2)_{15}(\text{C}_5\text{H}_4\text{NCO}_2)]\}_4]$	dominant AF	67
32	$\{[\text{Cu}_4(\text{OH})_4(\text{Me}_2\text{CO})]\{[\text{NH}_2\text{Pr}_2][\text{Cr}_7\text{NiF}_8((\text{CH}_3)_3\text{CCO}_2)_{15}(\text{O}_2\text{CC}_6\text{H}_4\text{CO}_2)]\}_4\}$	dominant AF	68
33	$\{[\text{Zn}_4\text{O}]\{[\text{NH}_2\text{Pr}_2][\text{Cr}_7\text{NiF}_8((\text{CH}_3)_3\text{CCO}_2)_{15}(\text{O}_2\text{CC}_6\text{H}_4\text{CO}_2)]\}_6\}$	dominant AF	68
34	$[\text{Ni}_{30}\text{La}_{20}(\text{OH})_{30}(\text{ida})_{30}(\text{CO}_3)_6(\text{NO}_3)_6(\text{H}_2\text{O})_{12}](\text{CO}_3)_6^{17}$	dominant F; $S \sim 20$	58, 59
35/Ln; Ln = Pr, Nd	$[\text{Ni}_{21}\text{Ln}_{20}(\text{OH})_{24}(\text{ida})_{21}(\text{C}_2\text{H}_2\text{O}_3)_6(\text{C}_2\text{O}_4)_3(\text{NO}_3)_9(\text{H}_2\text{O})_{12}](\text{NO}_3)_9^{17}$	dominant AF	58
36	$[\text{Ni}_{54}\text{Gd}_{54}(\text{OH})_{144}(\text{ida})_{48}(\text{CO}_3)_6(\text{H}_2\text{O})_{25}](\text{NO}_3)_{18}^{17}$	dominant AF	60

37	$[\text{Ni}_{76}\text{La}_{60}(\text{OH})_{158}(\text{ida})_{68}(\text{NO}_3)_4(\text{H}_2\text{O})_{44}](\text{NO}_3)_{34}$ ¹⁷	weak F	57
38	$[\text{Ni}_{12}\text{Gd}_{36}\text{O}_6(\text{OH})_{84}(\text{CH}_3\text{CO}_2)_{18}(\text{H}_2\text{O})_{54}(\text{NO}_3)\text{Cl}_2](\text{NO}_3)_6\text{Cl}_9$	dominant AF; large MCE ($-\Delta S_m=36.3 \text{ J kg}^{-1} \text{ K}^{-1}$ at 3 K for $\Delta H=7 \text{ T}$)	30
39/Ln; Ln=Gd, Dy	$[\text{Ni}_{10}\text{Ln}_{42}(\text{OH})_{68}(\text{CO}_3)_{12}(\text{CH}_3\text{CO}_2)_{30}(\text{H}_2\text{O})_{70}](\text{ClO}_4)_{24}$	Competing F and AF; 39/Dy : SMM; 39/Gd : large MCE ($-\Delta S_m=38.2 \text{ J kg}^{-1} \text{ K}^{-1}$ at 2 K for $\Delta H=7 \text{ T}$)	22
40/Ln; Ln=Gd, Dy	$[\text{Co}_{10}\text{Ln}_{42}(\text{OH})_{68}(\text{CO}_3)_{12}(\text{CH}_3\text{CO}_2)_{30}(\text{H}_2\text{O})_{70}](\text{ClO}_4)_{25}$	Competing F and AF; 40/Dy : SMM; 40/Gd : large MCE ($-\Delta S_m=41.26 \text{ J kg}^{-1} \text{ K}^{-1}$ at 2 K for $\Delta H=7 \text{ T}$)	22
41/Ln; Ln=Gd, Dy	$[\text{Co}_{16}\text{Ln}_{24}(\text{OH})_{50}(\text{pyacac})_{16}(\text{NO}_3)_{18}(\text{H}_2\text{O})_{12}][\text{Ln}(\text{H}_2\text{O})_8]_2(\text{NO}_3)_{16}(\text{OH})_{10}$ ¹⁸	Competing F and AF; 41/Dy : possible SMM; 41/Gd : large MCE ($-\Delta S_m = 26.0 \text{ J kg}^{-1} \text{ K}^{-1}$ at 3.8 K and $\Delta H=7 \text{ T}$)	29
42/Ln; Ln= Tb, Gd, Sm, La	$[\text{Cu}_{24}\text{Ln}_6(\text{OH})_{30}(\text{ala})_{12}(\text{CH}_3\text{CO}_2)_6(\text{ClO}_4)(\text{H}_2\text{O})_{12}](\text{ClO}_4)_{10}(\text{OH})_7$ ¹⁹	42/Sm , 42/La : dominant AF; 42/Tb , 42/Gd : competing F and AF; $S \sim 11$ for 42/Gd	51a
(43/Ln; Ln =Gd, Dy	$\text{Na}[\text{Cu}_{24}\text{Ln}_6(\text{OH})_{30}(\text{ala})_{12}(\text{CH}_3\text{CO}_2)_6(\text{NO}_3)_4(\text{H}_2\text{O})_{20}](\text{NO}_3)_8(\text{OH})_7$ ¹⁹	Competing F and AF; 43/Gd : large MCE ($-\Delta S_m = 21.2 \text{ J kg}^{-1} \text{ K}^{-1}$ at 2.5 K for $\Delta H = 7 \text{ T}$); 43/Dy SMM; $U_{\text{eff}} = 34 \text{ K}$	51b
44	$[\text{Cu}_{24}\text{Sm}_6(\text{OH})_{30}(\text{gly})_{12}(\text{CH}_3\text{CO}_2)_{12}(\text{ClO}_4)(\text{H}_2\text{O})_{16}](\text{ClO}_4)_9(\text{OH})_2$ ²⁰	not applicable	51a
45	$\text{Na}_4[\text{Cu}_{26}\text{Tb}_6(\text{OH})_{30}(\text{gly})_{18}(\text{ClO}_4)(\text{H}_2\text{O})_{22}](\text{ClO}_4)_{25}$ ²⁰	weak exchange interactions	52
46	$[\text{Cu}_{24}\text{Gd}_6(\text{OH})_{30}(\text{mala})_{16}(\text{ClO}_4)(\text{H}_2\text{O})_{22}](\text{ClO}_4)_{17}(\text{OH})_2$ ²¹	not applicable	52
47/Ln; Ln=Sm, Gd	$\{[\text{Cu}_{24}\text{Ln}_6(\text{OH})_{30}(\text{pro})_{12}(\text{CH}_3\text{CO}_2)_6(\text{ClO}_4)(\text{H}_2\text{O})_{13}]_2\text{Cu}(\text{pro})_2\}(\text{ClO}_4)_{18}(\text{OH})_{16}$ ²²	47/Gd : dominant F	52
48	$[\text{H}_3\text{O}][\text{Cu}_{24}\text{Dy}_8(\text{OH})_{42}(\text{Ph}_3\text{C-PO}_3)_6(\text{Ph}_3\text{C-PO}_3\text{H})_6(\text{CH}_3\text{CO}_2)_{12}(\text{CH}_3\text{CO}_2\text{H})_6(\text{NO}_3)(\text{H}_2\text{O})_6]$	competing F and AF; SMM; $U_{\text{eff}} \sim 4.6 \text{ K}$	20
49	$[(\text{Me}_4\text{N})_2\text{K}_2][\text{Cu}_{24}\text{Gd}_8(\text{OH})_{42}(\text{Ph}_3\text{C-PO}_3)_6(\text{Ph}_3\text{C-PO}_3\text{H})_6(\text{CH}_3\text{CO}_2)_{12}(\text{CH}_3\text{CO}_2\text{H})_{12}(\text{NO}_3)](\text{OH})_3$	competing F and AF; large S	20

50/Ln; $[\text{Cu}_3\text{Ln}_{24}(\text{OH})_{72}(\text{NO}_3)_6(\text{PhCO}_2)_{60}(\text{MeOH})_m(\text{H}_2\text{O})_n](\text{NO}_3)_6$ ²³ dominant AF; **50/Dy**: possible SMM; 21
 Ln=Dy, Gd **50/Gd**: large MCE ($-\Delta S_m = 21 \text{ J kg}^{-1} \text{ K}^{-1}$ at 2.1 K for $\Delta H=7 \text{ T}$)

^a Abbreviations and terms used in this table: AF = antiferromagnetic exchange interactions; F = ferromagnetic exchange interactions; small S - the compound displays a small spin ground state *S* which, however, has not been determined; large S - the compound displays a large spin ground state *S* the exact value of which, however, has not been determined; possible SMM - the compound displays frequency-dependent out-of-phase (χ''_M) signals at low T and a concomitant decrease of the in-phase ($\chi'_M T$) signals indicative of SMM behavior, but no further data to confirm such a conclusion have been reported.

¹ H₃thme = 1,1,1- tris(hydroxymethyl)ethane; ² bpy = 2,2'-bipyridine; ³ H₂Me-sao = 2'-hydroxyacetophenone oxime; ⁴ H₂pd = 1,3-propanediol; ⁵ H₂mpd = 2-methyl-1,3-propanediol; ⁶ L¹ = H₂O / CH₃CO₂⁻ / Mo₂O_{8/9}ⁿ⁻; ⁷ H₃tea = triethanolamine; ⁸ H₂L² = 2-pyridylphosphonic acid, X = ClO₄⁻, NO₃⁻ and OH⁻ for **16** and CF₃SO₃⁻ and OH⁻ for **17**; ⁹ H₂dcpz = 2,3-dicarboxypyrazine; ¹⁰ H₃tci = tris(2- carboxyethyl)isocyanurate; ¹¹ H₄TCA = p-tert-Butylthiacalix[4]arene; ¹² H₃ndpa = (nitrilodipropionic)acetic acid; ¹³ H₃ntp = 3,3',3''-Nitrilotripropionic acid; ¹⁴ PPN = bis(triphenylphosphoranylidene)ammonium cation; Hpz = pyrazole; ¹⁵ A schematic representation of the ligand H₄dpocco is shown in Fig. 18, top; ¹⁶ Hchp=6-chloro-2-hydroxypyridine; ¹⁷ H₂ida = iminodiacetic acid; ¹⁸ Hpyacac = 1,3-di(2-pyridyl)-1,3-propanedione; ¹⁹ Hala = L-alanine; ²⁰ Hgly = glycine; ²¹ Hmala = 2-methylalanine; ²² Hpro = L-proline; ²³ **50/Dy**: m = 14, n=0; **50/Gd**: m = 6, n= 12; ²⁴ The two types of complexes present in this compound interact weakly. Interestingly, although its main component (Ni₁₂ cluster) is a SMM, complex **30** does not display SMM behavior.

Conclusions

In this review, the synthetic, structural and magnetic aspects of clusters based on paramagnetic 3d or 3d/4f metal ions with nuclearities 30 or greater have been surveyed. The first discrete member of this family of compounds was a Mn_{30} cluster discovered in 2001,⁴ although a $\text{Fe}^{\text{III}}_{30}\text{Mo}^{\text{VI}}_{72}$ 3d/4d cluster had been reported earlier,⁷¹ and since then the family of giant clusters based on paramagnetic 3d metal ions has been greatly expanded. Thus, there are now known more than 50 such species, which are collected in Table 1 along with brief information about their magnetic properties. As it can be seen in Table 1, the highest nuclearity discrete cluster (0-D) is the $\text{Ni}_{76}\text{La}_{60}$ (compound **37**)⁵⁷ with the compounds $\text{Ni}_{54}\text{Gd}_{54}$ (compound **36**)⁶⁰ and Mn_{84} (compound **2**) to follow in the list.¹¹ The latter, which is also the largest homometallic 3d compound, possesses a 4-nm-diameter torus structure and SMM behaviour, thus being also the highest nuclearity SMM known to date.¹¹ It is noteworthy that the MW, nuclearities and dimensions of these species have been dramatically increased over the last years and currently become comparable with those of other categories of giant compounds. Thus, although in 2001 the highest nuclearity paramagnetic metal cluster in moderate oxidation states was compound **1** with nuclearity 30,⁴ MW $\sim 6100 \text{ g mol}^{-1}$ and diameter $\sim 3 \text{ nm}$, more than ten times smaller than the corresponding highest nuclearity POM (Mo_{368} : MW $\sim 80000 \text{ g mol}^{-1}$, largest dimension $\sim 6 \text{ nm}$),^{34a} or metal chalcogenide cluster (Ag_{490} : MW $\sim 70000 \text{ g mol}^{-1}$, narrow-waisted cylinder of dimensions 2.8–3.1 nm)^{31b} already known in 2004, these differences have been decreased significantly after the recent discovery of some giant 3d and 3d/4f complexes such as Mn_{84} (MW $\sim 15000 \text{ g mol}^{-1}$ and diameter $\sim 4.2 \text{ nm}$),¹¹ $\text{Ni}_{54}\text{Gd}_{54}$, (MW $\sim 25000 \text{ g mol}^{-1}$ and largest dimension $\sim 2.3 \text{ nm}$),⁶⁰ $\text{Ni}_{76}\text{La}_{60}$ (MW $\sim 28000 \text{ g mol}^{-1}$)⁵⁷ and largest dimension $\sim 3.4 \text{ nm}$) and $\text{Cu}_{36}\text{Ln}_{24}$ (MW: $\sim 17500 \text{ g mol}^{-1}$ and largest dimension $\sim 4.6 \text{ nm}$).²¹ This significant increase of

the nuclearity, molecular weight and size of the homometallic 3d and heterometallic 3d/4f species reflects the enormous evolution that took place in this chemistry during the last decade, achieving something that 10 years ago looked impossible, i.e. the isolation and characterization of compounds of comparable dimensions with those of POMs and metal chalcogenide clusters. It is also interesting that these compounds have similar sizes to those of the smallest magnetic nanoparticles of the classical world.⁷⁶ For example, a Co nanoparticle exhibiting a face-centered cubic structure and comprising around 1000 metal atoms has diameter 3 nm^{76a} which is smaller than the dimensions of many compounds described in this review.^{11,21,57,67} For this reason, the giant species are considered to be the meeting point of two different approaches towards new nanoscale magnetic materials, the molecular bottom-up and traditional top-down ones. In addition, their molecular nature, crystallinity and monodispersity together with the fact that their crystal structures can be functionalized and readily determined, bring all the required advantages for the manipulation of these giant species on surfaces, and thus they are excellent candidates for further employment in technological and biomedical applications and promising competitors of the currently used nanoparticles.^{76,79}

The dramatic development that took place the last decade in the chemistry of giant 3d and 3d/4f metal clusters in moderate oxidation states stems not only from the enchanting beauty of such species, but also from their very interesting magnetic properties. Thus, giant paramagnetic metal clusters sometimes exhibit single-molecule magnetism behavior and can reasonably be considered as the meeting point of the quantum and the classical worlds of nanoscale magnetism. In addition, the fact that such species are located at the quantum – classical physics boundary while maintaining their molecular advantages and large mesoscale size, could lead to the further discovery of new physical properties as well as to the better understanding of the existing ones,

such as the clear confirmation that these giant species still exhibit quantum tunneling of the magnetization, as mentioned in this review.^{4,11} However, the prediction that compounds based on high number of paramagnetic metal ions could lead to high spin and magnetoanisotropy values and thus enhanced SMM properties has not been proven to be entirely true. Although there are some giant species displaying SMM behavior, the largest U_{eff} is ~ 45 K for a Mn_{32} “double – decker” wheel (compound **4**),²³ significantly smaller than U_{eff} values reported for other lower nuclearity homometallic and heterometallic SMMs.^{7,9,10,77} The latter, apart from their larger U_{eff} values, also have other significant advantages since they are simpler systems and thus more amenable to a) an in-depth analysis of their magnetism behaviour (e.g. determination of the nature and strength of the exchange interactions between the metal ions, spin ground state and magnetoanisotropy values, etc) and b) various structural modifications that can lead to fine-tuning of their magnetic properties.

A recent discovery that increased the interest for giant metal clusters in moderate oxidation states was the appearance of enhanced MCE in a series of heterometallic compounds including $\text{Ni}_{12}\text{Gd}_{36}$ (compound **38** of Table 1),³⁰ $\text{M}_{10}\text{Gd}_{42}$ ($\text{M} = \text{Ni}$, **39**/Gd; $\text{M}=\text{Co}$, **40**/Gd of Table 1),²² $\text{Co}_{16}\text{Gd}_{24}$ (compound **41**/Gd of Table 1),²⁹ and $\text{Cu}_{36}\text{Gd}_{24}$ (compound **50**/Gd of Table 1),²¹ species. This can be explained by the fact that such compounds display a limited organic content combined with a huge number of unpaired electrons that could result in very high magnetization values and thus possess some of the required ingredients to achieve enhanced MCE. This is clearly proven in the case of **40**/Gd which displays a remarkably high MCE value ($-\Delta S_{\text{m}} = 41.26 \text{ J kg}^{-1} \text{ K}^{-1}$); in fact this MCE is very close to the world record for any discrete metal cluster ($-\Delta S_{\text{m}} = 46.9 \text{ J kg}^{-1} \text{ K}^{-1}$) and among the highest yet observed for any metal compound in general.^{46d,46e,78} The giant number of unpaired electrons that such high nuclearity species have can also lead to

abnormally high spin ground state values if their metal ions are ferromagnetically coupled. In fact, there have been reported several giant species possessing dominant ferromagnetic exchange interactions with the largest spin ground state values for such compounds being $51/2$ and 26 ± 1 for the $\text{Mn}_{28}\text{Cu}_{17}$ (compound **28** of Table 1)¹⁹ and $\text{Mn}_{36}\text{Ni}_4$ (compound **29** of Table 1) heterometallic clusters,⁶² respectively.

As expected, the isolation of a significant number of giant metal-organic species has increased our knowledge about the synthetic methods that can afford such compounds. Although the majority of these methods are still based on serendipitous assembly, there are some breakthroughs reported during recent years that can guide new synthetic efforts to even higher nuclearity species with interesting magnetic properties. A detailed discussion about the most important synthetic methods towards giant metal clusters, along with the main conclusions concerning the synthetic work that has been performed in this area, is included in section 2 of this review.

Clearly the chemistry of giant metal clusters based on 3d metal ions has been significantly developed during the last decade. This development has provided significant information about all aspects of this area of chemistry including synthetic methods, structural types that are stabilized, physical properties and potential applications. We feel confident that the future will see the isolation of clusters possessing even higher nuclearities and interesting physical properties, new controlled synthetic methods displaying greater elements of rational design, and the utilization of these fascinating species in a variety of areas of chemistry and materials science.

Acknowledgements: The synthetic chemistry from the groups of AJT and GC described in this Review has been carried out by our talented PhD students whose names appear in the reference

list. This work has been done in collaboration with a number of groups. The authors thank Dr. Wolfgang Wernsdorfer (Laboratoire Louis Néel) for micro-SQUID studies at very low temperatures. In addition, AJT, CP and EEM wish to thank Prof. Euan K. Brechin (University of Edinburgh) and his group, Prof. Rodolphe Clérac (CNRS, France) and his group, Dr. Yiannis Sanakis and Dr. Athanasios Boudalis (NCSR ‘Demokritos’, Athens), Prof. Vassilios Nastopoulos and Prof. Spyros P. Perlepes (University of Patras) and Dr Giannis S. Papaefstathiou (University of Athens). This work was supported by the University of Cyprus (internal grants awarded to AJT) and the Cyprus Research Promotion Foundation Grant “ANABAΘMISΗ/ΠAΓIO/0308/12” which is co-funded by the Republic of Cyprus and the European Regional Development Fund. GC acknowledges the generous support over many years from the National Science Foundation, most recently grant DMR-1213030. We also thank the European Union Seventh Framework Program (FP7/2007-2013) under Grant agreement number: PCIG09-GA-2011-293814 (AJT and CP) and the COST action CM1203 (AJT).

References

- 1 (a) *Physics and Chemistry of Metal Cluster Compounds*; L. J. de Jongh, Ed.; Kluwer Academic Publishers: The Netherlands, 1994;
- (b) M. Kawano, J. W. Bacon, C. F. Campana, B. E. Winger, J. D. Dudek, S. A. Sirchio, S. L. Scruggs, U. Geiser and L. F. Dahl, *Inorg. Chem.*, 2001, **40**, 2554;
- (c) E. G. Mednikov, S. A. Ivanov and L. F. Dahl, *Inorg. Chem.*, 2011, **50**, 11795.
- 2 (a) H. K. Jun, M. A. Careem and A. K. Arof, *Ren. Sust. En. Rev.*, 2013, **22**, 148;
- (b) N. Zheng, X. Bu, H. Lu, Q. Zhang and P. Feng, *J. Am. Chem. Soc.*, 2005, **127**, 11963.
- 3 (a) Y.-S. Bae, O. K. Farha, A. M. Spokoyny, C. A. Mirkin, J. T. Hupp and R. Q. Snurr, *Chem. Commun.*, 2008, 4135;
- (b) R. Kawamoto, S. Uchida and N. Mizuno, *J. Am. Chem. Soc.*, 2005, **127**, 10560;

- (c) Handbook of Porous Solids, Five Vols. (Eds.: F. Schüth, K. S. W. Sing, J. Weitkamp), Wiley-VCH, Weinheim, 2002;
- (d) Comprehensive Supramolecular Chemistry, Vol. 7 (Eds.: J. L. Atwood, J. E. D. Davies, D. D. MacNicol, F. Vögtle), Pergamon, Oxford, 1996.
- 4 (a) M. Soler, W. Wernsdorfer, K. Folting, M. Pink and G. Christou, *J. Am. Chem. Soc.*, 2004, **126**, 2156;
- (b) M. Soler, E. Rumberger, K. Folting, D. N. Hendrickson and G. Christou, *Polyhedron*, 2001, **20**, 1365.
- 5 (a) K. L. Taft, G. C. Papaefthymiou and S. J. Lippard, *Science*, 1993, **259**, 1302;
- (b) S.M. Gorun, G. C. Papaefthymiou, R. B. Frankel and S. J. Lippard, *J. Am. Chem. Soc.*, 1987, **109**, 3337;
- (c) K. H. Ebrahimi, P.-L. Hagedoorn and W. R. Hagen, *Chem. Rev.*, 2015, **115**, 295;
- (d) G. Jutz, P. van Rijn, B. S. Miranda and A. Böker, *Chem. Rev.*, 2015, **115**, 1653;
- (e) E. C. Theila, R. K. Behera and T. Tosha, *Coord. Chem. Rev.*, 2013, **257**, 579.
- 6 (a) G. C. Dismukes, R. Brimblecombe, G. A. N. Felton, R. S. Pryadun, J. E. Sheats, L. Spiccia and G. F. Swiegers, *Acc. Chem. Res.*, 2009, **42**, 1935;
- (b) G. Maayan and G. Christou, *Inorg. Chem.*, 2011, **50**, 7015;
- (c) W. Rüttinger and G. Charles Dismukes, *Chem. Rev.*, 1997, **97**, 1;
- (d) X.-J. Kong, L.-S. Long, Z. Zheng, R.-B. Huang and L.-S. Zheng, *Acc. Chem. Res.*, 2010, **43**, 201.
- 7 (a) D. Gatteschi, R. Sessoli and J. Villain in “*Molecular Nanomagnets*”, Oxford University Press, 2006.
- (b) O. Kahn in “*Molecular magnetism*”, Wiley, 1993;
- (c) M. Evangelisti in “*Molecule-based magnetic coolers: Measurement, design and application*”, (Eds.: J. Bartolomé, F. Luis and J. F. Fernández), Molecular Magnets, NanoScience and Technology, Springer-Verlag, Berlin, Heidelberg, 2014, pp. 365-387;
- (d) R. Sessoli, H. -L. Tsai, A. R. Schake, S. Wang, J. B. Vincent, K. Folting, D. Gatteschi, G. Christou and D. N. Hendrickson, *J. Am. Chem. Soc.*, 1993, **115**, 1804;
- (e) R. Sessoli, D. Gatteschi, A. Caneschi and M. A. Novak, *Nature*, 1993, **365**, 141.
- 8 (a) A. M. Ako, I. J. Hewitt, V. Mereacre, R. Clerac, W. Wernsdorfer, C. E. Anson and A. K. Powell, *Angew. Chem., Int. Ed.*, 2006, **45**, 4926;

- (b) C.-H. Ge, Z.-H. Ni, C.-M. Liu, A.-L. Cui, D.-Q. Zhang and H.-Z. Kou, *Inorg. Chem. Commun.*, 2008, **11**, 675.
- (c) E. E. Moushi, T. C. Stamatatos, W. Wernsdorfer, V. Nastopoulos, G. Christou and A. J. Tasiopoulos, *Inorg. Chem.*, 2009, **48**, 5049.
- 9 (a) G. Aromi and E. K. Brechin, *Struct. Bonding*, 2006, **122**, 1;
(b) C. J. Milios and R. E. P. Winpenny, *Struct. Bonding*, 2015, **164**, 1.
- 10 (a) R. Bagai and G. Christou, *Chem. Soc. Rev.*, 2009, **38**, 1011;
(b) G. Christou, D. Gatteschi, D. N. Hendrickson and R. Sessoli, *MRS Bull.*, 2000, **25**, 66;
(c) E. K. Brechin, *Chem. Commun.*, 2005, 5141;
(d) R. Inglis, C. J. Milios, L. F. Jones, S. Piligkos and E. K. Brechin, *Chem. Commun.*, 2012, **48**, 181;
(e) G. E. Kostakis, S. P. Perlepes, V. A. Blatov, D. M. Proserpio and A. K. Powell, *Coord. Chem. Rev.*, 2012, **256**, 1246;
(f) G. E. Kostakis, A. M. Ako and A. K. Powell, *Chem. Soc. Rev.*, 2010, **39**, 2238.
- 11 A. J. Tasiopoulos, A. Vinslava, W. Wernsdorfer, K. A. Abboud and G. Christou, *Angew. Chem. Int. Ed.*, 2004, **43**, 2117.
- 12 (a) L. Bogani and W. Wernsdorfer, *Nature Mater.*, 2008, **7**, 179;
(b) M. N. Leuenberger and D. Loss, *Nature*, 2001, **410**, 789.
- 13 (a) A. Kovalev, L. X. Hayden, G. E. W. Bauer and Y. Tserkovnyak, *Phys. Rev. Lett.*, 2011, **106**, 147203;
(b) D. A. Garanin and E. Chudnovsky, *Phys. Rev. X*, 2011, **1**, 011005;
(c) M. Ganzhorn, S. Klyatskaya, M. Ruben and W. Wernsdorfer, *Nature Nanotech.*, 2013, **8**, 165;
(d) S. Hill, R. S. Edwards, N. Aliaga-Alcalde and G. Christou, *Science*, 2003, **302**, 1015;
(e) R. Tiron, W. Wernsdorfer, D. Foguet-Albiol, N. Aliaga-Alcalde and G. Christou, *Phys. Rev. Lett.*, 2003, **91**, 227203(1-4).
- 14 (a) W. Wernsdorfer, S. Bhaduri, C. Boskovic, G. Christou and D. N. Hendrickson, *Phys. Rev. B*, 2002, **65**, 180403;
(b) W. Wernsdorfer, N. E. Chakov and G. Christou, *Phys. Rev. Lett.*, 2005, **95**, 037203.
- 15 (a) D. Gatteschi and R. Sessoli, *Angew. Chem. Int. Ed.*, 2003, **42**, 268;

- (b) E. del Barco, A. D. Kent, S. Hill, J. M. North, N. S. Dalal, E. M. Rumberger, D. N. Hendrickson, N. E. Chakov and G. Christou, *J. Low Temp. Phys.*, 2005, **140**, 119;
- (c) P. C. E. Stamp, *Nature*, 1996, **383**, 125.
- 16 (a) W. Wernsdorfer and R. Sessoli, *Science*, 1999, **284**, 133;
- (b) W. Wernsdorfer, M. Soler, G. Christou and D. N. Hendrickson, *J. Appl. Phys.*, 2002, **91**, 7164.
- 17 (a) F. Macia, J. M. Hernandez, J. Tejada, S. Datta, S. Hill, C. Lampropoulos and G. Christou, *Phys. Rev. B*, 2009, **79**, 092403;
- (b) S. T. Adams, E. H. da Silva Neto, S. Datta, J. F. Ware, C. Lampropoulos, G. Christou, Y. Myaesoedov, E. Zeldov and J. R. Friedman, *Phys. Rev. Lett.*, 2013, **110**, 087205.
- 18 (a) J. D. Rinehart and J. R. Long, *Chem. Sci.*, 2011, **2**, 2078;
- (b) P. Dechambenoit and J. R. Long, *Chem. Soc. Rev.*, 2011, **40**, 3249;
- (c) F. Habib and M. Murugesu, *Chem. Soc. Rev.*, 2013, **42**, 3278;
- (d) J.-L. Liu, J.-Y. Wu, Y.-C. Chen, V. Mereacre, A. K. Powell, L. Ungur, L. F. Chibotaru, X.-M. Chen and M.-L. Tong, *Angew. Chem. Int. Ed.*, 2014, **53**, 12966;
- (e) E. J. Schelter, F. Karadas, C. Avendano, A. V. Prosvirin, W. Wernsdorfer and K. R. Dunbar, *J. Am. Chem. Soc.*, 2007, **129**, 8139;
- (f) E. J. Schelter, A. V. Prosvirin and K. R. Dunbar, *J. Am. Chem. Soc.*, 2004, **126**, 15004;
- 19 W.-G. Wang, A.-J. Zhou, W.-X. Zhang, M.-L. Tong, X.-M. Chen, M. Nakano, C. C. Beedle and D. N. Hendrickson, *J. Am. Chem. Soc.* 2007, **129**, 1014.
- 20 V. Baskar, K. Gopal, M. Helliwell, F. Tuna, W. Wernsdorfer and R. E. P. Winpenny, *Dalton Trans.*, 2010, **39**, 4747.
- 21 J.-D. Leng, J.-L. Liu and M.-L. Tong, *Chem. Commun.*, 2012, **48**, 5286.
- 22 J.-B. Peng, Q.-C. Zhang, X.-J. Kong, Y.-Z. Zheng, Y.-P. Ren, L.-S. Long, R.-B. Huang, L.-S. Zheng and Z. Zheng, *J. Am. Chem. Soc.*, 2012, **134**, 3314.
- 23 M. Manoli, R. Inglis, M. J. Manos, V. Nastopoulos, W. Wernsdorfer, E. K. Brechin and A. J. Tasiopoulos, *Angew. Chem. Int. Ed.*, 2011, **50**, 4441.
- 24 S. K. Langley, R. A. Stott, N. F. Chilton, B. Moubaraki and K. S. Murray, *Chem. Commun.*, 2011, **47**, 6281.
- 25 (a) E. E. Moushi, C. Lampropoulos, W. Wernsdorfer, V. Nastopoulos, G. Christou and A. J. Tasiopoulos, *J. Am. Chem. Soc.*, 2010, **132**, 16146;

- (b) E. E. Moushi, C. Lampropoulos, W. Wernsdorfer, V. Nastopoulos, G. Christou and A. J. Tasiopoulos, *Inorg. Chem.*, 2007, **46**, 3795.
- 26 E. Warburg, *Ann. Phys. Chem.*, 1881, **13**, 141.
- 27 P. Debye, *Ann. Phys.*, 1926, **386**, 1154.
- 28 (a) T. Feder, *Phys. Today*, 2001, **62**, 21;
(b) Y.-Z. Zheng, G.-J. Zhou, Z. Zheng and R. E. P. Winpenny, *Chem. Soc. Rev.*, 2014, **43**, 1462;
(c) V. K. Pecharsky and K. A. Gschneidner Jr., *J. Magn. Magn. Mat.*, 1999, **200**, 44.
- 29 Z.-M. Zhang, L.-Y. Pan, W.-Q. Lin, J.-D. Leng, F.-S. Guo, Y.-C. Chen, J.-L. Liu and M.-L. Tong, *Chem. Commun.* 2013, **49**, 8081.
- 30 J.-B. Peng, Q.-C. Zhang, X.-J. Kong, Y.-P. Ren, L.-S. Long, R.-B. Huang, L.-S. Zheng and Z. Zheng, *Angew. Chem. Int. Ed.*, 2011, **50**, 10649.
- 31 (a) O. Fuhr, S. Dehnen and D. Fenske, *Chem. Soc. Rev.*, 2013, **42**, 1871;
(b) C. E. Anson, A. Eichhöfer, I. Issac, D. Fenske, O. Fuhr, P. Sevillano, C. Persau, D. Stalke and J. Zhang, *Angew. Chem. Int. Ed.*, 2008, **37**, 1326;
(c) D. Fenske, N. Zhu and T. Langetepe, *Angew. Chem., Int. Ed.*, 1998, **47**, 2639;
(d) X.-J. Wang, T. Langetepe, C. Persau, B.-S. Kang, G. M. Sheldrick and D. Fenske, *Angew. Chem. Int. Ed.*, 2002, **41**, 3818;
(e) G. Li, Z. Lei and Q.-M. Wang, *J. Am. Chem. Soc.*, 2010, **132**, 17678.
- 32 (a) M.-L. Fu, I. Issac, D. Fenske and O. Fuhr, *Angew. Chem. Int. Ed.*, 2010, **49**, 6899;
(b) D. Fenske and H. Krautscheid, *Angew. Chem. Int. Ed.*, 1990, **29**, 1452;
(c) H. Krautscheid, D. Fenske, G. Baum and M. Semmelmann, *Angew. Chem. Int. Ed.*, 1993, 1303;
(d) S. Dehnen and D. Fenske, *Chem. Eur. J.*, 1996, **2**, 1407;
(e) N. R. M. Crawford, A. G. Hee and J. R. Long, *J. Am. Chem. Soc.*, 2002, **124**, 14842.
- 33 (a) T. Vossmeier, G. Reck, B. Schulz, L. Katsikas and H. Weller, *J. Am. Chem. Soc.*, 1995, **117**, 12881;
(b) A. Eichhöfer, P. T. Wood, R. N. Viswanath and R. A. Mole, *Chem. Commun.*, 2008, 1596;
(c) S. Koenig, A. Eichhöfer, N. R. M. Crawford, R. Ahlrichs and D. Fenske, *Z. Anorg. Allg. Chem.*, 2007, 713;

- (d) D. Fenske, J. Ohmer and J. Hachgenei, *Angew. Chem. Int. Ed.*, 1985, **24**, 993;
- (e) D. Fenske, J. Ohmer, J. Hachgenei and K. Merzweiler, *Angew. Chem. Int. Ed.*, 1988, **27**, 1277.
- 34 (a) A. Müller, E. Beckmann, H. Bögge, M. Schmidtman and A. Dress, *Angew. Chem., Int. Ed.*, 2002, **41**, 1162;
- (b) D.-L. Long, R. Tsunashima and L. Cronin, *Angew. Chem. Int. Ed.*, 2010, **49**, 1736;
- (c) U. Kortz, A. Müller, J. van Slageren, J. Schnack, N. S. Dalal and M. Dressel, *Coord Chem. Rev.*, 2009, **253**, 2315;
- (d) A. Müller and P. Gouzerh, *Chem. Soc. Rev.*, 2012, **41**, 7431.
- 35 (a) A. Müller, M. Koop, H. Bögge, M. Schmidtman and C. Beugholt, *Chem. Commun.*, 1998, 1501;
- (b) S. Wang, X. Lin, Y. Wan, W. Yang, S. Zhang, C. Lu and H. Zhuang, *Angew. Chem. Int. Ed.*, 2007, **46**, 3490;
- (c) A. M. Todea, A. Merca, H. Bögge, J. van Slageren, M. Dressel, L. Engelhardt, M. Luban, T. Glaser, M. Henry and A. Müller, *Angew. Chem. Int. Ed.*, 2007, **46**, 6106;
- (d) K. Heussner, M. Grabau, J. Forster and C. Streb, *Eur. J. Inorg. Chem.*, 2011, 5125;
- (e) W. Yang, C. Lu, X. Lin and H. Zhuang, *Inorg Chem.*, 2002, **41**, 452;
- (f) W. Yang, C. Lu, X. Lin and H. Zhuang, *Chem. Commun.*, 2000, 1623;
- (g) C. Schäffer, H. Bögge, A. Merca, I. A. Weinstock, D. Rehder, E. T. K. Haupt and A. Müller, *Angew. Chem. Int. Ed.*, 2009, **48**, 8051;
- (h) A. Müller, A. M. Todea, J. van Slageren, M. Dressel, H. Bögge, M. Schmidtman, M. Luban, L. Engelhardt and M. Rusu, *Angew. Chem. Int. Ed.*, 2005, **44**, 3857;
- (i) A. Müller, H. Bögge, F. L. Sousa, M. Schmidtman, D. G. Kurth, D. Volkmer, J. van Slageren, M. Dressel, M. L. Kistler and T. Liu, *Small*, 2007, **3**, 986.
- 36 (a) D.-L. Long, H. Abbas, P. Kögerler and L. Cronin, *J. Am. Chem. Soc.*, 2004, **126**, 13880;
- (b) C. Streb, T. McGlone, O. Brücher, D.-L. Long and L. Cronin, *Chem. Eur. J.*, 2008, **14**, 8861;
- (c) C. Ritchie, M. Speldrich, R. W. Gable, L. Sorace, P. Kögerler and C. Boskovic, *Inorg. Chem.*, 2011, **50**, 7004;
- (d) J. Yan, D.-L. Long, E. F. Wilson and L. Cronin, *Angew. Chem. Int. Ed.*, 2009, **48**, 4376;
- (e) J. Gao, J. Yan, S. Beeg, D.-L. Long and L. Cronin, *J. Am. Chem. Soc.*, 2013, **135**, 1796.

- 37 (a) A. M. Todea, A. Merca, H. Bögge, T. Glaser, J. M. Pigga, M. L. K. Langston, T. Liu, R. Prozorov, M. Luban, C. Schröder, W. H. Casey and A. Müller, *Angew. Chem. Int. Ed.*, 2010, **49**, 514;
- (b) A. M. Todea, A. Merca, H. Bögge, T. Glaser, L. Engelhardt, R. Prozorov, M. Luban and A. Müller, *Chem. Commun.*, 2009, 3351;
- (c) B. Botar, A. Ellern, R. Hermann and P. Kögerler, *Angew. Chem. Int. Ed.*, 2009, **48**, 9080;
- (d) B. Botar, P. Kögerler, A. Müller, R. Garcia-Serres and C. L. Hill, *Chem. Commun.*, 2005, 5621;
- (e) A. Müller, B. Botar, H. Bögge, P. Kögerler and A. Berkle, *Chem. Commun.*, 2002, 2944.
- 38 (a) M. Nyman, *Dalton Trans.*, 2011, **40**, 8049;
- (b) R. P. Bontchev and M. Nyman, *Angew. Chem. Int. Ed.*, 2006, **45**, 6670;
- (c) J. Niu, P. Ma, H. Niu, J. Li, J. Zhao, Y. Song and J. Wang, *Chem. Eur. J.*, 2007, **13**, 8739.
- 39 (a) L.-H. Bi, S. S. Mal, N. H. Nsouli, M. H. Dickman, U. Kortz, S. Nellutla, N. S. Dalal, M. Prinz, G. Hofmann and M. Neumann, *J. Cluster Sci.*, 2008, **19**, 259;
- (b) S.-T. Zheng, M.-H. Wang and G.-Y. Yang, *Inorg. Chem.*, 2007, **46**, 9503;
- (c) J. Niu, F. Li, J. Zhao, P. Ma, D. Zhang, B. Bassil, U. Kortz and J. Wang, *Chem. Eur. J.*, 2014, **20**, 9852;
- (d) J. D. Sokolow, E. Trzop, Y. Chen, J. Tang, L. J. Allen, R. H. Crabtree, J. B. Benedict and P. Coppens, *J. Am. Chem. Soc.*, 2012, **134**, 11695.
- 40 (a) N. T. Tran, D. R. Powell and L. F. Dahl, *Angew. Chem. Int. Ed.*, 2000, **39**, 4121;
- (b) E. G. Mednikov and L. F. Dahl, *J. Am. Chem. Soc.*, 2008, **130**, 14813;
- (c) N. T. Tran and L. F. Dahl, *Angew. Chem. Int. Ed.*, 2003, **42**, 3533;
- (d) E. G. Mednikov, S. A. Ivanov and L. F. Dahl, *Angew. Chem. Int. Ed.*, 2003, **42**, 323.
- 41 N. T. Tran, D. R. Powell and L. F. Dahl, *Dalton Trans.*, 2004, 217.
- 42 (a) C. Femoni, M. C. Iapalucci, G. Longoni, P. H. Svensson and J. Wolowska, *Angew. Chem. Int. Ed.*, 2000, **39**, 1635;
- (b) M. Kawano, J. W. Bacon, C. F. Campana and L. F. Dahl, *J. Am. Chem. Soc.*, 1996, **118**, 7869.

- 43 (a) A. Ceriotti, F. Demartin, G. Longoni, M. Manassero, M. Marchionna, G. Piva and M. Sansoni, *Angew. Chem. Int. Ed.*, 1985, **24**, 697;
(b) C. Femoni, M. C. Iapalucci, G. Longoni, P. H. Svensson, P. Zanello and F. F. de Biani, *Chem. Eur. J.*, 2004, **10**, 2318;
(c) N. de Silva and L. F. Dahl, *Inorg. Chem.*, 2006, **45**, 8814;
(d) C. Femoni, M. C. Iapalucci, G. Longoni and P. H. Svensson, *Chem. Commun.*, 2004, 2274.
- 44 (a) M. Scheer, A. Schindler, R. Merkle, B. P. Johnson, M. Linseis, R. Winter, C. E. Anson and A. V. Virovets, *J. Am. Chem. Soc.*, 2007, **129**, 13386;
(b) M. Scheer, A. Schindler, C. Gröger, A. V. Virovets and E. V. Peresyphkina, *Angew. Chem. Int. Ed.*, 2009, **48**, 5046;
(c) J. Bai, A. V. Virovets and M. Scheer, *Science*, 2003, **300**, 781.
- 45 P. D. Mlynek, M. Kawano, M. A. Kozee and L. F. Dahl, *J. Cluster Sci.*, 2001, **12**, 313.
- 46 (a) F. Xu, H. N. Miras, R. A. Scullion, D.-L. Long, J. Thiel and L. Cronin, *PNAS*, 2012, 11609;
(b) R. A. Scullion, A. J. Surman, F. Xu, J. S. Mathieson, D.-L. Long, F. Haso, T. Liu and L. Cronin, *Angew. Chem. Int. Ed.*, 2014, **53**, 10032;
(c) X. Gu and D. Xue, *Inorg. Chem.*, 2007, **46**, 3212;
(d) F.-S. Guo, Y.-C. Chen, L.-L. Mao, W.-Q. Lin, J.-D. Leng, R. Tarasenko, M. Orendáč, J. Prokleška, V. Sechovský and M.-L. Tong, *Chem. Eur. J.*, 2013, **19**, 14876;
(e) J.-B. Peng, X.-J. Kong, Q.-C. Zhang, M. Orendáč, J. Prokleška, Y.-P. Ren, L.-S. Long, Z. Zheng and L.-S. Zheng, *J. Am. Chem. Soc.*, 2014, **136**, 17938;
(f) W.-J. Gong, Y.-Y. Liu, J. Yang, H. Wu, J.-F. Ma and T.-F. Xie, *Dalton Trans*, 2013, **42**, 3304;
(g) S. P. Argent, A. Greenaway, M. D. Gimenez-Lopez, W. Lewis, H. Nowell, A. N. Khlobystov, A. J. Blake, N. R. Champness and M. Schröder, *J. Am. Chem. Soc.*, 2012, **134**, 55;
(h) V. Chandrasekhar, R. K. Metre and D. Sahoo, *Eur. J. Inorg. Chem.*, 2014, 164;
(i) X.-J. Kong, Y. Wu, L.-S. Long, L.-S. Zheng and Z. Zheng, *J. Am. Chem. Soc.*, 2009, **131**, 6918;

- (j) X. Yang, Z. Li, S. Wang, S. Huang, D. Schipper and R. A. Jones, *Chem. Commun.*, 2014, **50**, 15569;
- (k) X. Yang, D. Schipper, L. Zhang, K. Yang, S. Huang, J. Jiang, C. Su and R. A. Jones, *Nanoscale*, 2014, **6**, 10569.
- 47 (a) M. Manoli, R. Inglis, M. J. Manos, G. S. Papaefstathiou, E. K. Brechin and A. J. Tasiopoulos, *Chem. Commun.*, 2013, **49**, 1061;
- (b) J.-J. Zhang, S.-Q. Xia, T.-L. Sheng, S.-M. Hu, G. Leibelng, F. Meyer, X.-T. Wu, S.-C. Xiang and R.-B. Fu, *Chem. Commun.*, 2004, 1186;
- (c) T. C. Stamatatos, D. Foguet-Albiol, W. Wernsdorfer, K. A. Abboud and G. Christou, *Chem. Commun.*, 2011, 274;
- (d) M. Wu, F. Jiang, X. Kong, D. Yuan, L. Long, S. A. Al-Thabaiti and M. Hong, *Chem. Sci.*, 2013, **4**, 3104;
- (e) J.-W. Cheng, J. Zhang, S.-T. Zheng, M.-B. Zhang and G.-Y. Yang, *Angew. Chem. Int. Ed.*, 2006, **45**, 73;
- (f) S. Xiang, S. Hu, T. Sheng, J. Chen and X. Wu, *Chem. Eur. J.*, 2009, **15**, 12496;
- (g) J.-J. Zhang, T.-L. Sheng, S.-M. Hu, S.-Q. Xia, G. Leibelng, F. Meyer, Z.-Y. Fu, L. Chen, R.-B. Fu and X.-T. Wu, *Chem. Eur. J.*, 2004, **10**, 3963;
- (h) C.-Z. Ruan, R. Wen, M.-X. Liang, X.-J. Kong, Y.-P. Ren, L.-S. Long, R.-B. Huang and L.-S. Zheng, *Inorg. Chem.*, 2012, **51**, 7587;
- (i) Z.-Y. Li, Y.-X. Wang, J. Zhu, S.-Q. Liu, G. Xin, J.-J. Zhang, H.-Q. Huang and C.-Y. Duan, *Cryst. Growth Des.*, 2013, **13**, 3429;
- (j) L. Chen, J.-Y. Guo, X. Xu, W.-W. Ju, D. Zhang, D.-R. Zhu and Y. Xu, *Chem. Commun.*, 2013, **49**, 9728.
- 48 Z.-M. Zhang, S. Yao, Y.-G. Li, R. Clérac, Y. Lu, Z.-M. Su and E.-B. Wang, *J. Am. Chem. Soc.*, 2009, **131**, 14600.
- 49 M. Wang, D.-Q. Yuan, C.-B. Ma, M.-J. Yuan, M.-Q. Hu, N. Li, H. Chen, C.-N. Chen and Q.-T. Liu, *Dalton Trans.*, 2010, **39**, 7276.
- 50 A. J. Tasiopoulos and S. P. Perlepes, *Dalton Trans.*, 2008, 5537.
- 51 (a) J.-J. Zhang, T.-L. Sheng, S.-Q. Xia, G. Leibelng, F. Meyer, S.-M. Hu, R.-B. Fu, S.-C. Xiang and X.-T. Wu, *Inorg. Chem.*, 2004, **43**, 5472; (b) G. Xiong, H. Xu, J. -Z. Cui, Q. -L. Wang and B. Zhao, *Dalton Trans.*, 2014, **43**, 5639.

- 52 J.-J. Zhang, S.-M. Hu, S.-C. Xiang, T. Sheng, X.-T. Wu and Y.-M. Li, *Inorg. Chem.*, 2006, **45**, 7173.
- 53 P. Alborés and E. Rentschler, *Angew. Chem. Int. Ed.*, 2009, **48**, 9366.
- 54 Y.-L. Bai, X. Bao, S. Zhu, J. Fang, M. Shao and H. Shi, *Eur. J. Inorg. Chem.*, 2014, 1275.
- 55 M. Murugesu, R. Clérac, C. E. Anson and A. K. Powell, *Chem. Commun.*, 2004, 1598.
- 56 M. Murugesu, R. Clérac, C. E. Anson and A. K. Powell, *Inorg. Chem.*, 2004, **43**, 7269.
- 57 X.-J. Kong, L.-S. Long, R.-B. Huang, L.-S. Zheng, T. D. Harris and Z. Zheng, *Chem. Commun.*, 2009, 4354.
- 58 X.-J. Kong, Y.-P. Ren, L.-S. Long, Z. Zheng, G. Nichol, R.-B. Huang and L.-S. Zheng, *Inorg. Chem.*, 2008, **47**, 2728.
- 59 X.-J. Kong, Y.-P. Ren, L.-S. Long, Z. Zheng, R.-B. Huang and L.-S. Zheng, *J. Am. Chem. Soc.*, 2007, **129**, 7016.
- 60 X.-J. Kong, Y.-P. Ren, W.-X. Chen, L.-S. Long, Z. Zheng, R.-B. Huang and L.-S. Zheng, *Angew. Chem. Int. Ed.*, 2008, **47**, 2398.
- 61 T. Liu, Y.-J. Zhang, Z.-M. Wang and S. Gao, *J. Am. Chem. Soc.*, 2008, **130**, 10500.
- 62 M. Charalambous, E. E. Moushi, C. Papatriantafyllopoulou, W. Wernsdorfer, V. Nastopoulos, G. Christou and A. J. Tasiopoulos, *Chem. Commun.*, 2012, **48**, 5410.
- 63 (a) A. Bilyk, J. W. Dunlop, R. O. Fuller, A. K. Hall, J. M. Harrowfield, M. W. Hosseini, G. A. Koutsantonis, I. W. Murray, B. W. Skelton, R. L. Stamps and A. H. White, *Eur. J. Inorg. Chem.*, 2010, 2106;
(b) A. Gehin, S. Ferlay, J. M. Harrowfield, D. Fenske, N. Kyritsakas and M. W. Hosseini, *Inorg. Chem.*, 2012, **51**, 5481.
- 64 Y. Bi, X.-T. Wang, W. Liao, X. Wang, X. Wang, H. Zhang and S. Gao, *J. Am. Chem. Soc.*, 2009, **131**, 11650.
- 65 (a) F. P. Schmidtchen and M. Berger, *Chem. Rev.*, 1997, **97**, 1609;
(b) P. A. Gale, *Coord. Chem. Rev.*, 2000, **199**, 181;
(c) P. A. Gale, *Coord. Chem. Rev.*, 2001, **213**, 79;
(d) J. J. Bodwin, A. D. Cutland, R. G. Malkani and V. L. Pecoraro, *Coord. Chem. Rev.*, 2001, **216-217**, 489;
(e) N. H. Evans and P. D. Beer, *Angew. Chem. Int. Ed.*, 2014, **53**, 11716;
(f) K. M. Mullen and P. D. Beer, *Chem. Soc. Rev.*, 2009, **38**, 1701;

- (g) H. N. Miras, G. I. Chilas, L. Cronin and T. A. Kabanos, *Eur. J. Inorg. Chem.*, 2013, 1620.
- 66 G. Mezei, P. Baran and R. G. Raptis, *Angew. Chem. Int. Ed.*, 2004, **43**, 574.
- 67 G. F. S. Whitehead, F. Moro, G. A. Timco, W. Wernsdorfer, S. J. Teat and R. E. P. Winpenny, *Angew. Chem. Int. Ed.*, **2013**, *52*, 9932.
- 68 G. F. S. Whitehead, J. Ferrando-Soria, L. G. Christie, N. F. Chilton, G. A. Timco, F. Moro and R. E. P. Winpenny, *Chem. Sci.*, 2014, **5**, 235.
- 69 R. T. W. Scott, S. Parsons, M. Murugesu, W. Wernsdorfer, G. Christou and E. K. Brechin, *Angew. Chem. Int. Ed.*, 2005, **44**, 6540.
- 70 T. C. Stamatatos, K. A. Abboud, W. Wernsdorfer and G. Christou, *Angew. Chem. Int. Ed.*, 2008, **47**, 6694.
- 71 (a) A. Müller, S. K. Das, E. Krickemeyer, P. Kögerler, H. Bögge and M. Schmidtman, *Solid State Sciences*, 2000, **2**, 847;
(b) A. Müller, S. Sarkar, S. Q. N. Shah, H. Bögge, M. Schmidtman, S. Sarkar, P. Kögerler, B. Hauptfleisch, A. X. Trautwein and V. Schünemann, *Angew. Chem. Int. Ed.*, 1999, **38**, 3238.
- 72 A. Müller, E. Krickemeyer, H. Bögge, M. Schmidtman and F. Peters, *Angew. Chem. Int. Ed.*, 1998, **37**, 3360.
- 73 C. M. Beavers, A. V. Prosverin, J. D. Cashion, K. R. Dunbar and A. F. Richards, *Inorg. Chem.*, 2013, **52**, 1670.
- 74 (a) G. Karotsis, S. Kennedy, S. J. Teat, C. M. Beavers, D. A. Fowler, J. J. Morales, M. Evangelisti, S. J. Dalgarno and E. K. Brechin, *J. Am. Chem. Soc.*, 2010, **132**, 12983;
(b) P. P. Cholewa and S. J. Dalgarno, *Cryst. Eng. Comm.*, 2014, **16**, 3655;
(c) Y. Bi, S. Du and W. Liao, *Chem. Commun.*, 2011, 4724;
(d) G. Karotsis, S. J. Teat, W. Wernsdorfer, S. Piligkos, S. J. Dalgarno and E. K. Brechin, *Angew. Chem. Int. Ed.*, 2009, *48*, 8285.
- 75 T. S. M. Abedin, L. K. Thompson, D. O. Miller and E. Krupicka, *Chem. Commun.*, 2003, 708.
- 76 (a) M. Jamet, W. Wernsdorfer, C. Thirion, D. Mailly, V. Dupuis, P. Melinon and A. Perez, *Phys. Rev. Lett.*, 2001, **86**, 4676;
(b) R. H. Kodama, *J. Magn. Magn. Mater.*, 1999, **200**, 359;
(c) W. Jiang, F. T. Birk and D. Davidović, *Appl. Phys. Lett.*, 2011, **99**, 032510;

- (d) S. Guéron, M. M. Deshmukh, E. B. Myers and D. C. Ralph, *Phys. Rev. Lett.*, 1999, **83**, 4148.
- 77 (a) C. J. Milios, A. Vinslava, W. Wernsdorfer, S. Moggach, S. Parsons, S. P. Perlepes, G. Christou and E. K. Brechin, *J. Am. Chem. Soc.*, 2007, **129**, 2754;
(b) C. Papatriantafyllopoulou, W. Wernsdorfer, K. A. Abboud and G. Christou, *Inorg. Chem.*, 2011, **50**, 421;
(c) M. Holynska, D. Premuzic, I.-R. Jeon, W. Wernsdorfer, R. Clerac and S. Dehnen, *Chem. Eur. J.*, 2011, **17**, 9605.
- 78 (a) L.-X. Chang, G. Xiong, L. Wang, P. Cheng and B. Zhao, *Chem. Commun.*, 2013, **49**, 1055;
(b) G. Lorusso, M. A. Palacios, G. S. Nichol, E. K. Brechin, O. Roubeau and M. Evangelisti, *Chem. Commun.*, 2012, **48**, 7592;
(c) S. Biswas, A. Adhikary, S. Goswami and S. Konar, *Dalton Trans.*, 2013, **42**, 13331;
(d) G. Lorusso, J. W. Sharples, E. Palacios, O. Roubeau, E. K. Brechin, R. Sessoli, A. Rossin, F. Tuna, E. J. L. McInnes, D. Collison and M. Evangelisti, *Adv. Mater.*, 2013, **25**, 4653.
- 79 (a) A.-H. Lu, E. L. Salabas and F. Schüth, *Angew. Chem. Int. Ed.*, 2007, **46**, 1222;
(b) T. Hyeon, *Chem. Commun.*, 2003, 927.



Constantina Papatriantafyllopoulou is a Researcher at the University of Cyprus. She completed her BSc degree at the University of Ioannina (Greece) and then moved to the University of Patras (Greece) and performed PhD research under the supervision of Professor Spyros P. Perlepes. After postdoctoral work with Prof. George Christou at the University of Florida, she was granted with a Marie Curie fellowship and joined Tasiopoulos' group in February 2011. Constantina's research interests are focused on the synthesis and magnetostructural characterization of 3d and 3d/4f metal complexes.



Eleni E. Moushi (born in 1981, Paralimni, Cyprus) obtained her PhD degree in 2009 under the supervision of Prof. Anastasios Tasiopoulos at the Department of Chemistry, University of Cyprus, Cyprus. Since 2009 she is working as a Postdoctoral Fellow at the University of Cyprus. Part of her postdoctoral research was performed under the supervision of Prof. Mercuri Kanatzidis at the Department of Chemistry, Northwestern University, USA. Her research

interests concern the design and synthesis of new coordination complexes and their structural characterization and the study of their magnetic and sorption properties.



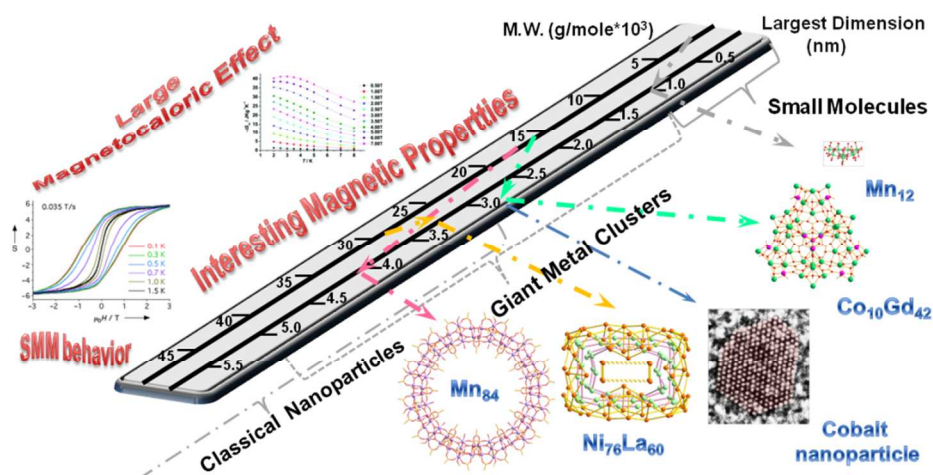
George Christou received his PhD in Chemistry from Exeter University, and was a Postdoctoral Fellow at Manchester and a NATO Fellow at Stanford and Harvard Universities. He became a lecturer at Imperial College, before moving to Indiana University in 1983. In 2001 he took up the Drago Chair of Chemistry at the University of Florida, where he is also Distinguished Professor. His research is in the synthesis and physical-inorganic chemistry of 3d metal clusters of various nuclearities, and their relevance to bioinorganic chemistry and magnetic materials.



Anastasios J. Tasiopoulos is Associate Professor of Inorganic Chemistry at the University of Cyprus. He was born in Korydallos, Greece. He completed both his *BSc* (1995) and *PhD* (1999) degrees at the University of Ioannina (Greece), the latter under the supervision of Professor Themistoklis A. Kabanos. After postdoctoral work with Professor George Christou at the

University of Florida, he was appointed Lecturer at the University of Cyprus in 2004. His research is focused on the synthesis and study of metal clusters and multidimensional coordination polymers with interesting properties and potential applications in various areas such as magnetism, sensing and gas storage and separation.

Table of Contents graphic



The syntheses, structures and magnetic properties of giant molecular 3d and 3d/4f paramagnetic metal clusters in moderate oxidation states are surveyed. Such complexes display fascinating crystal structures and interesting magnetic properties, combining sizes comparable to those of classical magnetic nanoparticles with the quantum behavior appearing in molecular species, and thus providing a powerful bottom-up approach to nanoscale magnetic materials.